

2018 Fall

“Phase Transformation *in* Materials”

12.04.2018

Eun Soo Park

Office: 33-313

Telephone: 880-7221

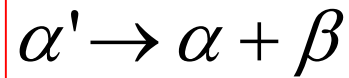
Email: espark@snu.ac.kr

Office hours: by an appointment

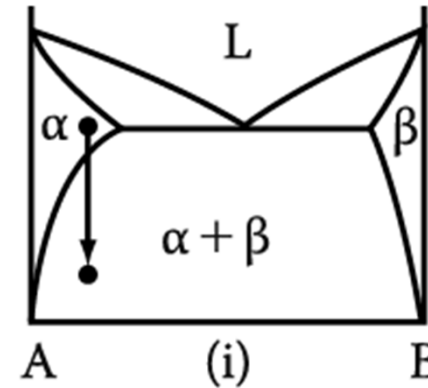
5. Diffusion Transformations in solid

: diffusional nucleation & growth

(a) Precipitation



Metastable supersaturated
Solid solution



Homogeneous Nucleation

$$\Delta G = -V\Delta G_V + A\gamma + V\Delta G_S$$

Heterogeneous Nucleation

$$\Delta G_{het} = -V(\Delta G_V - \Delta G_S) + A\gamma - \Delta G_d$$

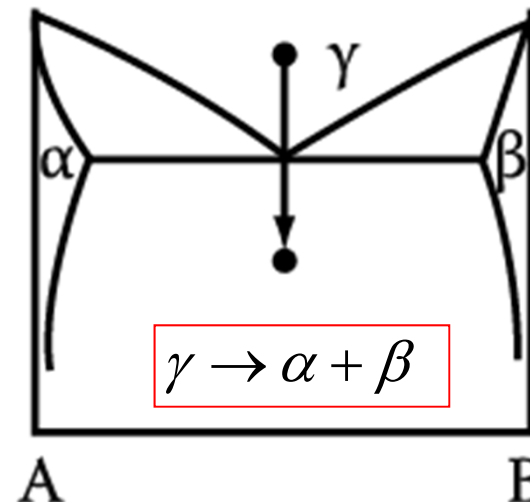
$$N_{hom} = \omega C_0 \exp\left(-\frac{\Delta G_m}{kT}\right) \exp\left(-\frac{\Delta G^*}{kT}\right)$$

→ suitable nucleation sites ~ nonequilibrium defects
(creation of nucleus ~ destruction of a defect (-ΔG_d))

(b) Eutectoid Transformation

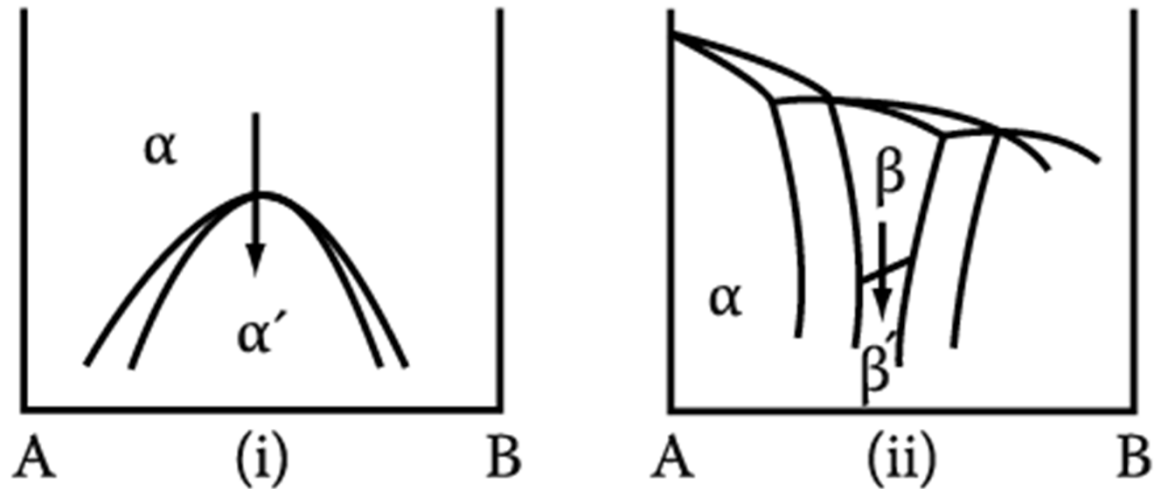
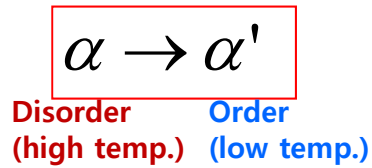
Composition of product phases
differs from that of a parent phase.
→ **long-range diffusion**

Which transformation proceeds
by short-range diffusion?



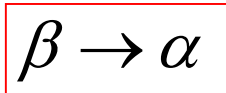
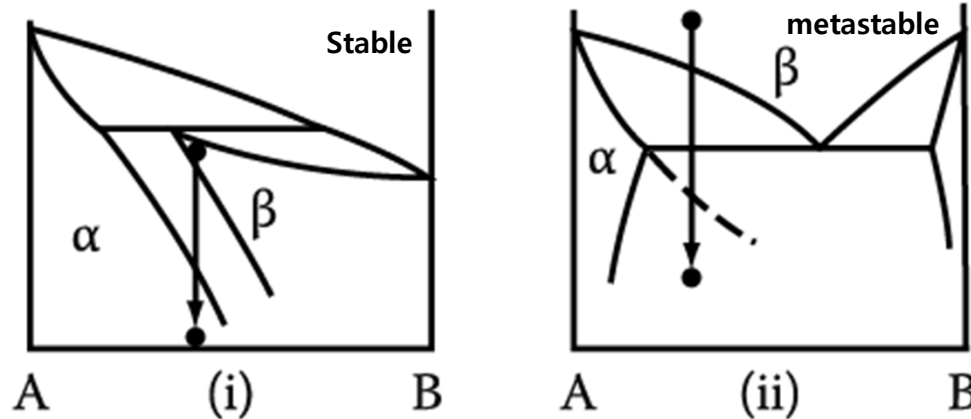
5. Diffusion Transformations in solid

(c) Order-Disorder Transformation

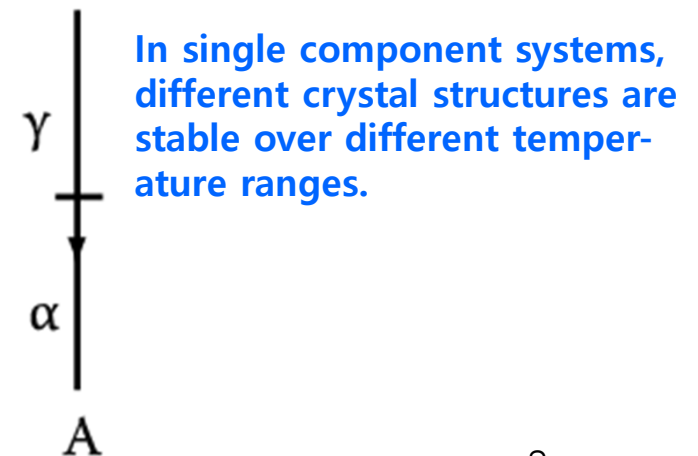


(d) Massive Transformation

: The original phase decomposes into one or more new phases which have the same composition as the parent phase, but different crystal structures.



(e) Polymorphic Transformation

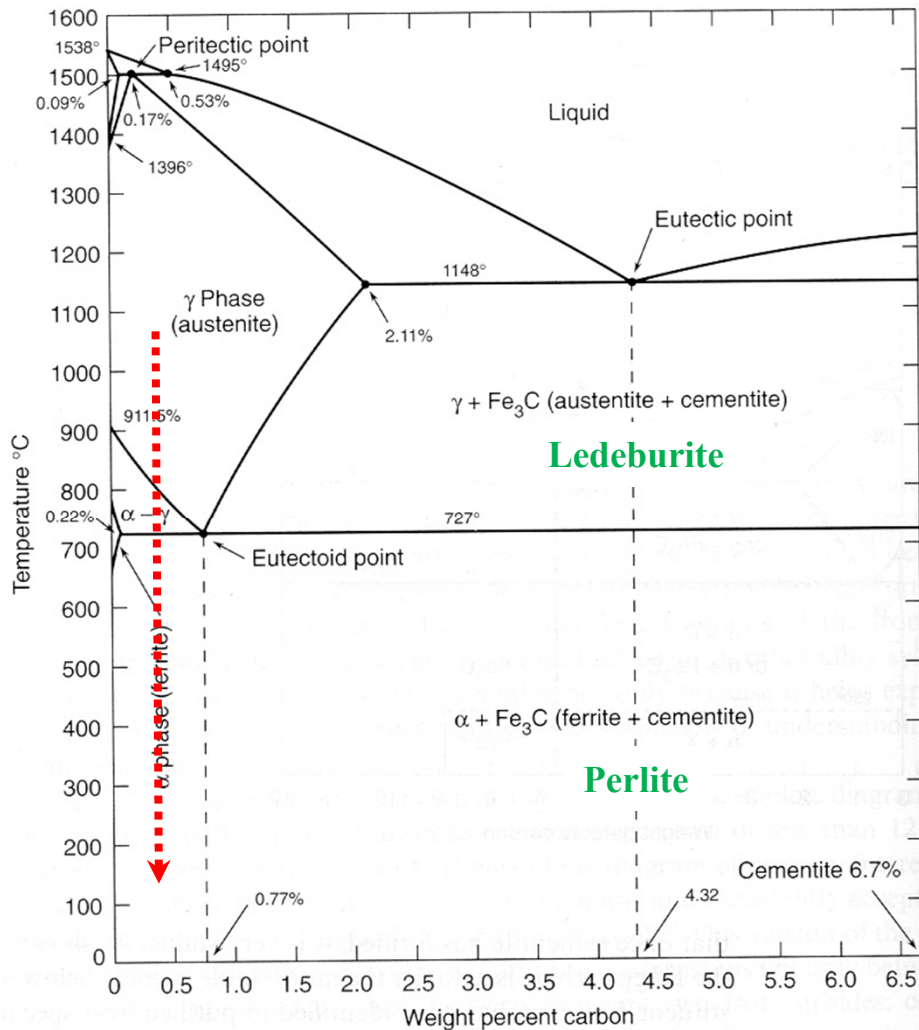


3) Precipitation of equilibrium phase by diffusional transformation

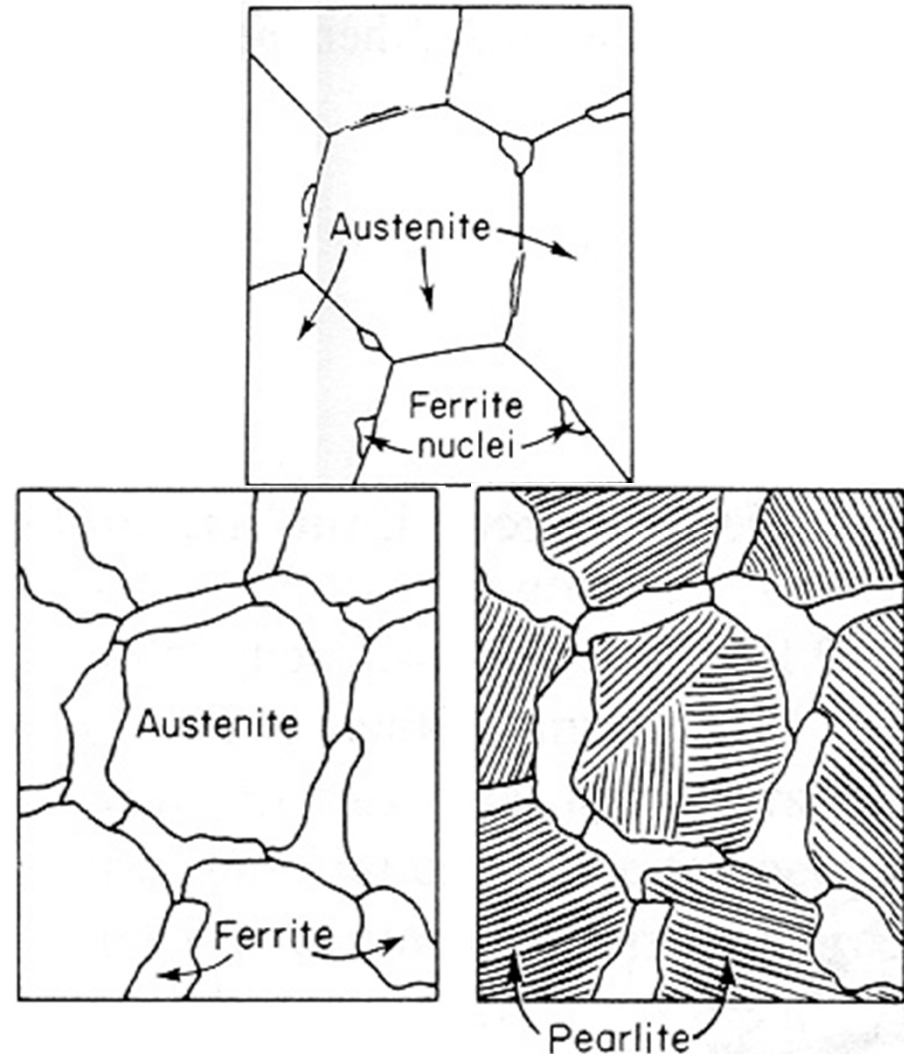
5.6. The Precipitation of Ferrite from Austenite ($\gamma \rightarrow \alpha$)

(Most important nucleation site: Grain boundary and the surface of inclusions)

The Iron-Carbon Phase Diagram

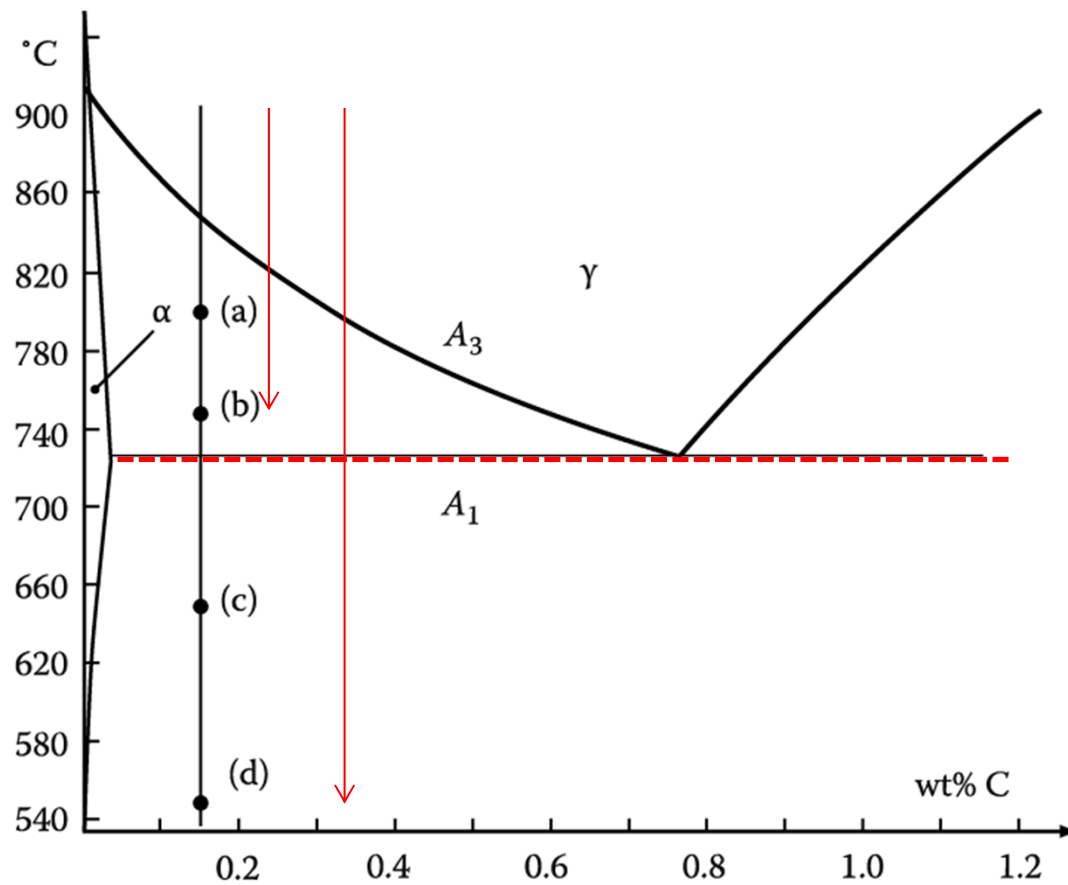


Microstructure (0.4 wt%C) evolved by slow cooling (air, furnace) ?



5.6. The Precipitation of Ferrite from Austenite

Diffusional Transformation of Austenite into Ferrite



Fe-0.15 wt%C

After being austenitized, held at

(a) 800°C for 150 s

(b) 750°C for 40 s

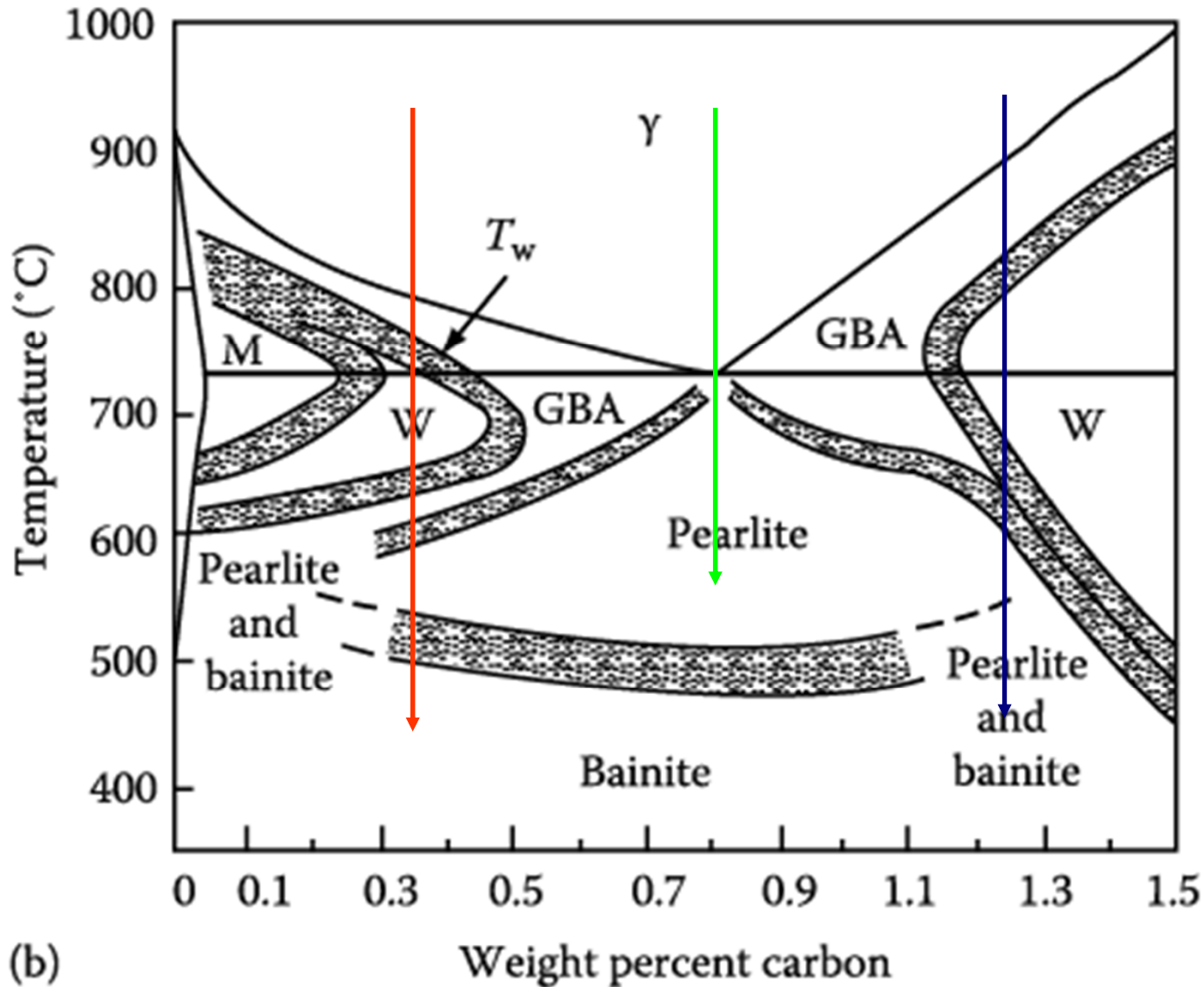
(c) 650°C for 9 s

(d) 550°C for 2 s and
then quenched to room T.

**What would be the
microstructures?**

Figure 5.45 Holding temperature for steel in Figure. 5.46

For alloys of different carbon content, A_3 and T_w vary and show parallel manner each other.



(GBA: GB allotriomorphs, W: Widmanstätten sideplates/intermolecular plates, M: Massive ferrite)

Figure 5.48 (b) Temperature-composition regions in which the various morphologies are dominant at late reaction times in specimens with ASTM grain size Nos. 0-1. 6

Growth of Pearlite: analogous to the growth of a lamellar eutectic

Min. possible: $(S^*) \propto 1/\Delta T$ / Growth rate : mainly lattice diffusion $v = kD_c \gamma (\Delta T)^2$

Interlamellar spacing of pearlite colonies : mainly boundary diffusion $v = kD_b (\Delta T)^3$

Relative Positions of the Transformation curves for Pearlite and Bainite in Plain Carbon Eutectoid Steels.

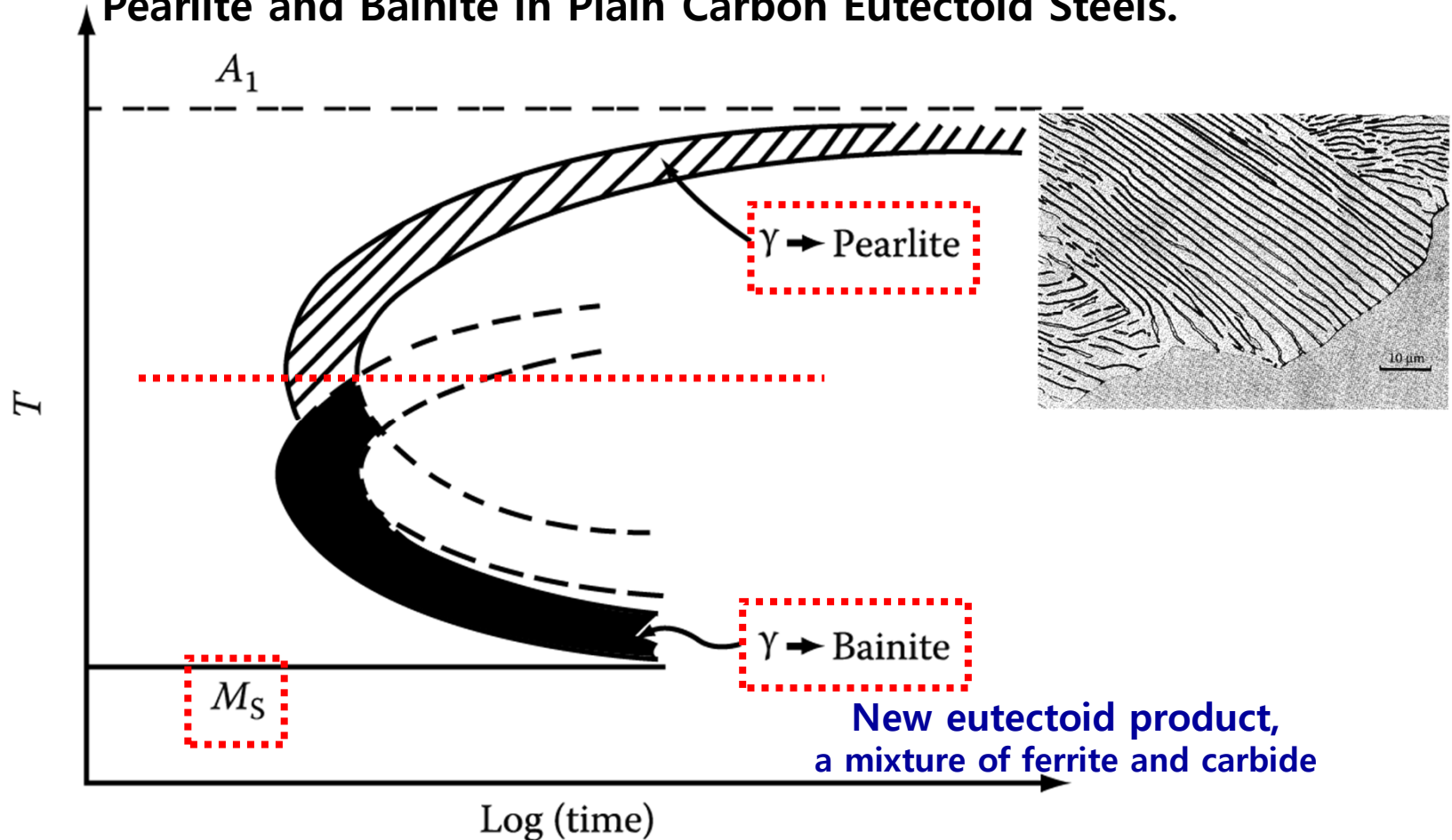


Figure 5.64 Schematic diagram showing relative positions of the transformation curves for pearlite and bainite in plain carbon eutectoid steel.

* Massive, Martensite Transformation

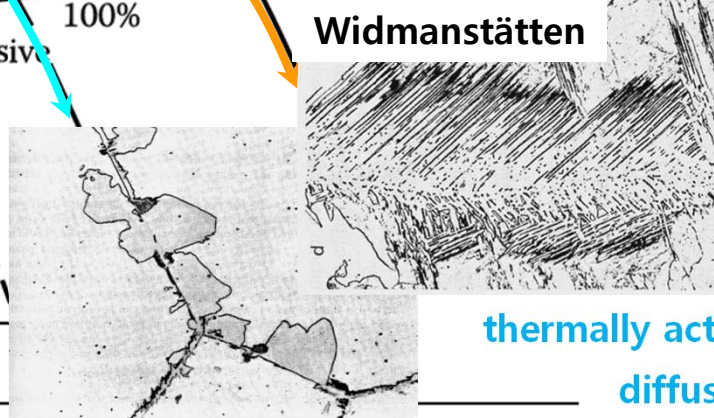
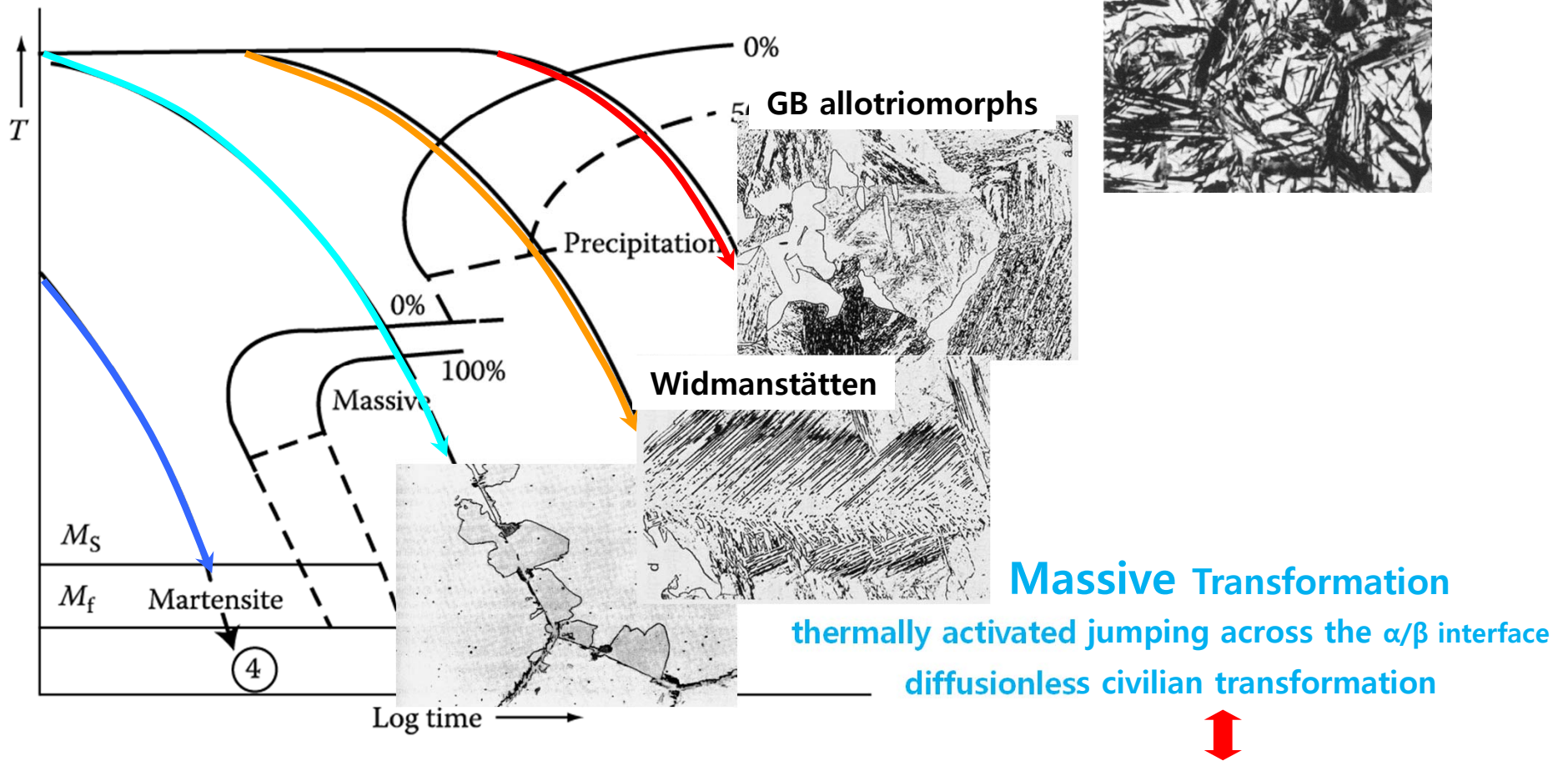


Fig. 5.75 A possible CCT diagram for systems showing a massive transformation. Slow cooling (1) produces equiaxed α . Widmanstätten morphologies result from faster cooling (2). Moderately rapid quenching (3) produces the massive transformation, while the highest quench rate (4) leads to a martensitic transformation.

β is sheared into α by the cooperative movement of atoms across a glissile interface
 diffusionless military transformation
Martensite Transformation

Contents in Phase Transformation

Background
to understand
phase
transformation

(Ch1) Thermodynamics and Phase Diagrams

(Ch2) Diffusion: Kinetics

(Ch3) Crystal Interface and Microstructure

Representative
Phase
transformation

(Ch4) Solidification: Liquid \rightarrow Solid

(Ch5) Diffusional Transformations in Solid: Solid \rightarrow Solid

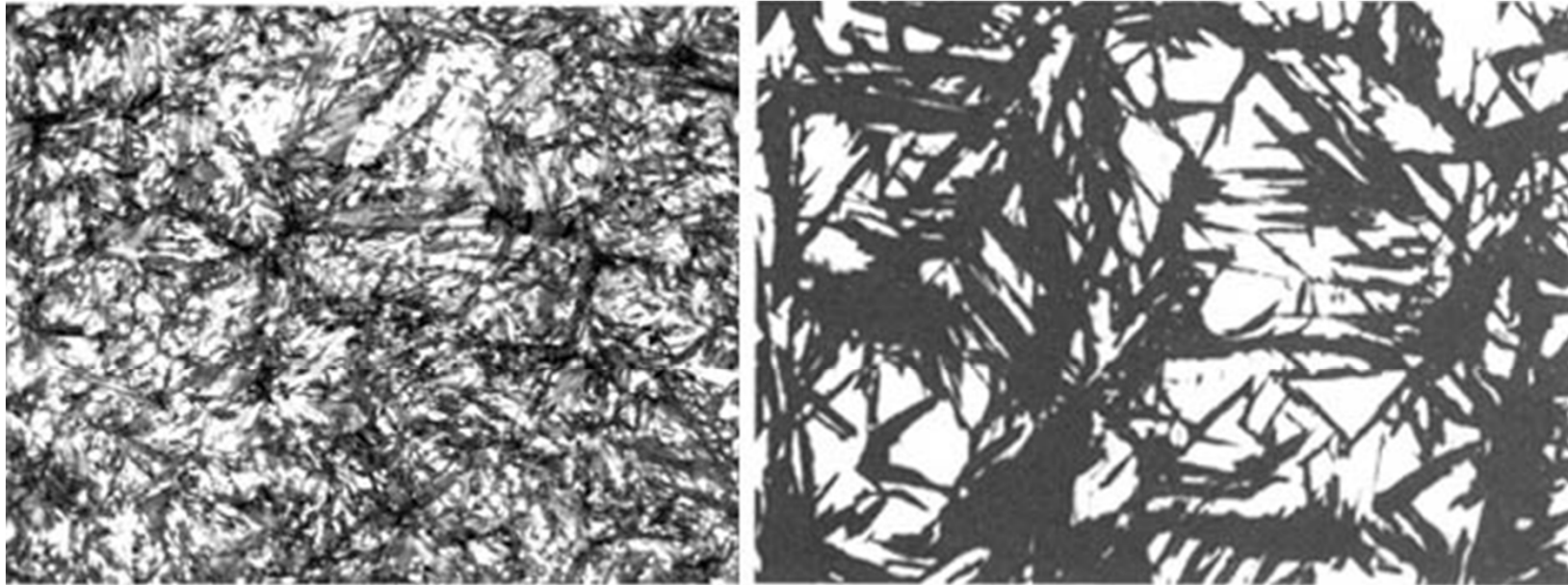
(Ch6) Diffusionless Transformations: Solid \rightarrow Solid

One of the most important technological processes is the hardening of steel by quenching.

Chapter 6 Diffusionless Transformation

Individual atomic movements are less than one interatomic spacing.

→ **Martensite Transformation**



($\gamma \rightarrow \alpha$) Martensite with some retained austenite

"Needle like" Structure of martensite

Supersaturated solid solution of carbon in α -Fe

Named for the German metallurgist **Adolph Martens**, Martensite is **the hardened phase of steel** that is obtained by cooling Austenite fast enough to **trap carbon atoms within the cubic iron matrix distorting it into a body centered tetragonal structure**. Now, martensite is used in physical metallurgy to describe any diffusionless trans. product.

Military Transformations

- What is a martensitic transformation?

Most phase transformations studied in this course have been diffusional transformations where long range diffusion is required for the (nucleation and) growth of the new phase(s).

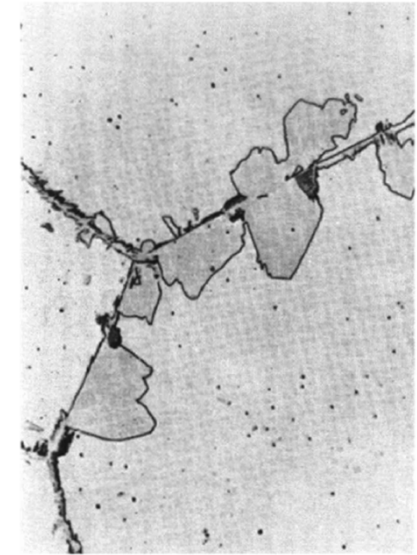
- There is a whole other class of *military transformations* which are *diffusionless transformations* in which the atoms move only short distances (**less than one interatomic spacing**) in order to join the new phase.
- These transformations are *also* subject to the constraints of nucleation and growth. They are (almost invariably) associated with *allotropic transformations* (동소변태).

Classification of Transformations

	Civilian	Military
Diffusion Required	Precipitation, Spinodal Decomposition	?
Diffusionless	Massive Transformations	Martensitic Transformations

Massive vs. Martensitic Transformations

- There are two basic types of diffusionless transformations.
- One is the **massive transformation**. In this type, a diffusionless transformation takes place ① without a definite orientation relationship. The interphase boundary (between parent and product phases) migrates so as to allow the new phase to grow. It is, however, a ② **diffusionless transformation** because the atoms move individually.
- The other is the **martensitic transformation**. In this type, the change in phase involves a ① definite orientation relationship because the atoms have to ② move in a coordinated manner. There is always a ③ change in shape which means that there is a strain associated with the transformation. The strain is a general one, meaning that all six (independent) coefficients can be different.



Microstructure of Martensite

- The microstructural characteristics of martensite are:
 - the product (martensite) phase has a well defined crystallographic relationship with the parent (matrix).
- 1) martensite (designated α') forms as **platelets within grains**.

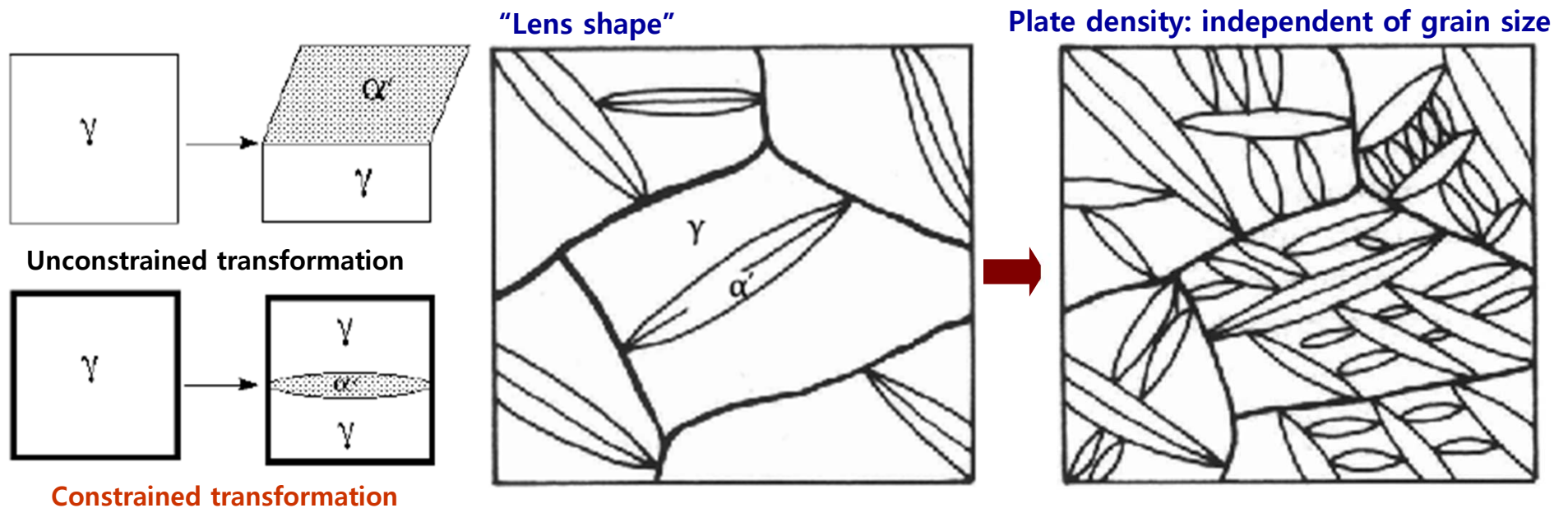


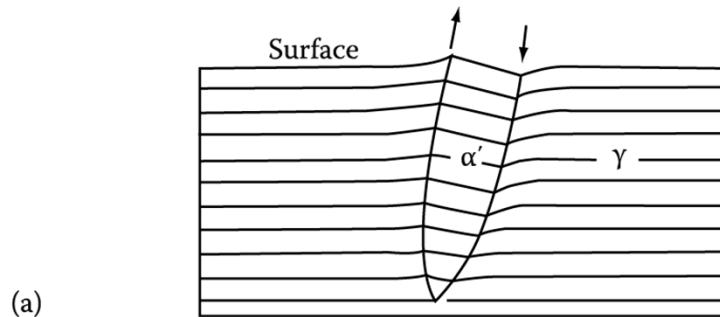
Fig. 6.1 Growth of martensite with increasing cooling below M_s .
→ Martensite formation rarely goes to completion

Microstructure of Martensite

- The microstructural characteristics of martensite are:
 - each platelet is accompanied by a **shape change**.
 - the shape change appears to be a **simple shear parallel to a habit plane** (the common, coherent plane between the phases) and a **“uniaxial expansion (dilatation) normal to the habit plane”**.

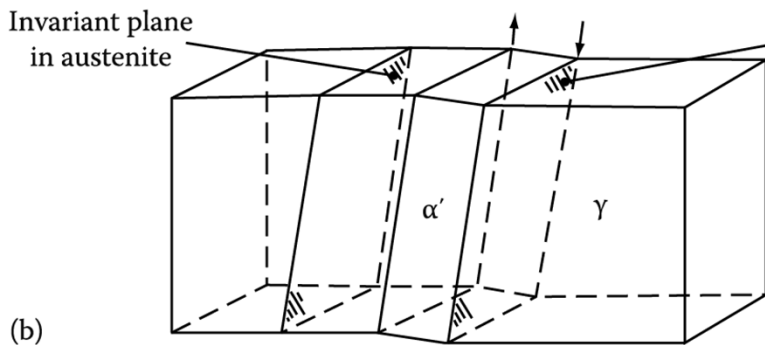
strain associated with the transformation

Polished surface_elastic deformation or tilting
→ but, remain continuous after the transformation



Intersection of the lenses with the surface of the specimen does not result in any discontinuity.

A fully grown plate spanning a whole grain $\sim 10^{-7}$ sec
→ v of α'/γ interface \propto speed of sound in solid

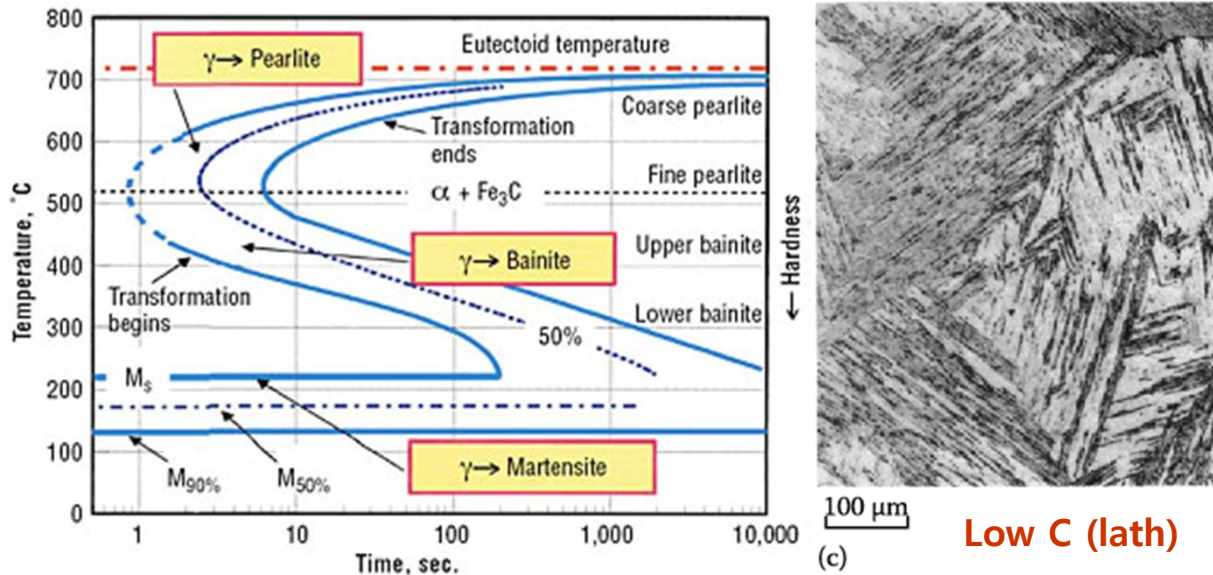


: difficult process to study M nucleation and growth experimentally

Fig. 6.2 Illustrating how a martensite plate remains macroscopically coherent with the surrounding austenite and even the surface it intersects.

Microstructures

M_f temperature (M finish) corresponds to that temperature
 Below which further cooling does not increase the amount of M.
 → 10-15% retained γ : common feature of higher C content alloys



(d) Medium C (plate)



(e) Fe-Ni (plate, some isothermal growth)

Fig. 6.1 (c-e) Different martensite morphologies in iron alloys

Control of Mechanical Properties By Proper Heat Treatment in Iron-Carbon Alloy



Martensite

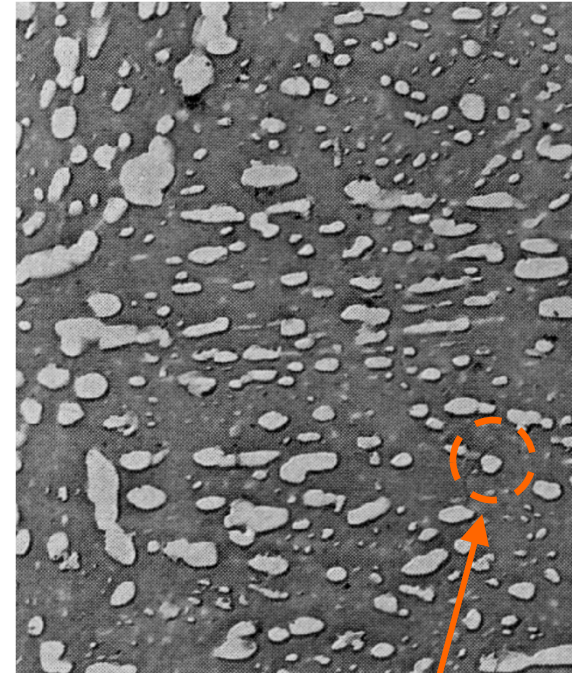
Tip of needle shape grain

Nucleation site of fracture

Brittle



Proper
heat treatment
(tempering)



Tempered martensite

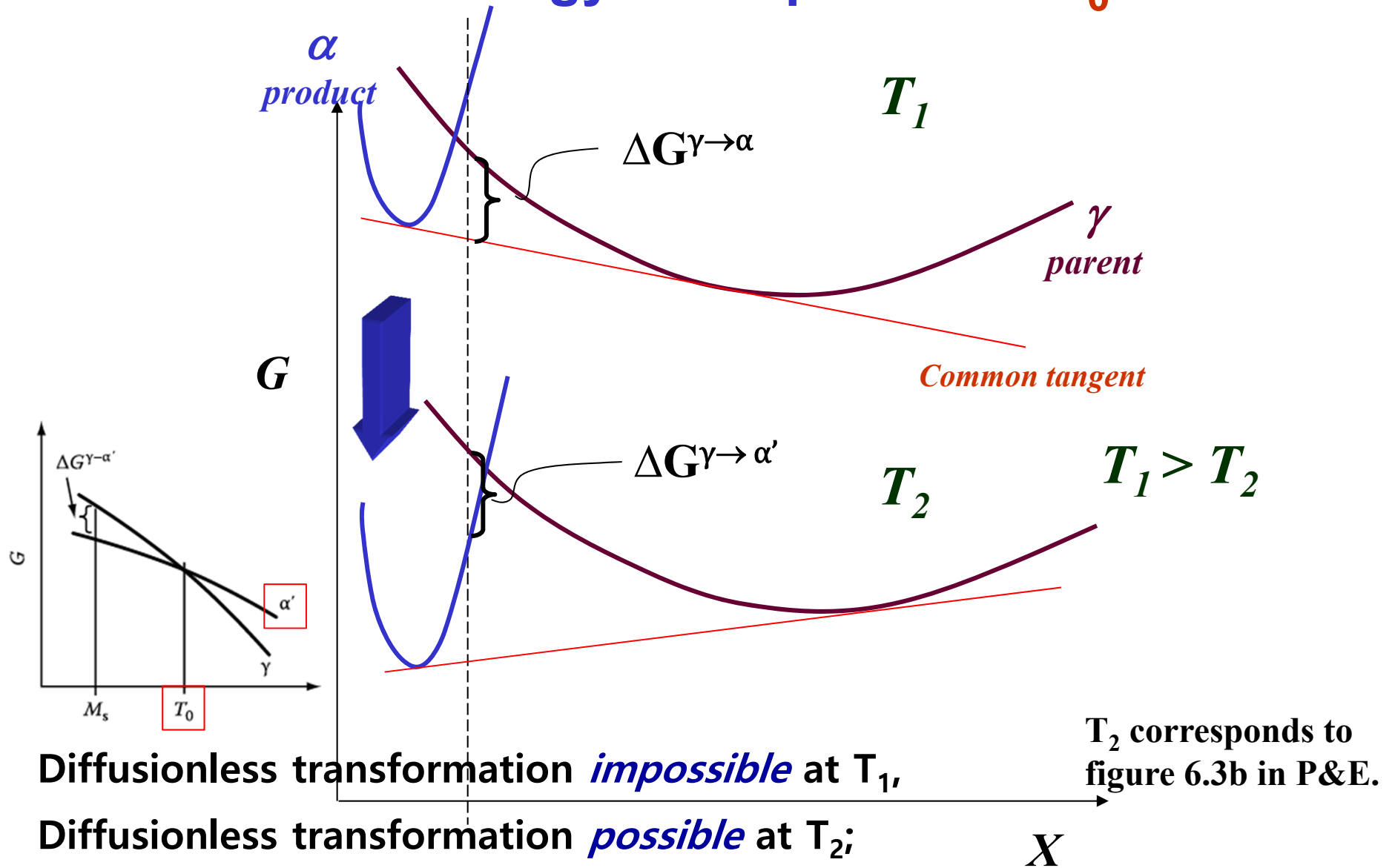
Very small & spherical shape grain

Good strength, ductility, toughness

Driving Forces

- These transformations require **larger driving forces** than for diffusional transformations. (= large undercooling, ΔT)
- Why? In order for a transformation to occur without long range diffusion, it must take place **without a change in composition**.
- This leads to the so-called **T_0 concept**, which is the temperature at which the new phase can appear with a net decrease in free energy at the same composition as the parent (matrix) phase.
- As the following diagram demonstrates, the temperature, T_0 , at which segregation-less transformation becomes possible (i.e. a decrease in free energy would occur), is always less than the liquidus temperature.

Free Energy - Composition: T_0



“ T_0 ” is defined by no difference in free energy between the phases, $\Delta G=0$.

Driving Force Estimation

- The driving force for a martensitic transformation can be estimated in exactly the same way as for other transformations such as solidification.
- Provided that an enthalpy (latent heat of transformation) is known for the transformation, the driving force can be estimated as proportional to **the latent heat** and **the undercooling below T_0** .

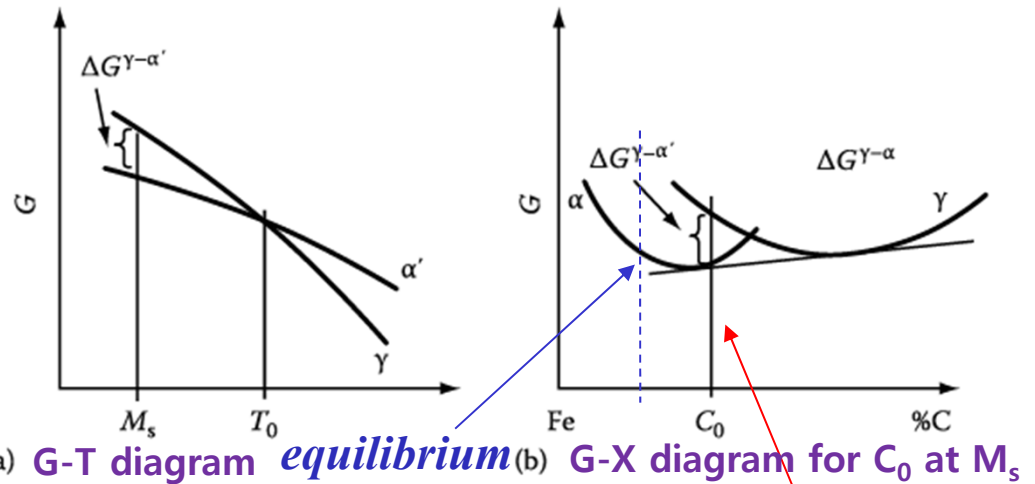
$$\Delta G = \frac{L\Delta T}{T_m} \Rightarrow \Delta G^{\gamma \rightarrow \alpha'} = \Delta H^{\gamma \rightarrow \alpha'} \Delta T / T_0 = \Delta H^{\gamma \rightarrow \alpha'} \frac{(T_0 - M_s)}{T_0}$$

Alloy	$\Delta H^{\gamma \rightarrow \alpha'}$ (J mol ⁻¹)	$T_0 - M_s$ (K)	$-\Delta G^{\gamma \rightarrow \alpha'}$ (J mol ⁻¹)
Ti-Ni	1550	20	92
Cu-Al	170-270	20-60	19.3 ± 7.6
Au-Cd	290	10	11.8
Fe-Ni 28%	1930	140	840
Fe-C			1260
Fe-Pt 24%	340	10	17
Ordered	* Large differences in $\Delta G^{\gamma \rightarrow \alpha'}$ btw disordered and ordered alloys (a relatively small ΔT)		
Fe-Pt	2390	~150	~1260
Disordered			

Source: From Guénin, G., PhD thesis, Polytechnical Institute of Lyon, 1979.

Table 6.1. Comparisons of Calorimetric Measurements of Enthalpy and Undercooling in some M alloys

Various ways of showing the martensite transformation

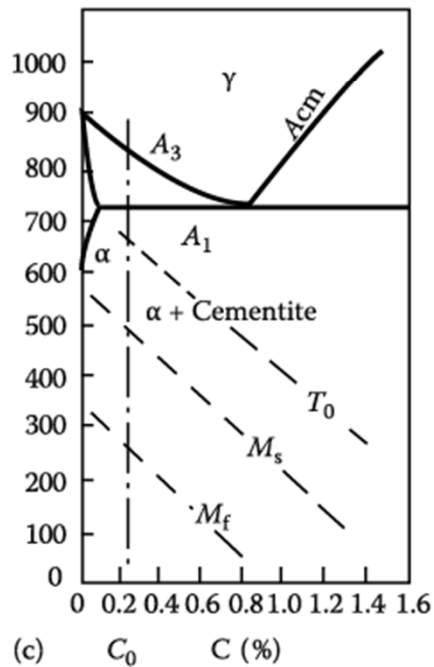


(a) G-T diagram *equilibrium* (b) G-X diagram for C_0 at M_s

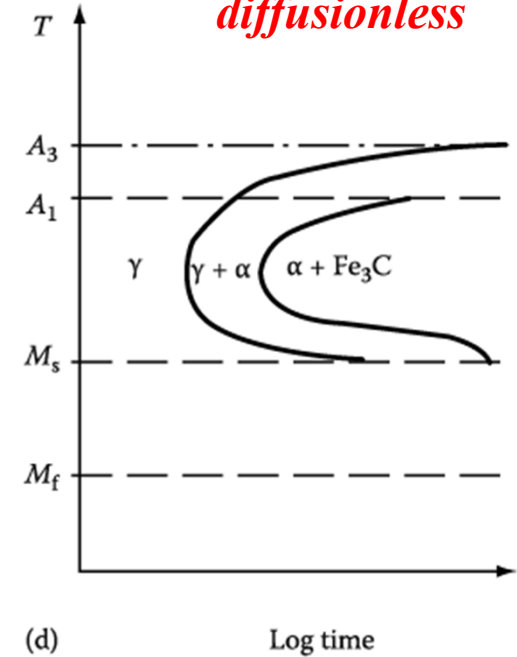
diffusionless

Note that the M_s line is horizontal in the TTT diagram; also, the M_f line.

Some retained austenite can be left even below M_f . In particular, as much as 10%-15% retained austenite is a common feature of especially the higher C content alloys such as those used for ball bearing steels.



(c) Fe-C phase diagram
Variation of $T_0/M_s/M_f$



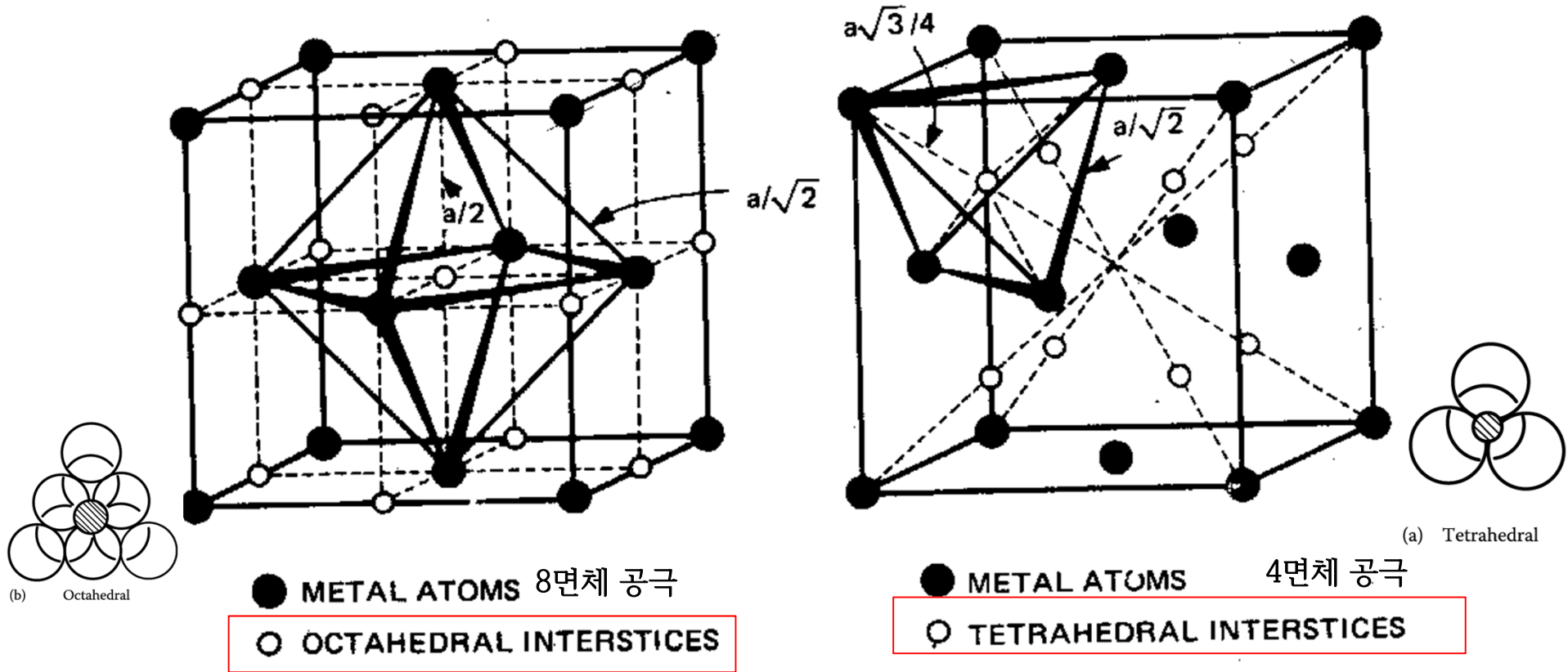
(d) TTT diagram
for alloy C_0 in (c)

Mechanisms for martensitic transformations

- The mechanisms of martensitic transformations are not entirely clear.
- Why does martensite require heterogeneous nucleation?
The reason is the large critical free energy for nucleation outlined above
- Possible mechanisms for martensitic transformations include
 - (a) dislocation based
 - (b) shear based
- (a) • ***Dislocations*** in the parent phase (austenite) clearly provide sites for heterogeneous nucleation.
 - Dislocation mechanisms are thought to be important for ***propagation/growth of martensite platelets or laths***.
- (b) • Martensitic transformations **strongly constrained** by crystallography of the parent and product phases.
 - This is analogous to **slip (dislocation glide)** and twinning, especially the latter.

6.1.1 Solid Solution of carbon in Iron (철의 탄소고용체)

Figure 6.4 Illustrating possible sites for interstitial atoms in the fcc or hcp lattices.



Six nearest neighbors/ $d_6 = 0.414D = 1.044 \text{ \AA}$ surrounded by four atoms/ $d_4 = 0.225D = 0.568 \text{ \AA}$

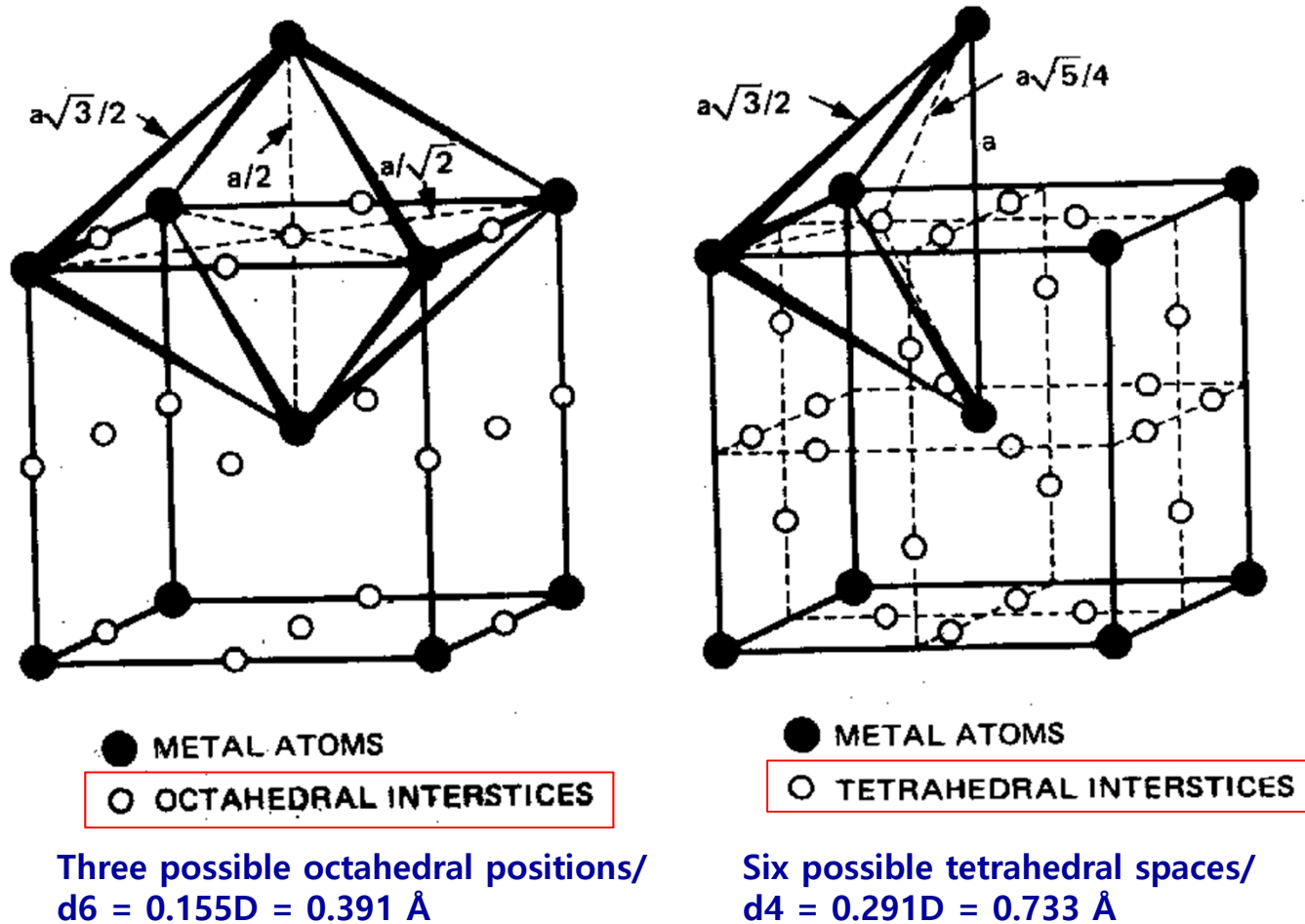
D is the diameter of the parent atoms/ d_4 and d_6 are the maximum interstitial diameters

Diameter of a carbon atom: 1.54 Å

: This means that **considerable distortion** of the γ austenite lattice must occur to contain carbon atoms in solution and that the **octahedral interstices should be the most favorable.**

6.1.1 Solid Solution of carbon in Iron

Figure. Illustrating possible sites for interstitial atoms in the bcc lattices.



D is the diameter of the parent atoms/ d_4 and d_6 are the maximum interstitial diameters

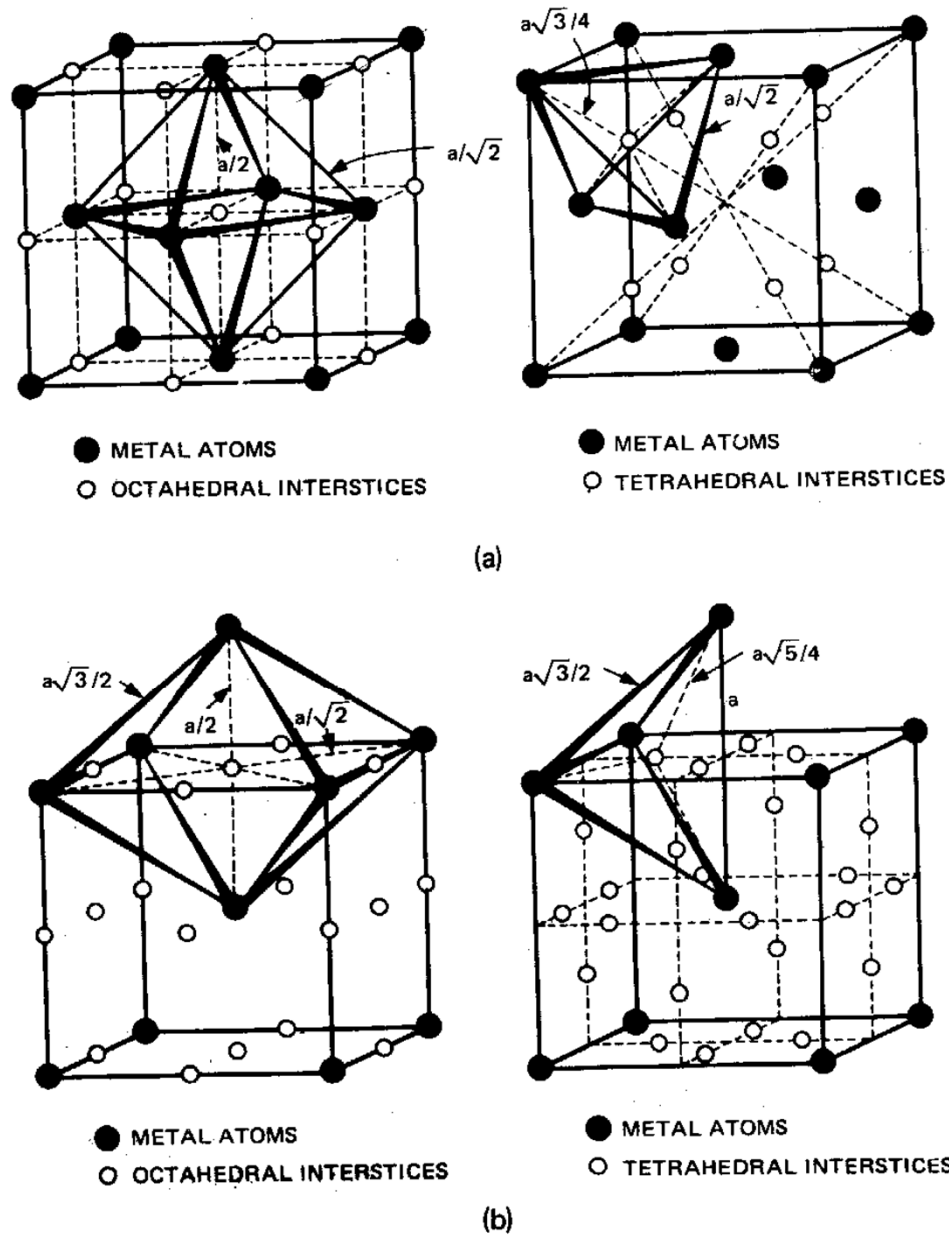
Free space: FCC < BCC but space available per interstitial: FCC > BCC

- * **In spite of $d_6 < d_4$, C & N prefer to occupy the octahedral positions in BCC.**
- **required considerable distortion but <100> directions~weaker** due to the lower number of near and next nearest neighbors compared to the tetrahedral interstitial position

Interstitial sites for C in Fe

fcc:
carbon occupies
the **octahedral**
sites

bcc:
carbon occupies
the
octahedral sites



[Leslie]

Figure II-1. Interstitial voids in iron. (a) Interstitial voids in the fcc structure, octahedral (1) and tetrahedral (2). (b) Interstitial voids in the bcc structure; octahedral (1) and tetrahedral (2). (From C.S. Barrett and T.B. Massalski, *Structure of Metals*, 3d ed., copyright 1966, used with the permission of McGraw-Hill Book Co., New York.)

Carbon in BCC ferrite

- One consequence of the occupation of the octahedral site in ferrite is that the carbon atom has only two nearest neighbors.
- Each carbon atom therefore distorts the iron lattice in its vicinity.
- The distortion is a *tetragonal distortion*.
- If all the carbon atoms occupy the *same type of site* then the entire lattice becomes tetragonal, as in the martensitic structure.
- Switching of the carbon atom between adjacent sites leads to strong internal friction peaks at characteristic temperatures and frequencies.

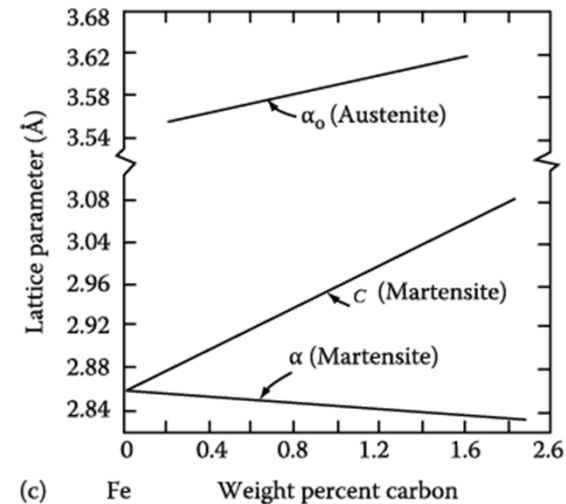
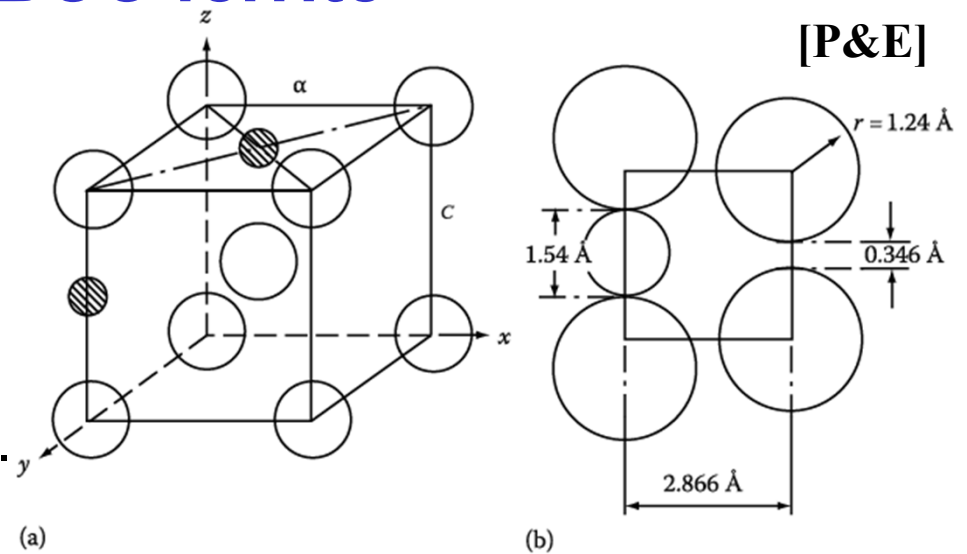


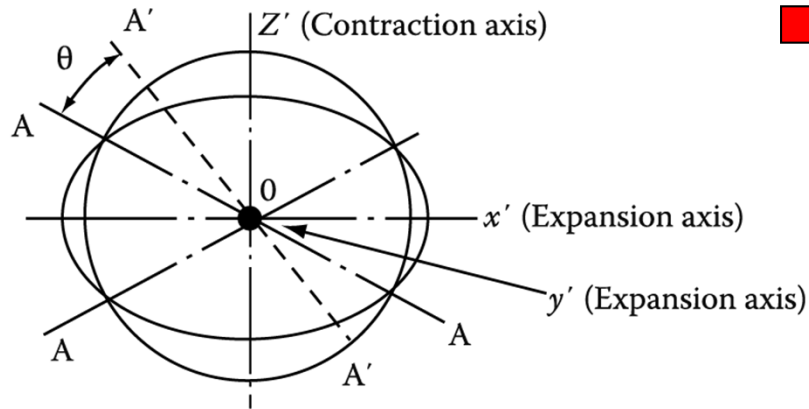
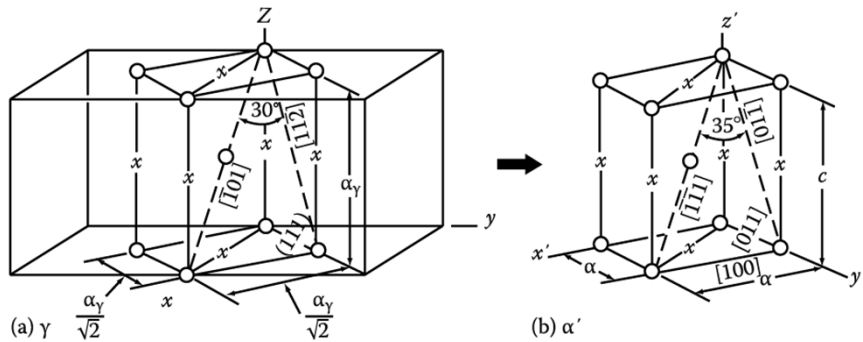
Fig. 6.5 Illustrating (a) possible sites for interstitial atoms in bcc lattice, and (b) the large distortion necessary to accommodate a carbon atom (1.54 \AA diameter) compared with the space available (0.346 \AA). (c) Variation of a and c as a function of carbon content.

Why tetragonal Fe-C martensite?

- At this point, it is worth stopping to ask why a tetragonal martensite forms in iron. The answer has to do with the preferred site for carbon as an interstitial impurity in bcc Fe.
- Remember: Fe-C martensites are unusual for being so strong (& brittle). Most martensites are not significantly stronger than their parent phases.
- Interstitial sites:
 - fcc: octahedral sites radius= 0.052 nm
tetrahedral sites radius= 0.028 nm
 - bcc: octahedral sites radius= 0.019 nm
tetrahedral sites radius= 0.036 nm
- Carbon atom radius = 0.08 nm.
- Surprisingly, it occupies the octahedral site in the bcc Fe structure, despite the smaller size of this site (compared to the tetrahedral sites) presumably because of the low modulus in the <100> directions.

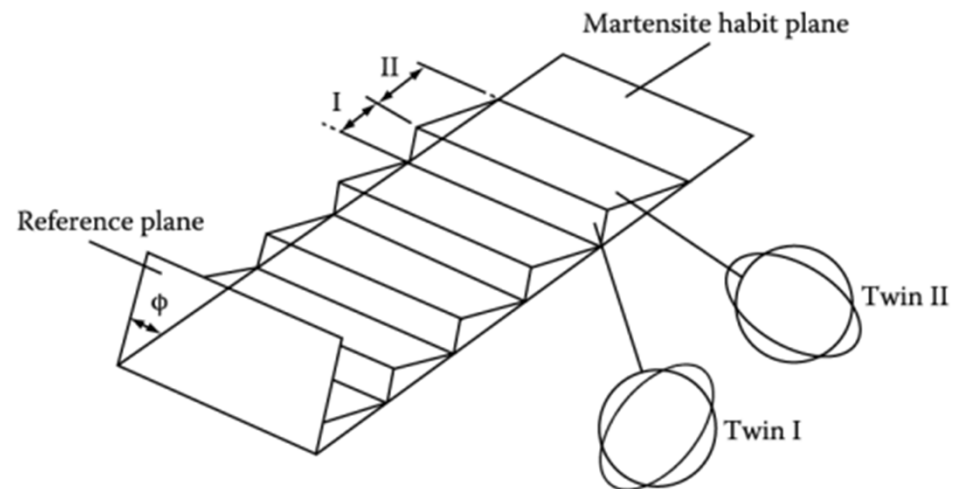
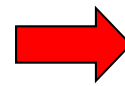
6.2. Martensite crystallography (Orientation btw M & γ)

- $\gamma \rightarrow \alpha'$:
- (1) Habit plane of M: not distorted by transformation
 - (2) A homogeneous shear (s) parallel to the habit plane
 - (3) ~4% expansion_dilatation normal to the habit plain (lens)



Bain Model for martensite

Applying the twinning analogy to the Bain model,



Twins in Martensite

may be self-accommodating and reduce energy by having alternate regions of the austenite undergo the Bain strain along different axes.

Possible atomic model for martensitic transformation: the Bain Model: fcc \rightarrow bct transformation

- For the case of **FCC Fe transforming to BCT ferrite** (Fe-C martensite), there is a basic model known as the **Bain model**.
- The essential point of the Bain model is that it accounts for the structural transformation with a *minimum of atomic motion*.
- Start with two FCC unit cells: contract by 20% in the z direction, and expand by 12% along the x and y directions.

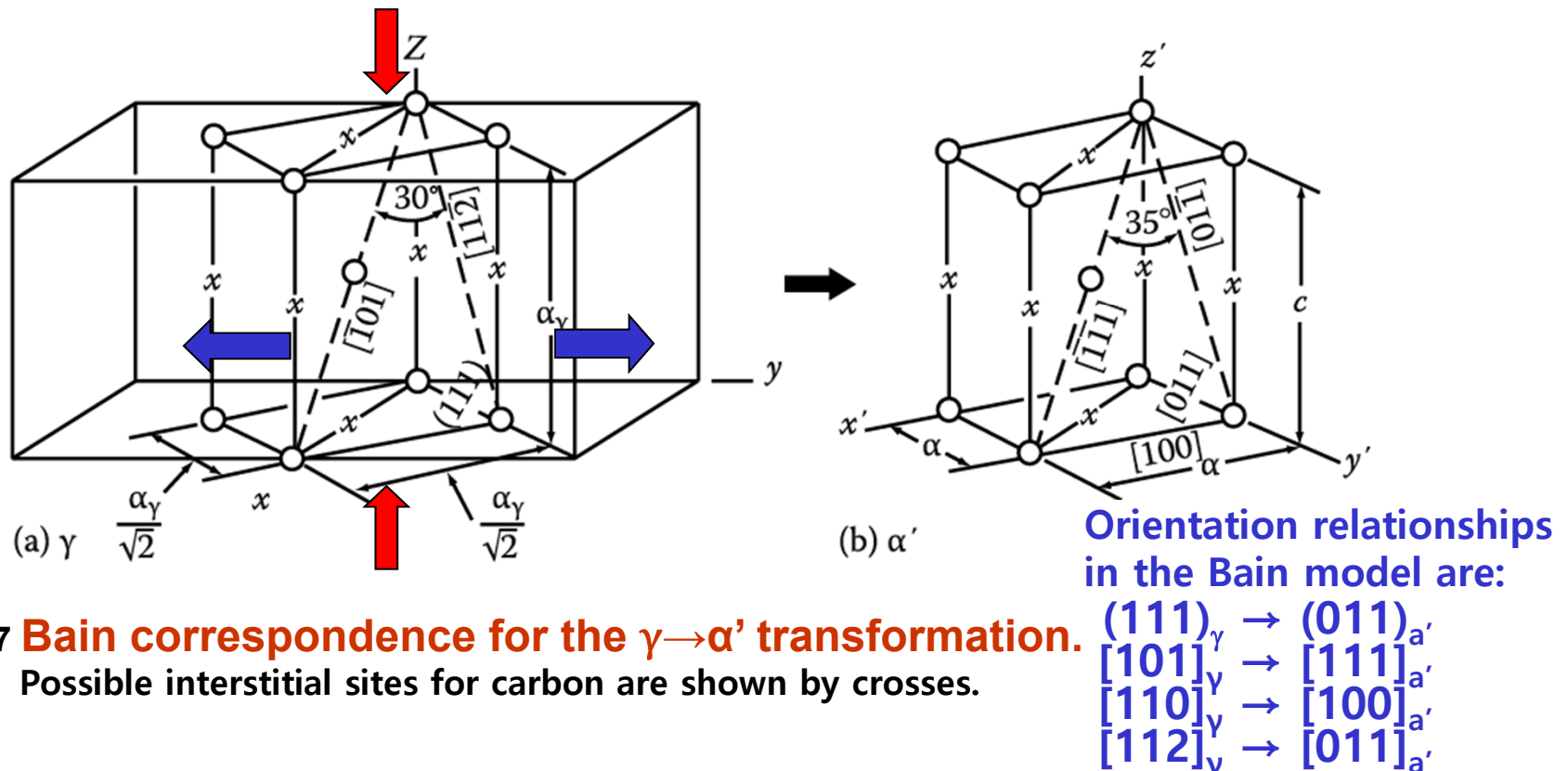


Figure. 6.7 **Bain correspondence for the $\gamma \rightarrow \alpha'$ transformation.**
Possible interstitial sites for carbon are shown by crosses.

Crystallography, contd.

- Although the Bain model explains several basic aspects of martensite formation, additional features must be added for complete explanations (not discussed here).
- **The missing component of the transformation strain is an additional shear that changes the character of the strain so that an invariant plane exists.** This is explained in fig. 6.8.

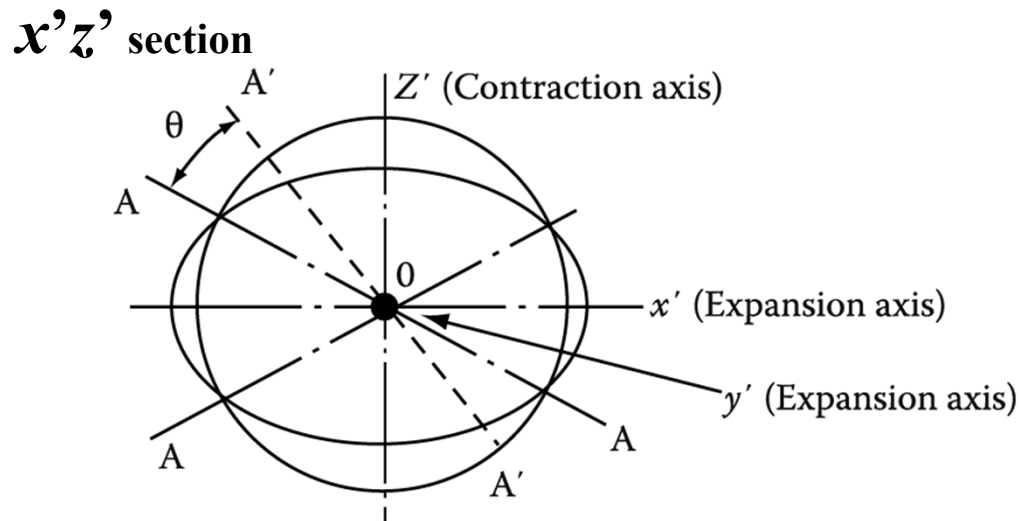


Fig. 6.8 Bain deformation is here simulated by the pure deformation in compressing a sphere elastically to the shape of an oblate ellipsoid. **As in the bain deformation, this transformation involves two expansion axes and one contraction axis.**

Bain deformation = Pure deformation

In this plane, the only vectors that are not shortened or elongated by the Bain distortion are OA or O'A'.

However, the vector OY' (perpendicular to the diagram) must be undistorted.

This is clearly not true and therefore **the Bain transformation does not fulfill the requirements of bringing about a transformation with an undistorted plane.** * 변형되지 않는 평면 설명 못함

Hence, the key to the crystallographic theory of martensitic transformations is to postulate an additional distortion which reduces the extension of y' to zero (in fact a slight rotation, θ , of the AO plane should also be made as shown in the figure).

→ The second deformation can be in the form of dislocation slip or twinning.

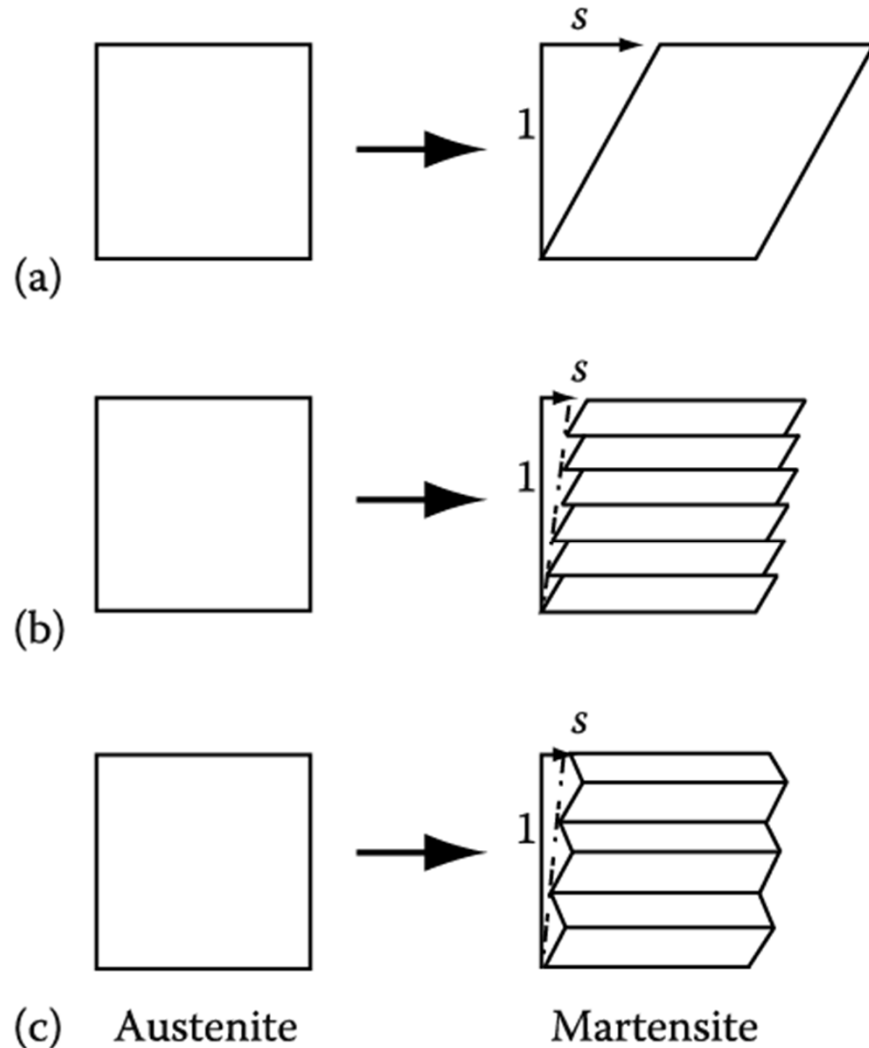
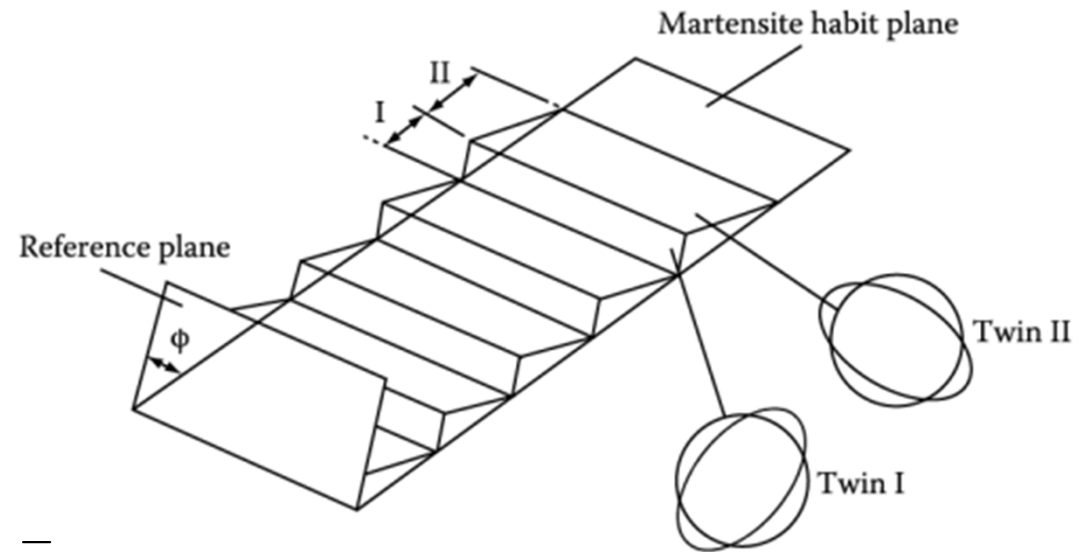
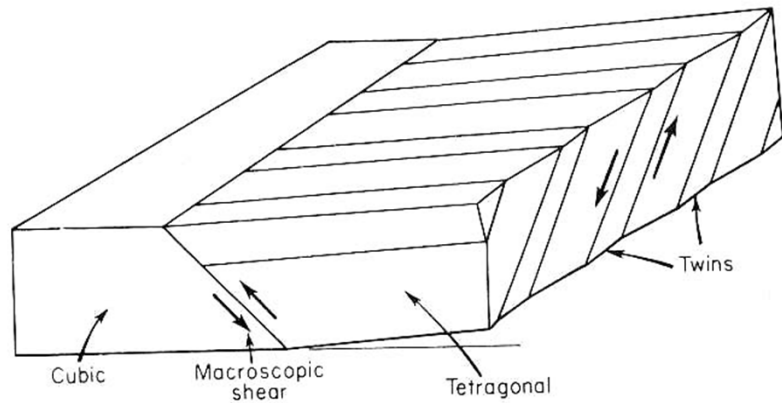


Figure. 6.9 Schematic illustration of **how dislocation glide or twinning of the martensite** can compensate for a pure lattice deformation such as a Bain deformation and thereby reduce the strain of the surrounding austenite. The **transformation shear (s) is defined**. Note **how s can be reduced by slip or twinning**.

Applying the twinning analogy to the Bain model,
the physical requirements of the theory are satisfied.



Slip or Twinning on
 $\{11\bar{2}\} \langle 111 \rangle$ in α $\{110\} \langle 1\bar{1}0 \rangle$ in γ

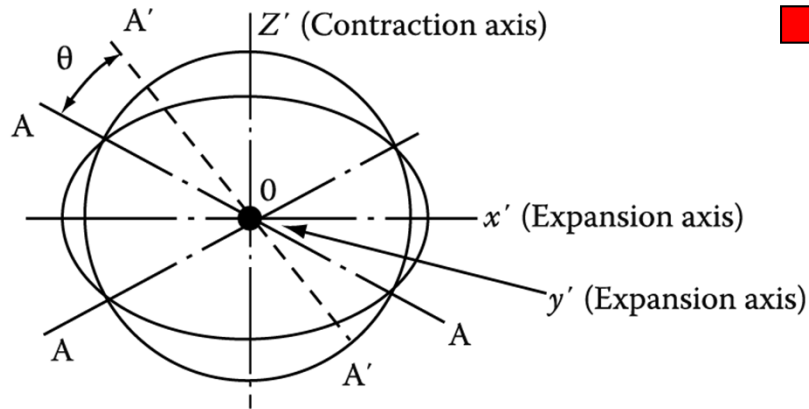
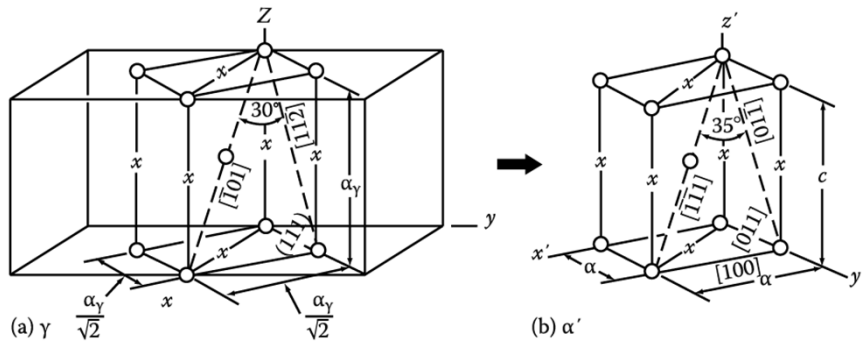
Twins in Martensite

may be self-accommodating and reduce energy by having alternate regions of the austenite undergo the Bain strain along different axes.

- On the basis, the habit plane of the M plate can be defined as a plane in the austenite which undergoes **not net (macroscopic) distortion (=average distortion over many twins is zero)**
- Local strain ϵ by twins at the edge of the plate, but if the plate is very thin (a few atomic spacings) this strain can be relatively small.

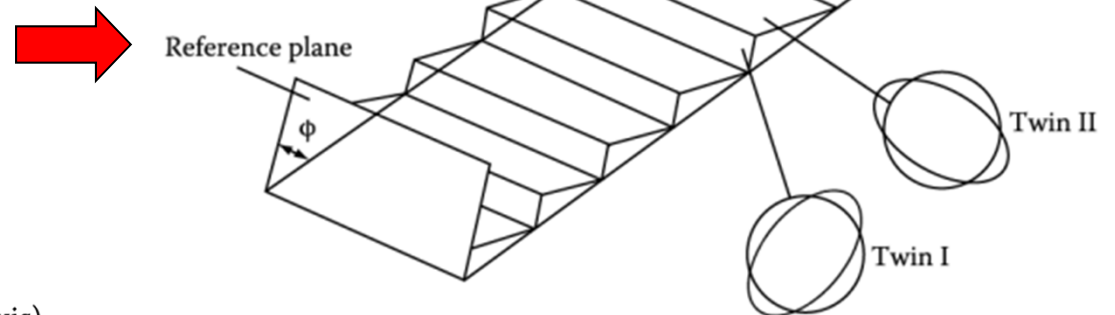
6.2. Martensite crystallography (Orientation btw M & γ)

- $\gamma \rightarrow \alpha'$:
- (1) Habit plane of M: not distorted by transformation
 - (2) A homogeneous shear (s) parallel to the habit plane
 - (3) ~4% expansion_dilatation normal to the habit plain (lens)



Bain Model for martensite

Applying the twinning analogy to the Bain model,



Twins in Martensite

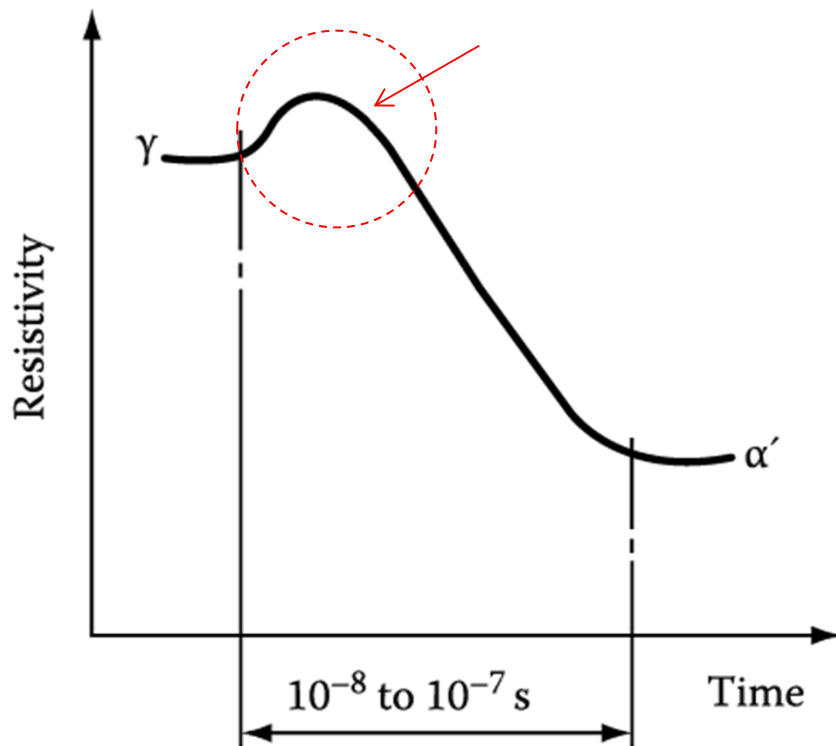
may be self-accommodating and reduce energy by having alternate regions of the austenite undergo the Bain strain along different axes.

6.3. Theories of Martensite Nucleation

: A single plate of M in steel: 10^{-5} to 10^{-7} s, ~the speed of sound

Using resistivity changes to monitor the growth of individual plates of M

e.g. Fe-Ni alloys: **speed of 800-1100 m/s ~ difficult to study experimentally**



- α' gives lower resistivity than γ .
- Smaller initial increase in resistivity
= initial strain of γ lattice by the M nucleus
= **initial M nucleus ~ coherent with parent γ**

Figure. 6.13 Resistivity changes during the growth of single plates of martensite across a grain in a Fe-Ni alloy. From this it can be calculated that the velocity of growth is about 1000 m/s.

6.3.1 Formation of Coherent Nuclei of Martensite (Homogenous nucleation)

Free Energy Change Associated with the Nucleation

Negative and Positive Contributions to ΔG ?

1) Volume Free Energy :

$$-V\Delta G_V$$

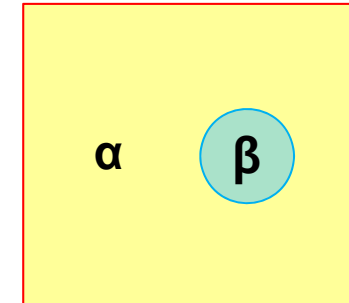
2) Interface Energy :

$$A\gamma$$

3) Misfit Strain Energy :

$$V\Delta G_S$$

$$\Delta G = -V\Delta G_V + A\gamma + V\Delta G_S$$



This expression does not account for possible additional energies (e.g. thermal stresses during cooling, externally applied stresses, and stresses produced ahead of rapidly growing plates, etc).

In M transformations, the strain energy (ΔG_s) of the coherent nucleus is much more Important than the surface energy, since the shear component of the pure Bain strain is as high as $s = 0.32$ which produces large strains in the surrounding austenite. However, the interfacial (surface) energy (γ) of a fully coherent nucleus is relatively small.

6.3.1 Formation of Coherent Nuclei of Martensite (Homogenous nucleation)

for thin ellipsoidal nucleus (radius **a**, semi thickness **c** and volume **V**),

$$\Delta G = A\gamma + V\Delta G_s - V\Delta G_v$$

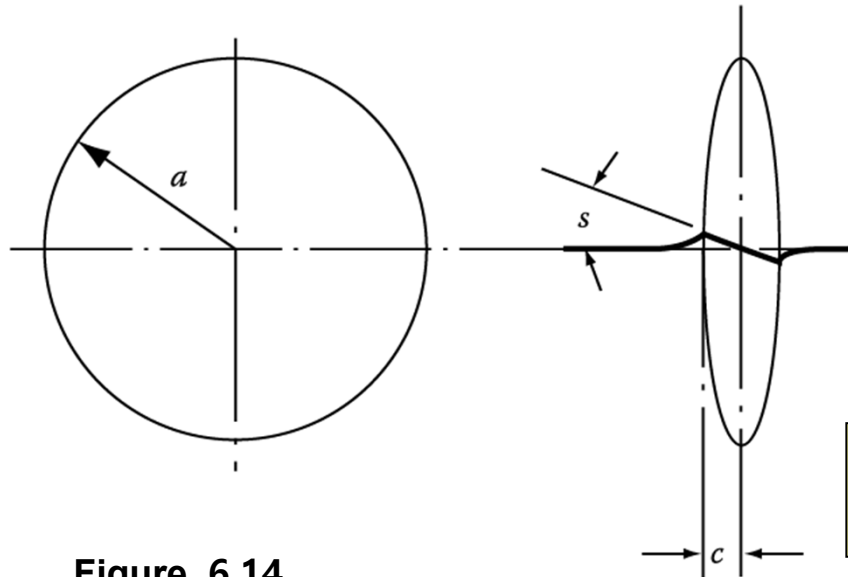


Figure. 6.14
Schematic representation of a M nucleus.

Assumption: 1) Nucleation does not necessarily occur at grain boundaries.
2) Nucleation occurs homogeneously without the aid of any other types of lattice defects.

→ The Nucleus forms by a simple shear, s , parallel to the plane of the disc, and complete coherency is maintained at the interface.

$$\Delta G = 2\pi a^2 \gamma + 2\mu V (s/2)^2 \frac{2(2-\nu)}{8(1-\nu)} \pi c / a - \frac{4}{3} \pi a^2 c \cdot \Delta G_v$$

If $\nu=1/3$,

$$\Delta G = \underbrace{2\pi a^2 \gamma}_{\text{Surface E}} + \underbrace{\frac{16\pi}{3} (s/2)^2 \mu a c^2}_{\text{Elastic E (shear component of strain only)}} - \underbrace{\frac{4\pi}{3} a^2 c}_{\text{Volume E}} \cdot \Delta G_v$$

Eq. (6.7)

6.3.1 Formation of Coherent Nuclei of Martensite

By differentiating Eq. (6.7) with respect to **a** and **c**, respectively

→ **Min. free energy barrier to nucleation: extremely sensitive to “ γ , ΔG_s and s ”**

$$\Delta G^* = \frac{512}{3} \cdot \frac{\gamma^3}{(\Delta G_v)^4} \cdot (s/2)^4 \mu^2 \pi \quad (\text{joules/nucleus})$$

→ **Critical nucleus size (c^* and a^*): highly dependent to “ γ , ΔG_s and s ”**

$$c^* = \frac{2\gamma}{\Delta G_v}$$

$$a^* = \frac{16\gamma\mu(s/2)^2}{(\Delta G_v)^2}$$

Eq. (6.9) & (6.10)

For steel, 1) typically $\Delta G_v = 174 \text{ MJm}^{-3}$, and

2) s (varies according to whether the net shear of a whole plate (e.g. as measured from surface markings) or shear of fully coherent plate (as measured from lattice fringe micrographs)
= 0.2 (macroscopic shear strain in steel)

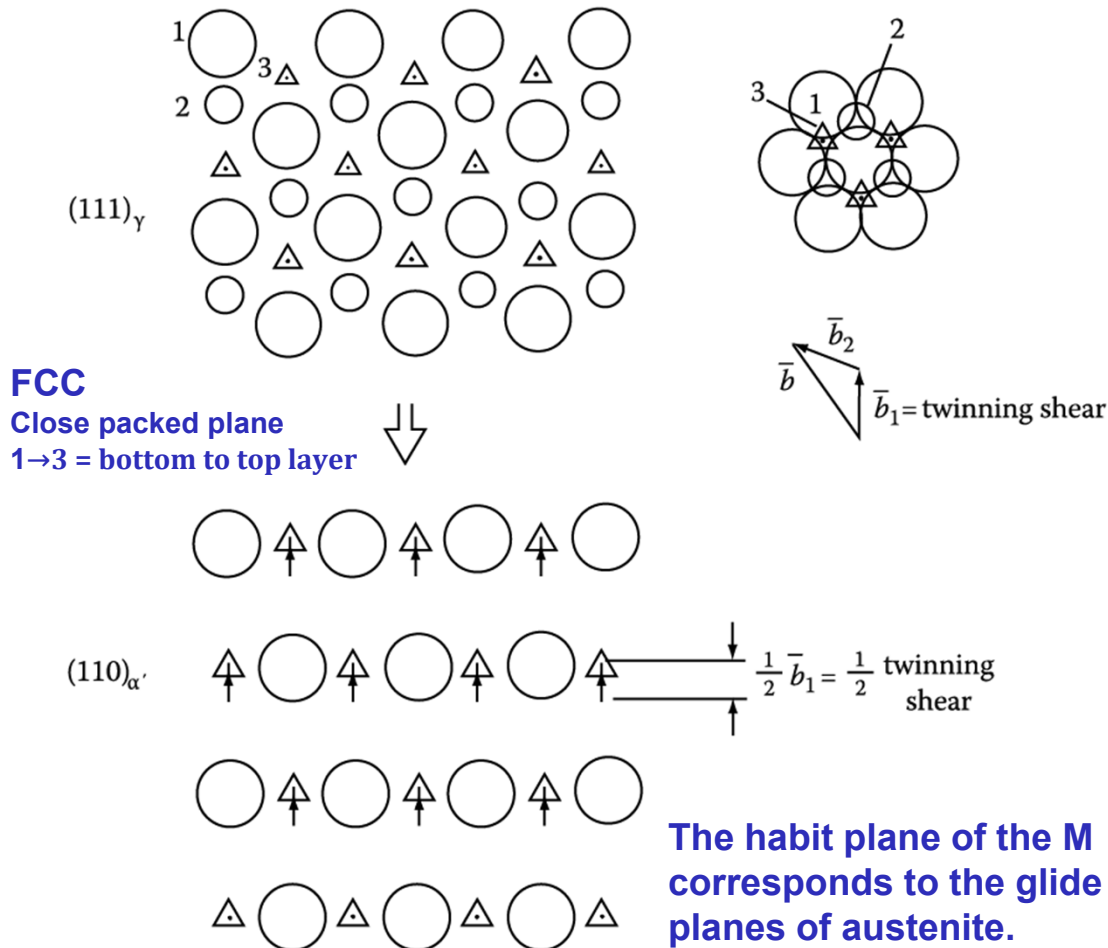
3) $\gamma = 20 \text{ mJm}^{-2}$ (fully coherent nucleus)

→ **$c^*/a^* \sim 1/40$, $\Delta G^* \sim 20 \text{ eV}$: too high for thermal fluctuation alone to overcome (at 700 K, $kT = 0.06 \text{ eV}$)**

→ **“M nucleation = heterogeneous process” : possibly in dislocation**

6.3.2 Role of Dislocations in Martensite Nucleation : based on atomic shuffles within the dislocation core

- 1) Zener: demonstrated how the **movement of $\langle 112 \rangle_\gamma$ partial dislocations** during twinning could **generate in thin bcc region of lattice from an fcc one.**



$$\bar{b} = \bar{b}_1 + \bar{b}_2$$

$$\frac{a}{2} [\bar{1}110] = \frac{a}{6} [\bar{2}11] + \frac{a}{6} [\bar{1}2\bar{1}]$$

In order to generate the bcc structure it requires that all the 'triangular' (Level 3) atoms jumps forward by

$$\frac{1}{2} \bar{b}_1 = \frac{a}{12} [\bar{2}11]$$

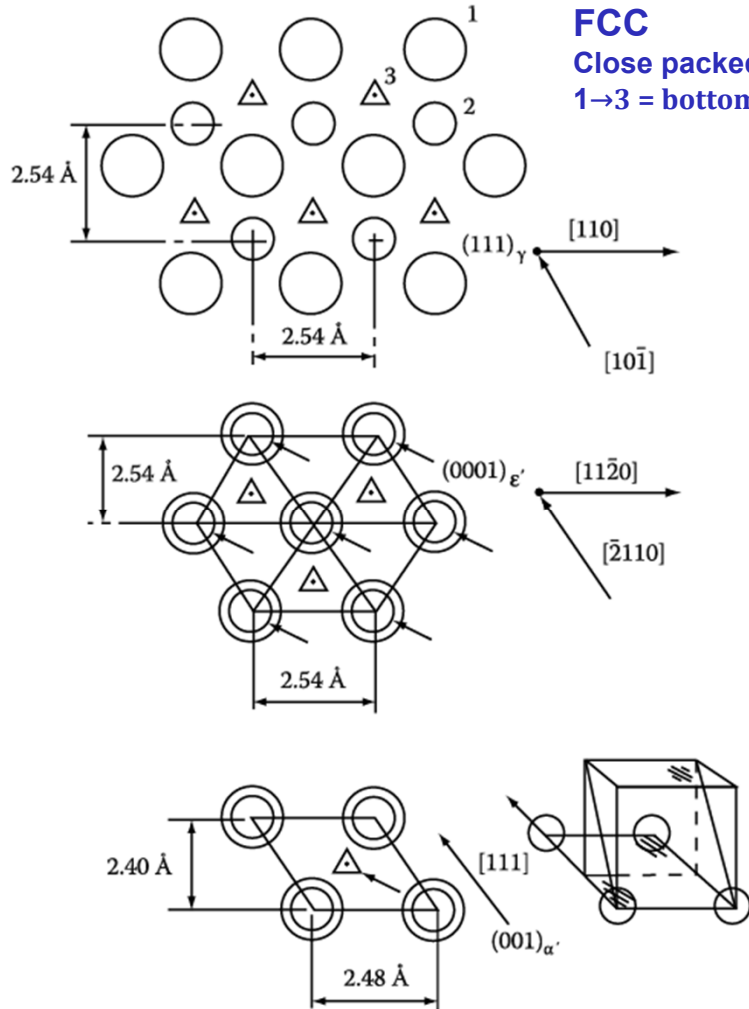
In fact, the lattice produced is only two atom layer thickness and not quite the bcc one after this shear, but requires an additional dilatation to bring about the correct lattice spacings.

Figure. 6.15 Zener's model of the generation of two-atom-thick martensite by a half-twinning shear

Region with dislocation pile-ups
→ possible to form **thicker M nuclei**

6.3.2 Role of Dislocations in Martensite Nucleation

- 2) Venables: M transformation induced by **half-twinning shear in fcc mater.**
 a. in the case of **alloys of low stacking fault energy** (e.g. steel, etc)



$$\gamma \text{ (fcc)} \rightarrow \epsilon' \text{ (hcp)} \rightarrow \alpha' \text{ (bcc)}$$

ε'-martensite structure thickens by inhomogenous half-twinning shears of $\frac{a}{12}[\bar{2}11]$ on every other {111}γ plane.

→ Indeed, α' regions have been observed to form in conjunction with M.

→ But, no direct evidence of the ε'→α' transition

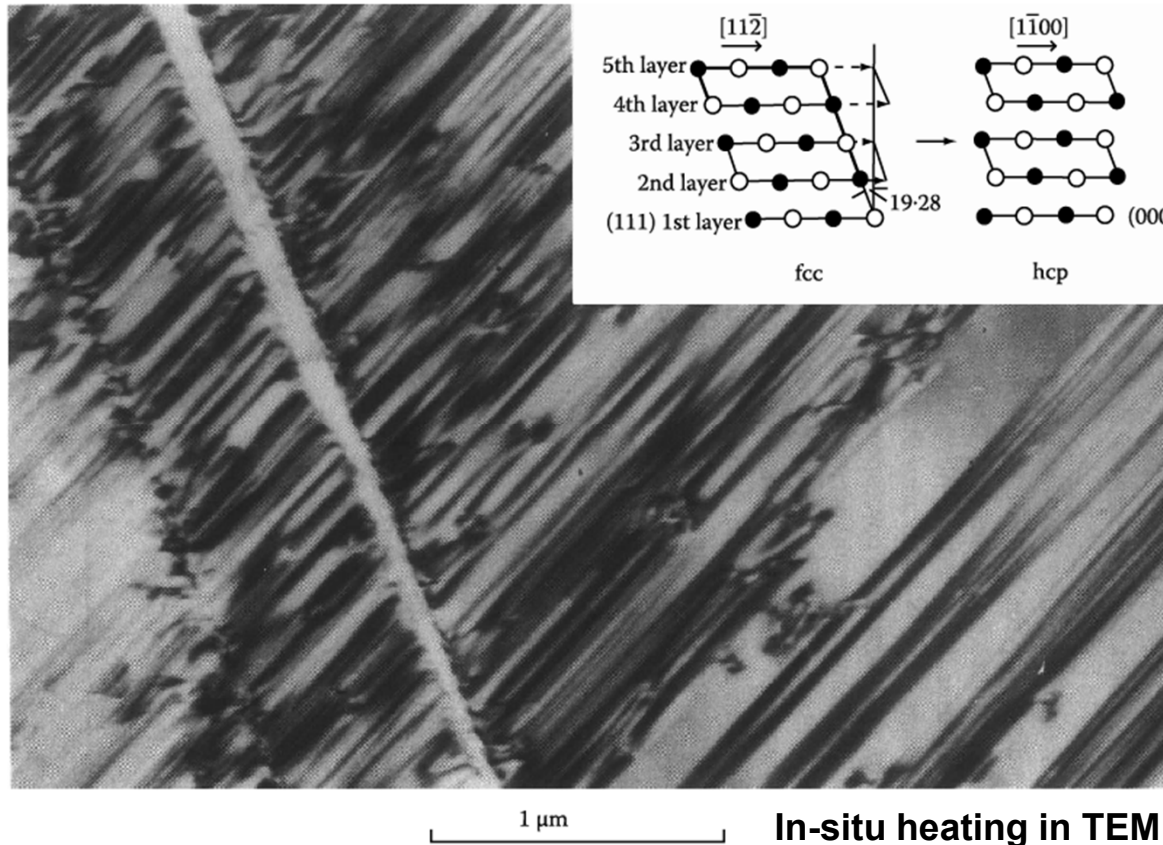
→ possible γ→ε' and γ→α' by different mechanism

Figure. 6.16 Venables's model for the γ→ε'→α'

6.3.2 Role of Dislocations in Martensite Nucleation

- 2) Venables: M transformation induced by **half-twinning shear in fcc mater.**
 b. M transformation of Co : i) **fcc** → **hcp** transformation at around 390 °C

habit plane $\{111\}_\gamma$ Orientation relationship $(111)_\gamma // (0001)_{\alpha'}$ → Generation of large number of

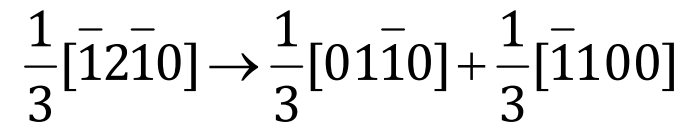


$\frac{a}{6} \langle 11\bar{2} \rangle_\gamma$ partial dislocations

on $\{111\}_\gamma$ plane → G.B. initiation
 of stacking fault

ii) **hcp** → **fcc** reaction at 430 °C

Dissociation of dislocation on the hcp basal plane:



The reaction has to occur on every other hcp plane in order to generate the fcc structure

Figure. 6.18 Dislocation-assisted M transformation in cobalt. The insert illustrates the way stacking fault formation induces the fcc → hcp transformation.

6.3.2 Role of Dislocations in Martensite Nucleation

- **It is thus seen that some types of M can form directly by the systematic generation and movement of extended dislocations.**
→ M_s temperature : a transition from positive to negative SFE
- **However, 1) this transition type cannot occur in ① high SFE nor in ② thermoelastic martensites → need to consider alternative way in which dislocations can nucleate martensite other than by changes at their cores.**

2) this transition is also difficult to understand ③ twinned martensite, merely on the basis of dislocation core changes.

6.3.3 Dislocation strain energy assisted transformation : help of the elastic strain field of a dislocation for M nucleation

- Assumption: coherent nuclei are generated by a pure Bain strain, as in the classical theories of nucleation

The strain field associated with a dislocation can in certain cases provide a favorable interaction with the strain field of the martensite nucleus, such that one of the components of the Bain strain is neutralized thereby reducing the total energy of nucleation.

→ the dilatation associated with the extra half plane of the dislocation contributes to the Bain strain.

→ Alternatively, the shear component of the dislocation could be utilized for M transformation.

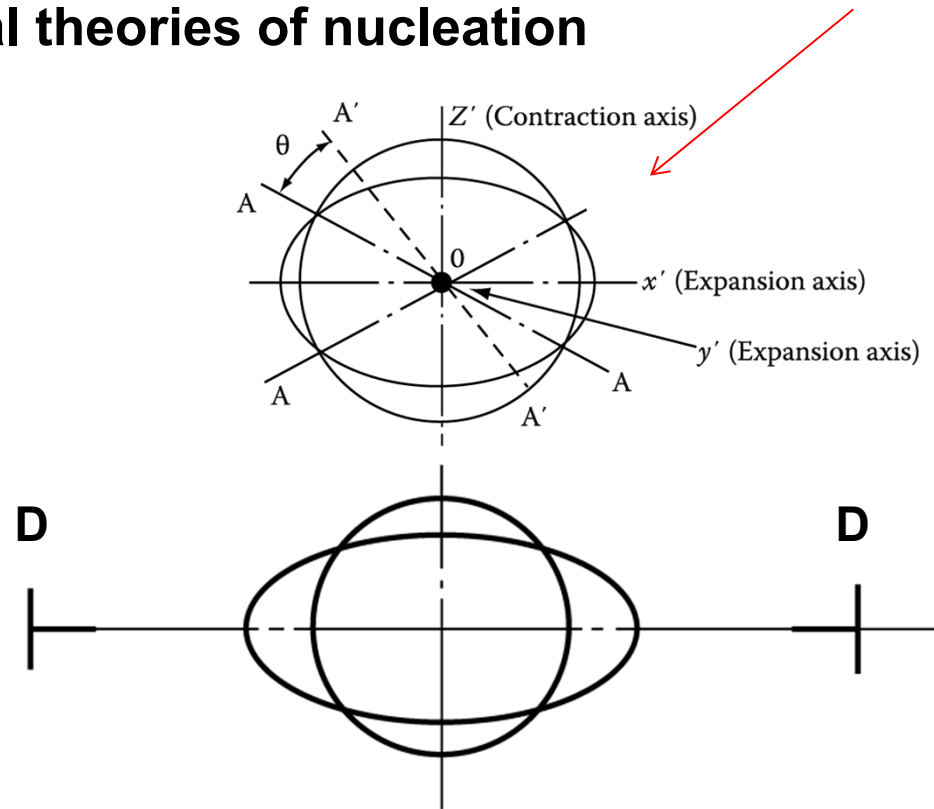


Figure. 6.19 Illustrating how one of the strain components of the Bain deformation may be compensated for by the strain field of a dislocation which in this case is tending to push atom planes together.

6.3.3 Dislocation strain energy assisted transformation : help of the elastic strain field of a dislocation for M nucleation

$$\Delta G = A\gamma + V\Delta G_s - V\Delta G_v - \Delta G_d$$

Creation of nucleus ~ destruction of a defect ($-\Delta G_d$)

→ Dislocation interaction energy which reduces the nucleation energy barrier

$$\Delta G_d = 2\mu s\pi \cdot ac \cdot \bar{b}$$

where \bar{b} = Burgers vector of the dislocation,
s = shear strain of the nucleus

$$\Delta G = 2\pi a^2 \gamma + \frac{16\pi}{3} (s/2)^2 \mu ac^2 - \frac{4\pi}{3} a^2 c \cdot \Delta G_v - 2\mu s\pi ac \cdot \bar{b} \quad \text{Eq. (6.16)}$$

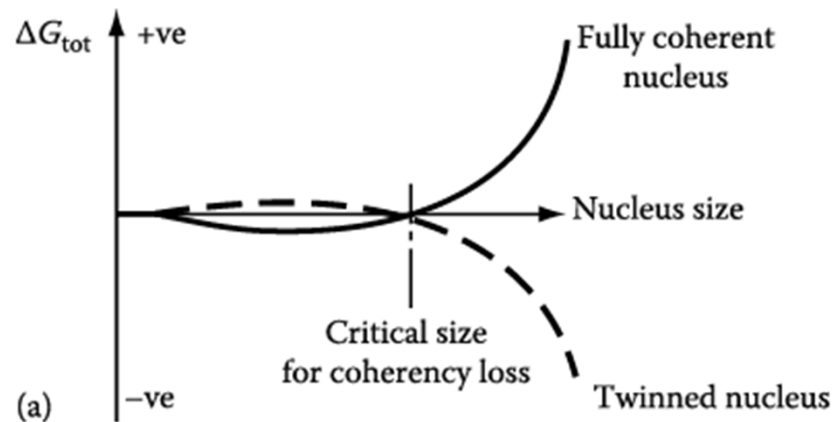


Figure. 6.20 (a) schematic diagram based on Eq. 6.16, illustrating the need for the nucleus to twin if it is to grow beyond a certain critical size.

→ Total energy of martensite nucleus:
as a function of 1) diameter and thickness (a, c)
(whether it is twinned or not (this affect "s"))
2) Degree of assistance from the strain field of a
dislocation (or group of dislocations)

e.g. A fully coherent nucleus from partial interaction
with the strain field of a dislocation ~ 20 nm dia.
& 2-3 atoms in thickness → further growth need
to twin and slip formation

6.3.3 Dislocation strain energy assisted transformation

: help of the elastic strain field of a dislocation for M nucleation

Burst phenomenon

: autocatalytic process of rapid, successive M plate formation occurs over a small temperature range , e.g. Fe-Ni alloys

(Large elastic stresses set up ahead of a growing M plate → Elastic strain field of the M plate act as the interaction term of elastic strain field of dislocation in Eq. (6.16) → reduces the M nucleation energy barrier)

In summary,

- we have not dealt with all the theories of martensite nucleation in this section as recorded in the literature, or even with all alloys exhibiting martensitic transformations.
- Instead we have attempted to illustrate some of the difficulties associated with explaining a complex event which occurs at such great speeds as to exclude experimental observation.
- A general, all embracing theory of martensite nucleation has still evaded us, and may not even be feasible.

6.4 Martensite Growth

- Once the nucleation barrier has been **overcome**, the chemical volume free energy term (ΔG_v) so large that **the martensite plate grows rapidly until it hits a barrier such as another plate or a high angle grain boundary.**
 - High speed of M growth → interface btw austenite and M must be a **glissile semi-coherent boundary** consisting of a set of parallel dislocations or twins with Burgers vector common to both phases, i.e. transformation dislocations → dislocation motion brings about required **lattice invariant shear transformation** (may or may not generate an irrational habit plane)
 - **Increased alloying lowers the Ms temperature** and that it is the temp. of transformation that dictates the **mode of lattice invariant shear.**
 - **Slip-twinning transition in a crystal at low temperatures:** increased difficulty of nucleating whole dislocations needed for slip, but not so temp dependence (as the Peierls stress for a perfect dislocation) of critical stress needed for the nucleation of a partial twinning dislocation & chemical energy for transformation ~ independent of M_s temp.
 - **when Ms temperature is lowered, the mechanism of M transformation chosen is governed ① by the growth process having least energy.**
- Other factor affecting mode of growth = ② how the nucleus forms**

* Two main cases of rational (lath) and irrational (plate) M growth in steel

6.4.1 Growth of Lath Martensite



- Morphology of a lath with dimensions $a > b \gg c$ growing on a $\{111\}_\gamma$ plane → thickening mechanism involving the nucleation and glide of transformation dislocations moving on discrete ledges behind the growing front, e.g. NiTi M and steel M

- Due to the large misfit between the bct and fcc lattices dislocations could be self-nucleated at the lath interface. → the stress at the interface exceeds the theoretical strength of the material.

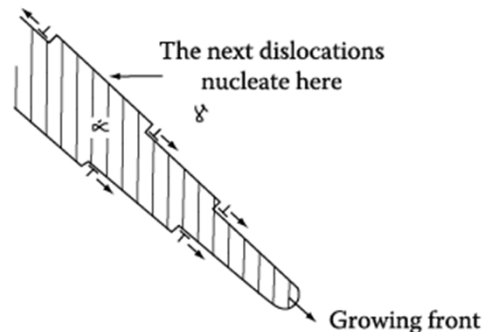
- Eshelby's approach: for thin ellipsoidal plate ($a \gg c$)

Maximum shear stress at the interface btw M and γ due to shear transformation

$$\sigma \cong 2\mu s c / a \quad \mu = \text{shear modulus of } \gamma$$

~Sensitive to ① particle shape and ② angle of shear (s)

: Of course in practice it is very difficult to define the morphology of M in such simple c/a terms, but this gives us at least a qualitative idea of what may be involved in the growth kinetics of M.



(b)

Figure. 6.20 (b) Lattice image of the tip of a martensite plate in a Ti-Ni alloy. The first interfacial dislocation behind the growing front is indicated.

6.4.1 Growth of Lath Martensite

- **Lath M growth by shear loop nucleation** ($\because \sigma/\mu > \text{threshold stress}$) :
by nucleating dislocations at the highly strained interface of the laths, the misfit energy reduced and the lath M can continue to grow into γ

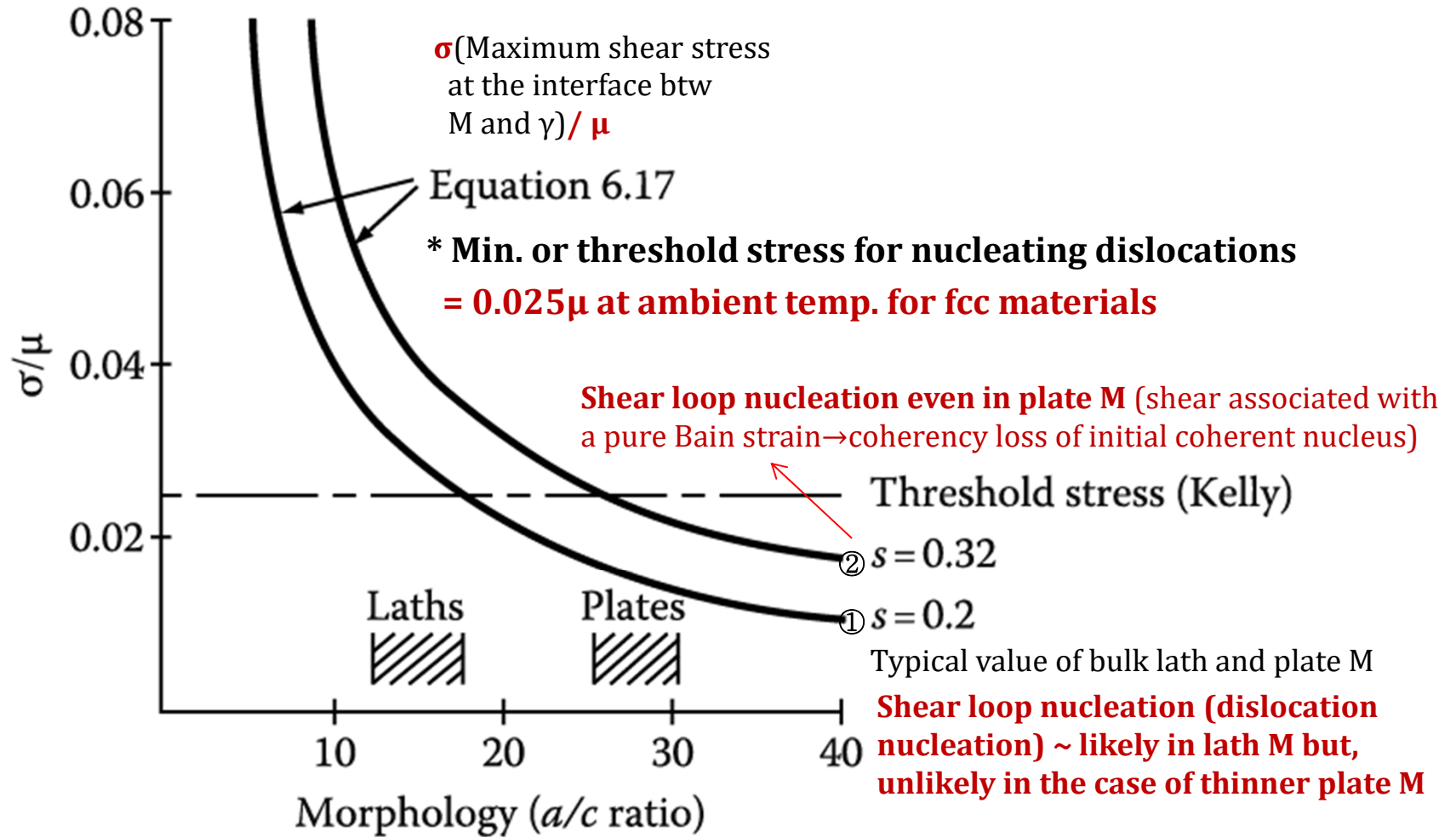
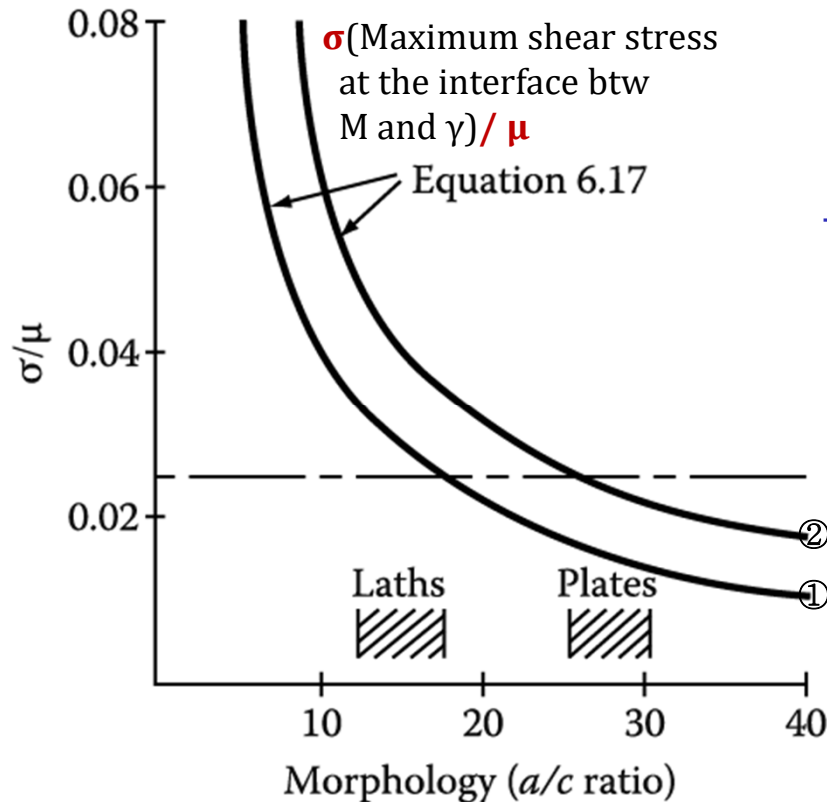


Figure. 6.21 Eq. 6.17 plotted for two values of shear corresponding to a pure Bain deformation ($s=0.32$) and a twinned plate ($s=0.2$)

6.4.1 Growth of Lath Martensite

- **Lath M growth by shear loop nucleation** ($\because \sigma/\mu > \text{threshold stress}$) :
by nucleating dislocations at the highly strained interface of the laths, the misfit energy reduced and the lath M can continue to grow into γ



- By internal friction measurements,

Density of carbon in lath M : cell walls > within cell
suggesting that **limited diffusion of carbon** takes place following or during the transformation

- **M transformation (at least at higher Ms like lath M)** → produce adiabatic heating which may affect ① diffusion of carbon and ② dislocation recovery (by dislocation climb and cell formation). ~ **a certain relationship between lower bainite and M**

Threshold stress (Kelly)

- ② $s = 0.32$ Shear loop nucleation lath M and plate M
- ① $s = 0.2$ Shear loop nucleation in lath M

- **High growth speed of lath M**

→ **interface of predominantly screw dislocation**

- **Volume of retained γ ~relatively small in lath M**

(important to the mechanical properties of low-carbon steel)

due to sideways growth of screw dislocation not too difficult

* **Figure. 6.21** Eq. 6.17 plotted for two values of shear corresponding to a pure Bain deformation ($s=0.32$) and a twinned plate ($s=0.2$)

6.4.2 Plate Martensite

- In medium and high carbon steels, or high nickel
Morphology: Lath M → Plate M (lower M_s temp. and more retained γ)
much thinner than lath M or bainite

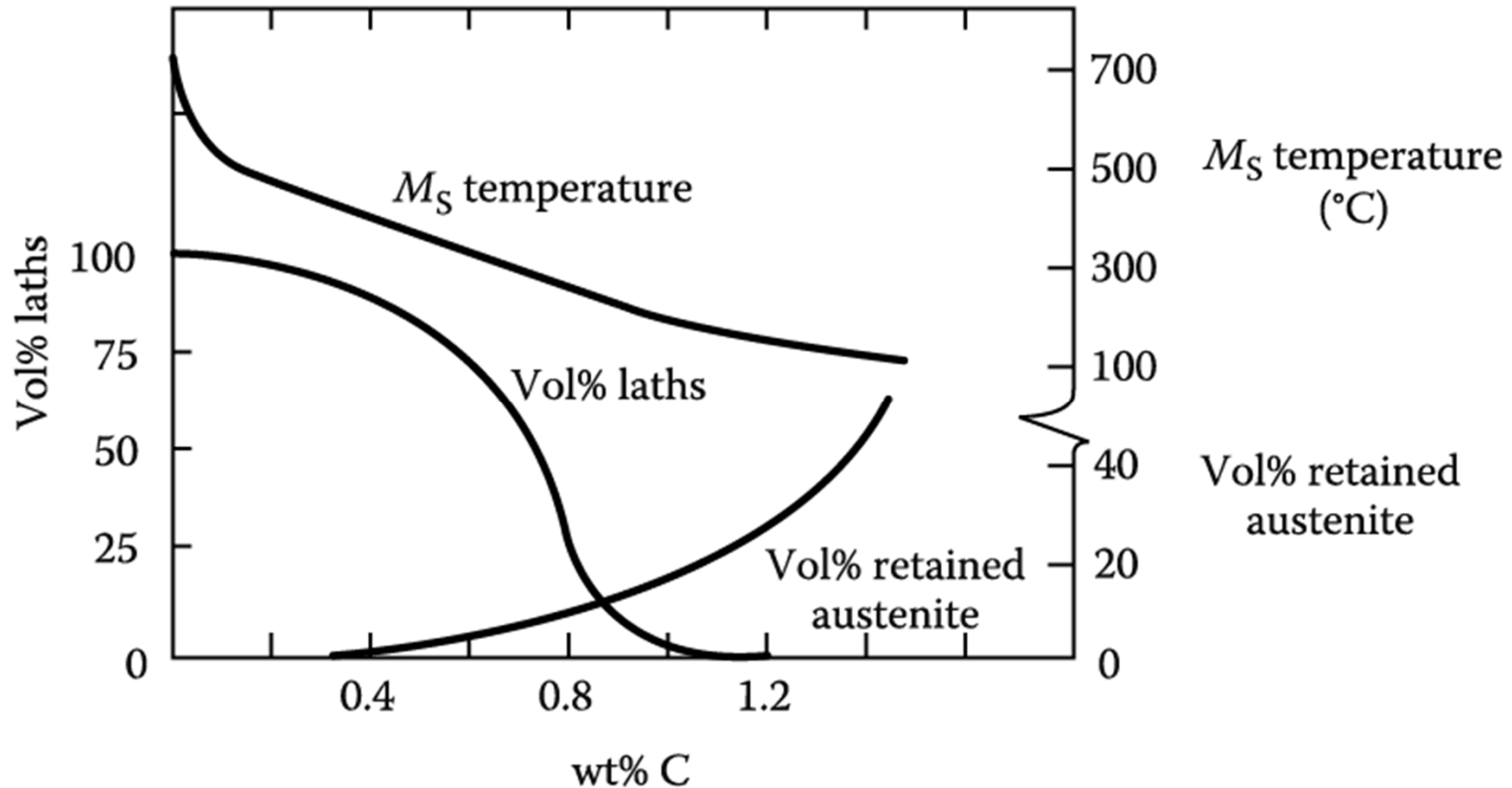


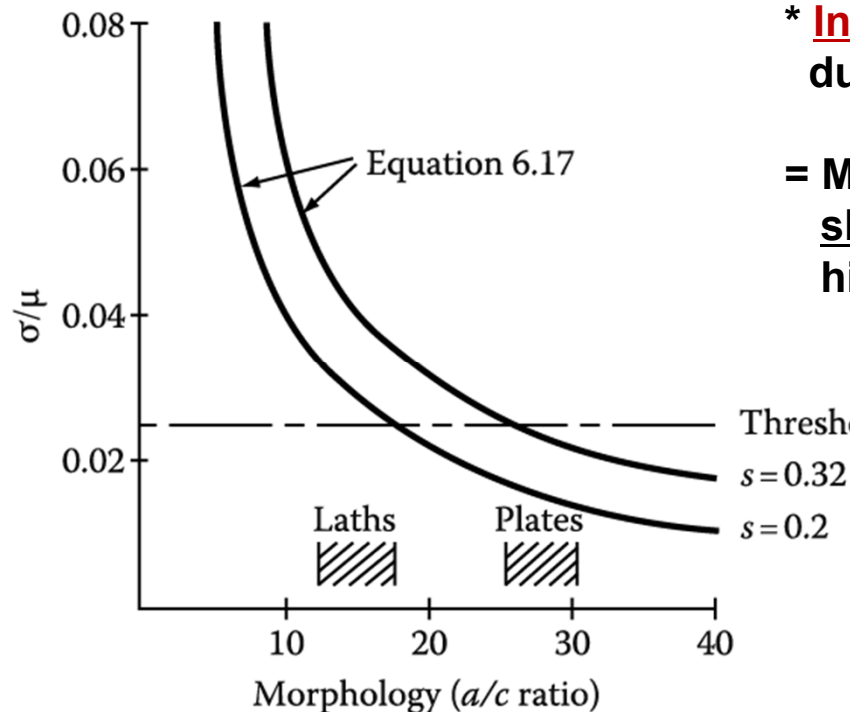
Figure. 6.22 Approximate relative percentages of lath martensite and retained austenite as function of carbon content in steels.

6.4.2 Plate Martensite

- In medium and high carbon steels, or high nickel
Morphology: Lath M \rightarrow Plate M (lower M_s temp. and more retained γ)
much thinner than lath M or bainite
- Transition from plates from growing on $\{225\}_\gamma$ planes to $\{259\}_\gamma$ planes with increasing alloy contents

In lower carbon or nickel, $\{225\}_\gamma$ M = plates with a central twinned 'midrib', the outer (dislocation) regions of the plate being free of twins

In high carbon and nickel, $\{259\}_\gamma$ M = completely twined & less scattered habit plane



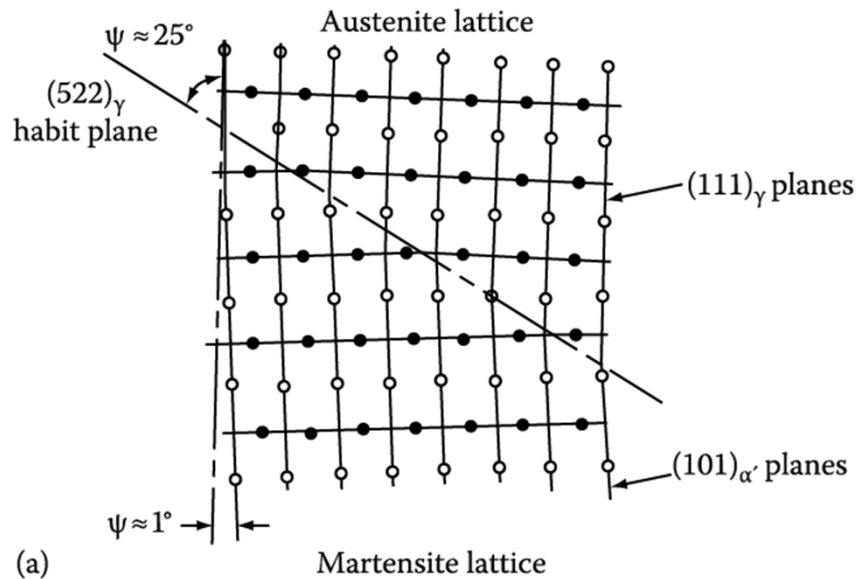
* In Midrib M, transition from twinning \rightarrow dislocations due to a change in growth rate after the midrib forms

= M formed at higher temp. or slower rates grows by a slip mechanism, while M formed at lower temp and higher growth rates grows by a twinning mode.

- 1) $s=2$, problem in nucleating whole dislocations in the case of growing plate M, but **partial twining dislocations evidently can nucleate**.
 \rightarrow Once nucleated, twinned M grows extremely rapidly, but the mechanism is unclear.

6.4.2 Plate Martensite

* Dislocation generated $\{225\}_\gamma$ M (Frank)



Close-packed plane

: slight misfit along the $[01\bar{1}]_\gamma$ & $[11\bar{1}]_{\alpha'}$

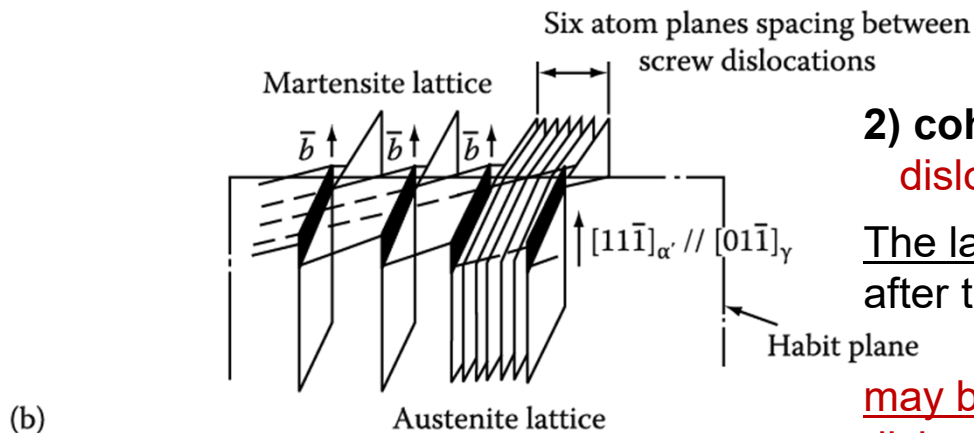
= M lattice parameter is ~2% less than that of γ

→ Insertion of an array of screw dislocations

with a spacing of six atom planes in the interface

* In terms of the min. shear stress criterion (Fig. 6.21), when the midrib reaches some critical a/c ratio further expansion and thickening of a $\{225\}_\gamma$ twinned midrib by a Frank dislocation interface could occur.

→ “No detailed explanation”



2) coherent nucleus with $s=0.32$: possible for dislocation nucleation to occur to relieve coherency.

The larger amount of chemical free energy, available after the critical size for growth has been exceeded,

may be sufficient to homogeneously nucleate dislocations particularly in the presence of the large strain energy of the rapidly growing plate.

Figure. 6.23 Model for the $\{225\}_\gamma$ habit austenite-martensite interface in steel.

- * Other factors for affecting the growth of M: ③ phenomenon of stabilization, ④ external stresses, and ⑤ grain size

6.4.3 Stabilization

- * In intermittent cooling between M_s and M_f , transformation does not immediately continue, and the total amount of transformed M is less than obtained by continuous cooling throughout the transformation range.

6.4.4 Effect of External Stresses

$$\Delta G = -V\Delta G_v + A\gamma + V\Delta G_s - ES$$

- * In view of the dependence of M growth on dislocation nucleation, it is expected that an externally applied stress (ES) will aid the generation of dislocations and hence the growth of M.

- a) ES lowers the nucleation barrier for coherency loss of second phase precipitates.
 - b) ES aid M nucleation if the ① external elastic strain components contribute to the Bain strain.
→ Ms temperature can be raised. But, if plastic deformation occurs, there is an upper limiting value of M_s defined as “the M_d temperature”.
 - c) ② Under hydrostatic compression, M_s temperature can be suppressed to lower temp.
($P \uparrow \rightarrow$ stabilizes the phase with the smaller atomic volume (close-packed austenite) \rightarrow lowering the driving force ΔG_v for the transformation to M)
 - d) ③ large magnetic field can raise the M_s temperature on the grounds that it favors the formation of the ferromagnetic phase.
 - e) Plastic deformation of samples can aid both nucleation and growth of M, but too much plastic deformation may in some cases suppress the transformation (nucleation \uparrow & nuclei growth \downarrow).
- * **Ausforming process** : plastically deforming the austenite prior to transformation \rightarrow number of nucleation sites and hence refining M plate size \rightarrow High strength (fine M plate size + solution hardening (due to carbon) and dislocation hardening)

- * Other factors for affecting the growth of M: ③ phenomenon of stabilization, ④ external stresses, and ⑤ grain size

6.4.5 Role of Grain Size

- * Martensite growth ~ maintaining a certain coherency with the surrounding austenite
 - high-angle grain boundary is an effective barrier to plate growth.
 - While grain size does not affect the number of M nuclei in a given volume, the **1) final M plate size** is a function of the grain size.
- * **2) Degree of residual stress** after transformation is completed.
 - In large grain sized materials: dilatation strain associated with the transformation
 - Large residual stresses to built up btw adjacent grains
 - **GB rupture (quench cracking)** and substantially increase of dislocation density in M
 - In fine grain-sized metals: dilatation strain associated with the transformation
 - more self-accommodating & smaller M plate size
 - **stronger & tougher material**
- * In summary, **theories of M nucleation and growth are far from developed to a state where they can be used in any practical way** – such as helping to control the fine structure of the finished product. It does appear that **nucleation is closely associated with the presence of dislocations (dislocation density)** and the process of ausforming (deforming the austenite prior to transformation) could possibly be influenced by this feature if we know more of the mechanism of nucleation. However, **growth mechanisms, particularly by twining, are still far from clarified.**

6.5, 6.6 & 6.7 Skip

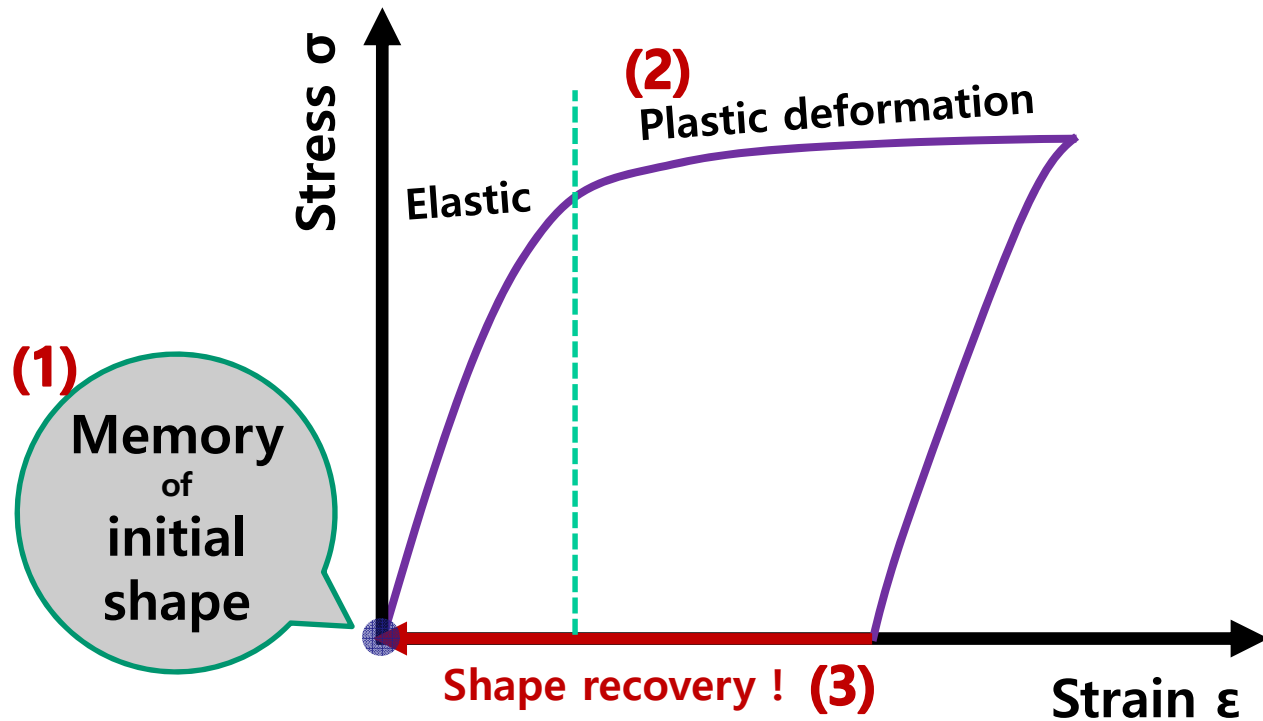
Representative Diffusionless Transformation

Martensitic transformation in Ni-Ti alloy ;
55~55.5 wt%Ni - 44.5~45 wt%Ti (“Nitinol”)

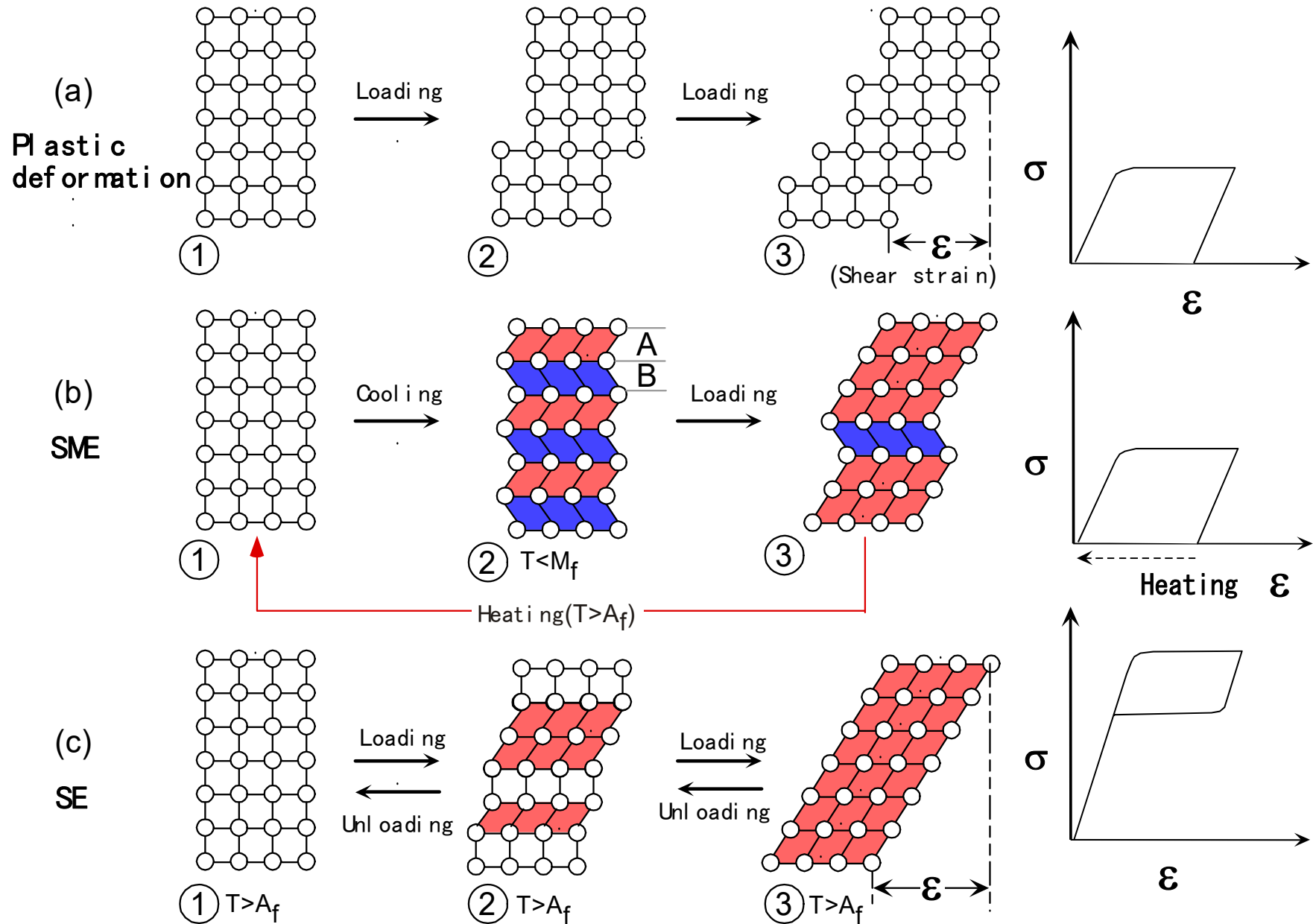


Ex) Shape memory alloy

Introduction - Shape-memory effect



	Elastic Deformation	Plastic Deformation	Transformation Deformation
Ceramics	○	×	×
Conventional Metals, Alloys & Plastics	○	○	×
Shape Memory Alloys	○	○	○
	<u>Recoverable</u> Small Deformation ↓ Elasticity	Permanent <u>Large Deformation</u> ↓ Plasticity	<u>Recoverable</u> Large Deformation ↓ Shape Memory Effect Superelasticity (Pseudoelasticity)



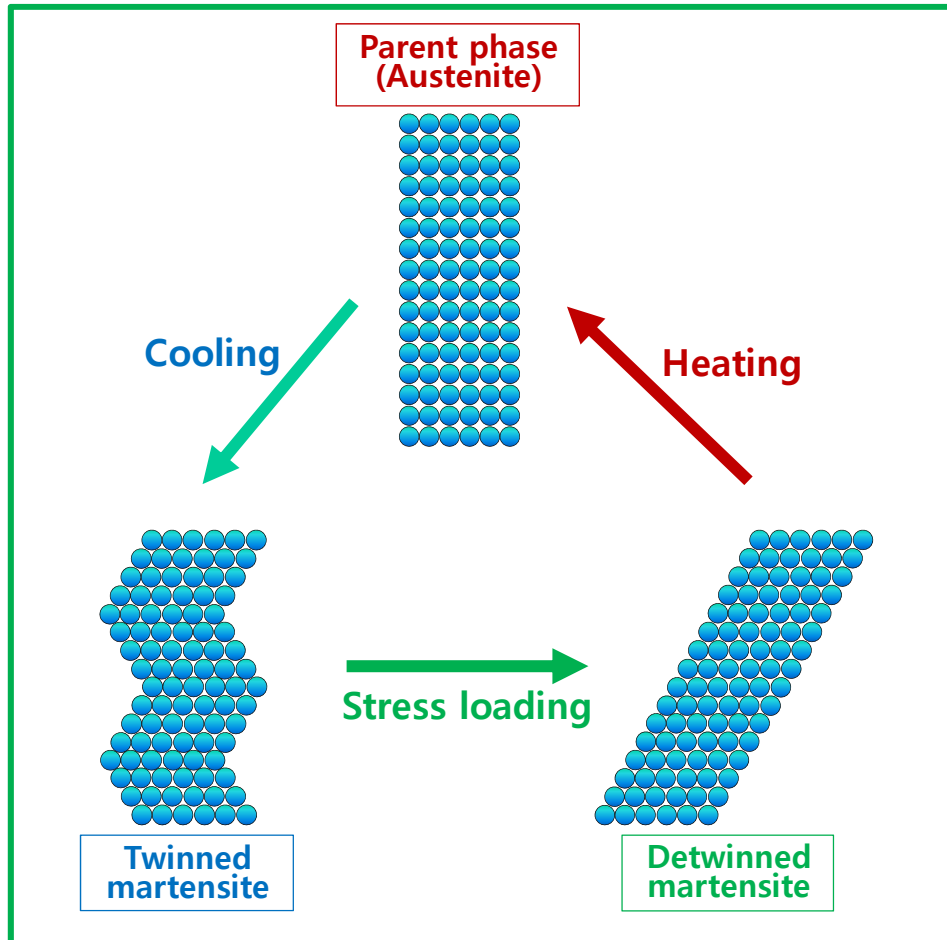
Principles

How can shape memory effect occur?

Principles

How can shape memory effect occur?

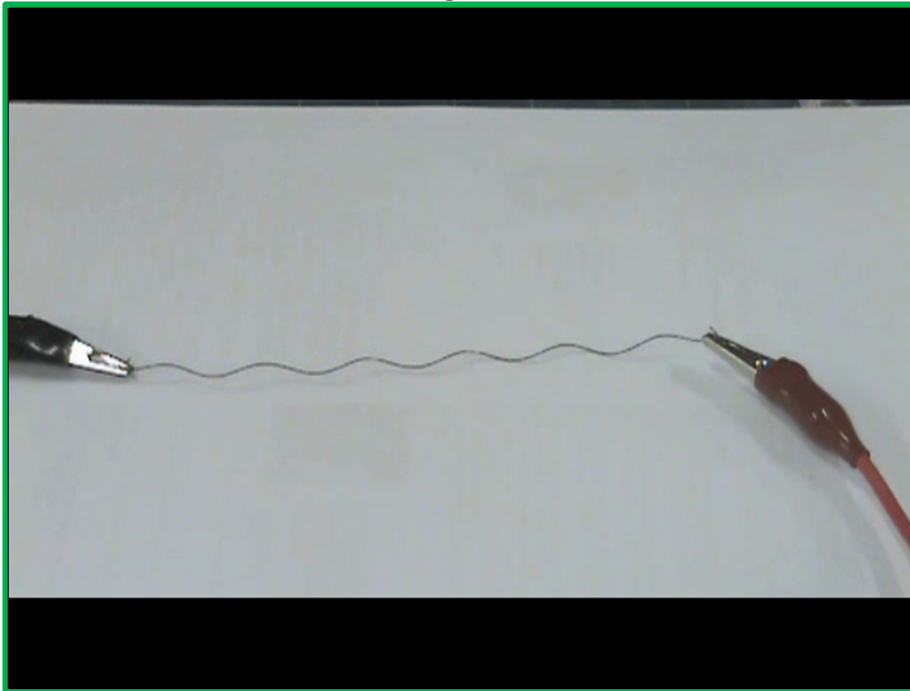
Principles- shape memory process



1. A_f 이상의 온도로 열처리를 통해 Austenite 상에서 형상 기억
2. M_s 이하의 온도로 냉각시 Twinned martensite 생성
3. 항복강도 이상의 응력을 가하면 Twin boundary의 이동에 의한 소성 변형
4. A_f 이상으로 가열해주면 martensite 에서 다시 Austenite로 변태
 → 기억된 형상으로 회복

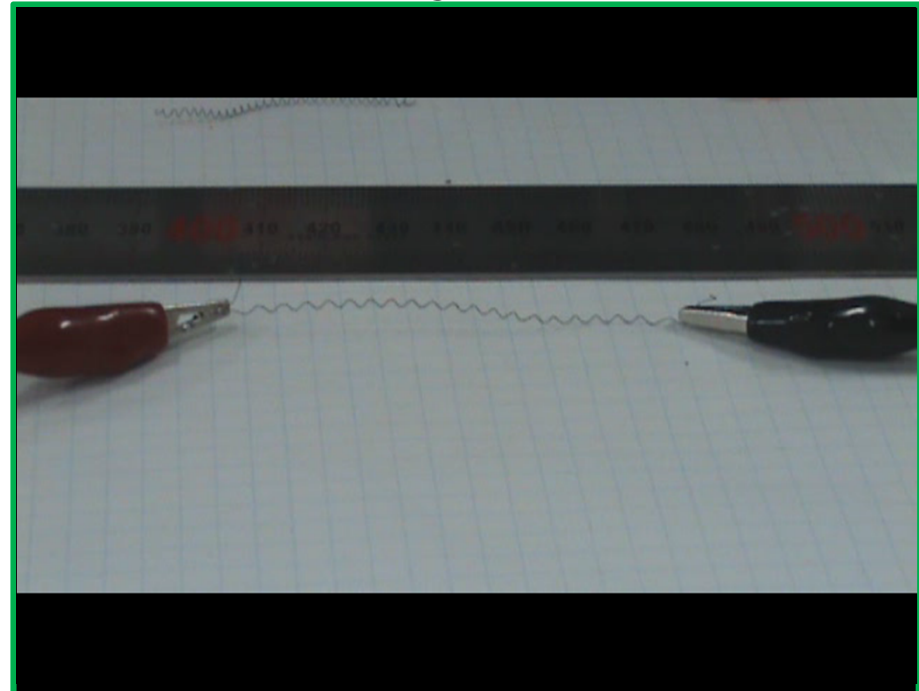
* One-way / Two-way shape memory effect

▼ One-way SME



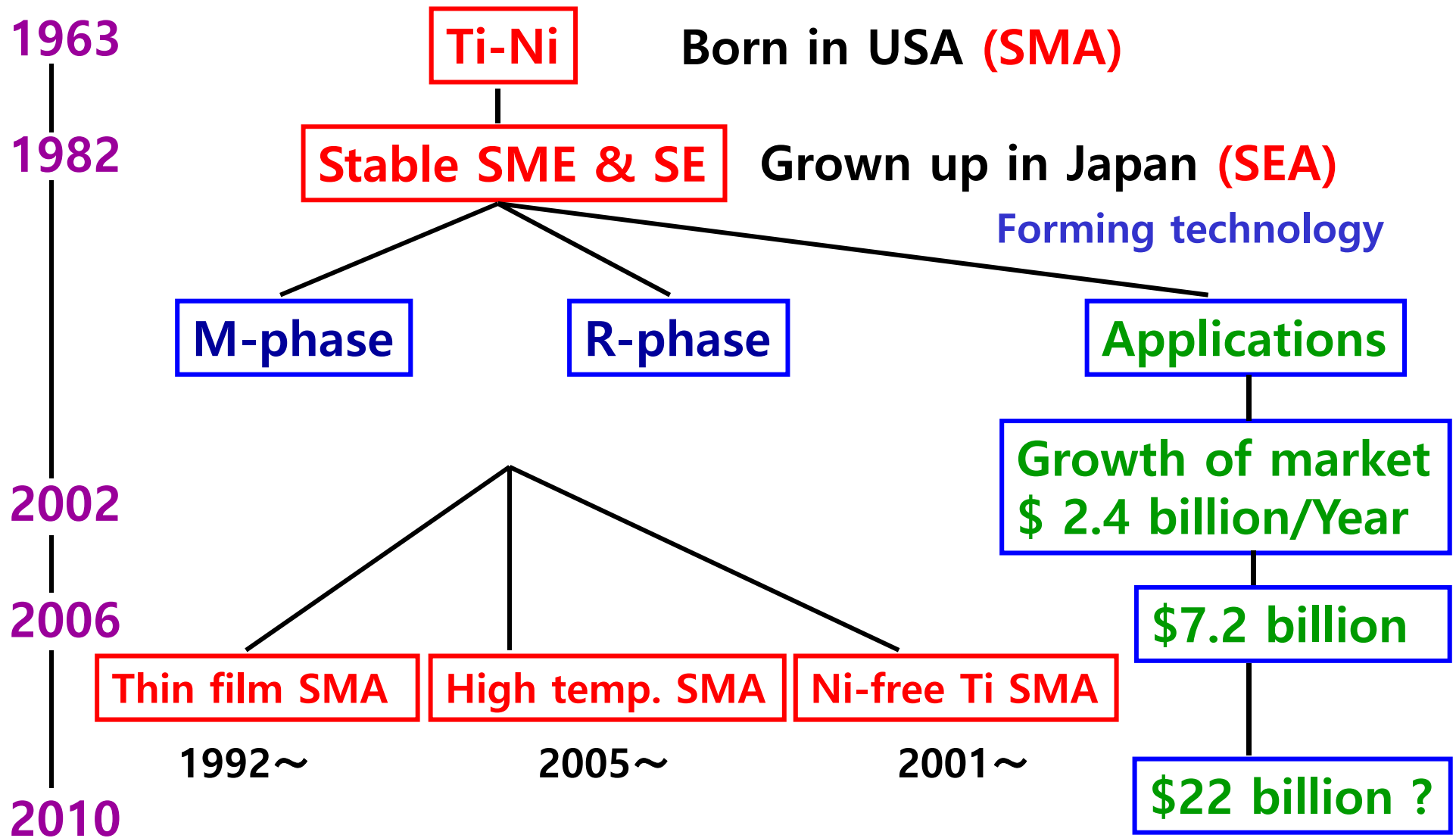
- ↳ A_f 이상의 고온 형상만을 기억
 - 저온($< M_f$)에서 소성변형 후 A_f 이상의 고온으로 가열
 - 기억된 고온 형상으로 회복

▼ Two-way SME



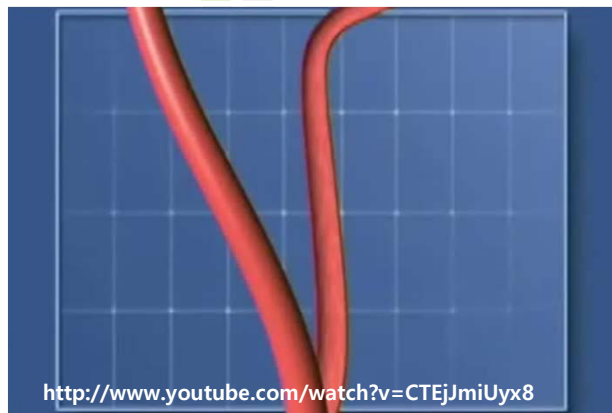
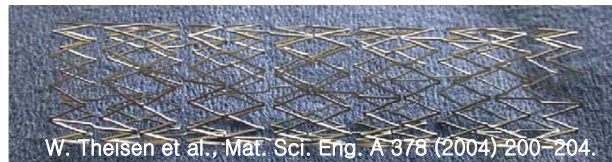
- ↳ 고온($> A_f$) 형상과 저온($< M_f$) 형상을 모두 기억
 - 반복적인 변형으로 인한 형상기억합금 내 전위 밀도의 상승 & 특정방향 응력장의 형성
 - 저온에서 반복소성변형 방향으로 회복

Summary



* Application of SMAs

▼ 산업 부문: 부품소재 (파이프 이음, 스위치소자나 온도제어용 장치 등)



▲ 생체의료 부문: 첨단의료재료
(stent, 치열교정용 강선 등)



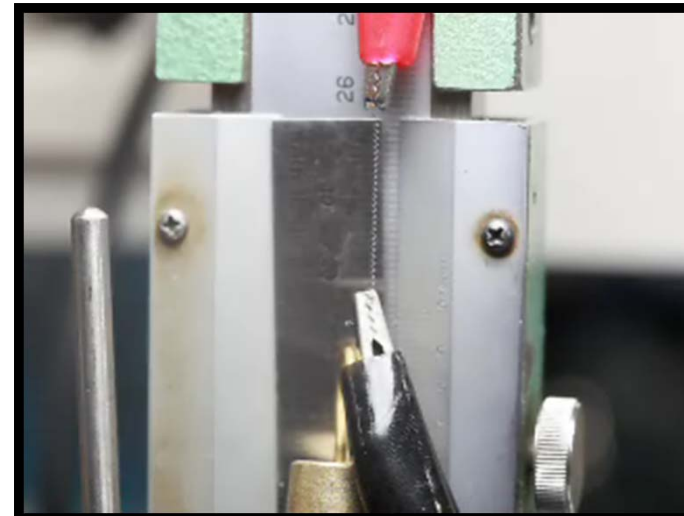
▲ 심해저/우주항공 부문: 극지재료
(잠수함, 태양전지판 등)

* SMA Actuator

▶ 액츄에이터(Actuator) : 전기 에너지, 열에너지 등의 에너지를 운동에너지로 전환하여 기계장치를 움직이도록 하는 구동소자

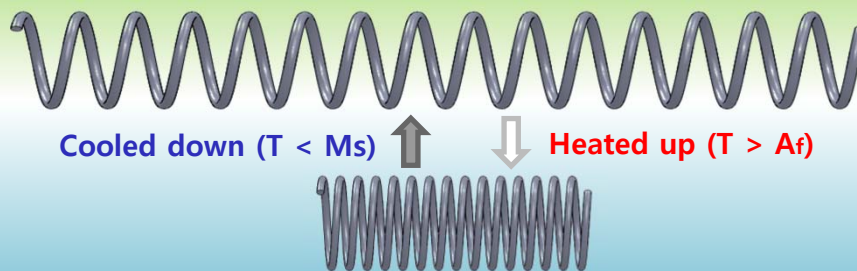


▲ 기존의 매크로 스케일 액츄에이터 (모터-기어 방식)



▲ SMA 스프링 액츄에이터

SMA Spring Actuator



재료의 수축과 신장을 통하여 기계적인 동작을 가능하게 함.

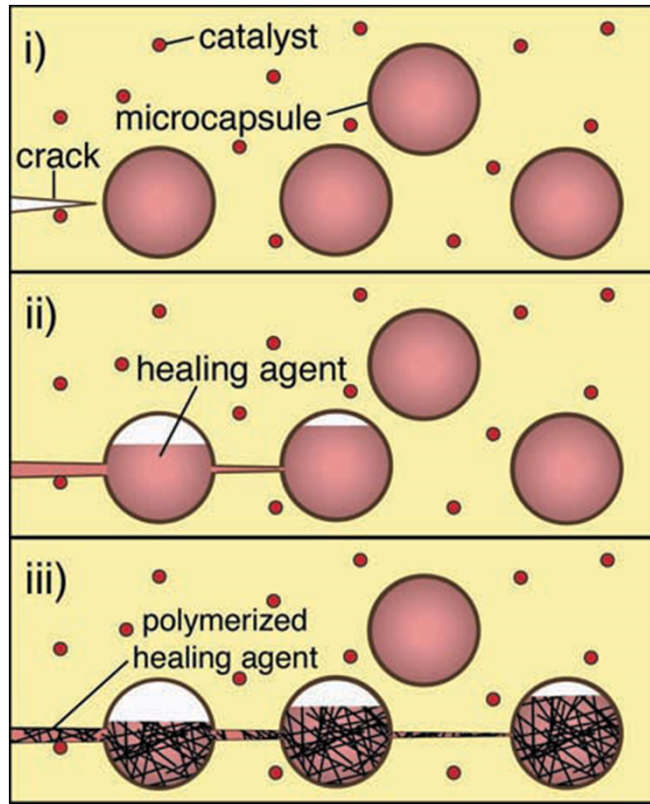
1. 단위 체적당 출력이 높음
2. 모터 구동에 비해 매우 단순한 구조
3. 온도에 의한 제어가 용이
4. 소형화가 쉬움.



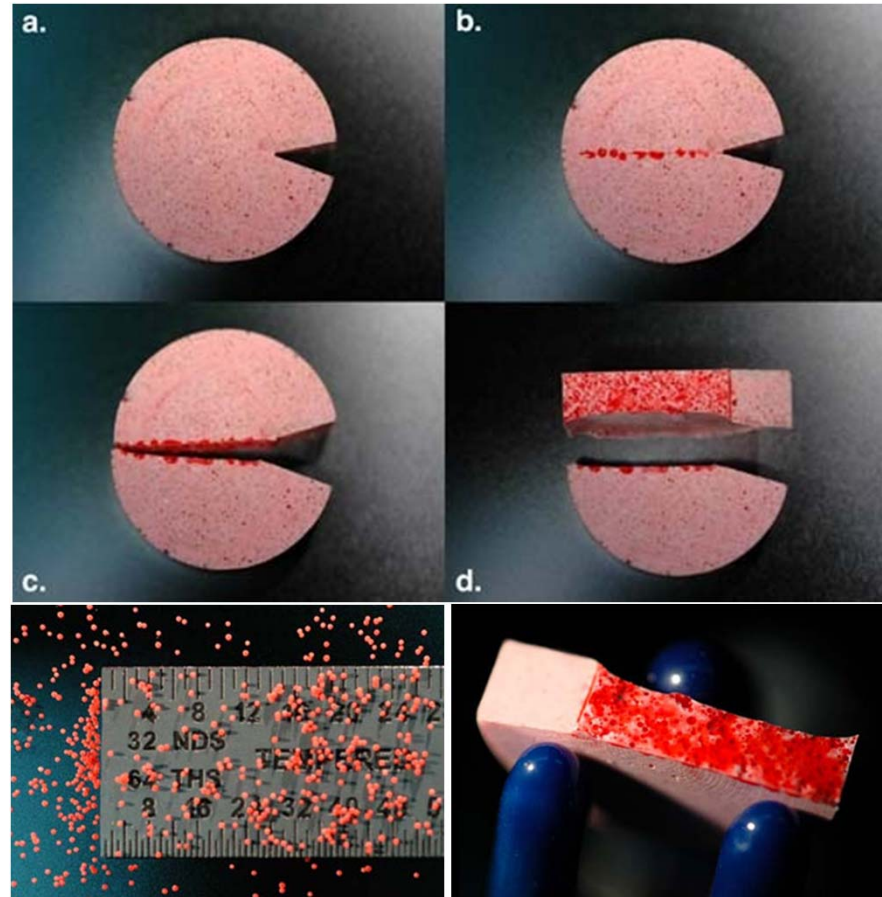
자가 치유가 가능한 금속

Self-healing Metallic Materials

Self-healing : Microencapsulation approaches

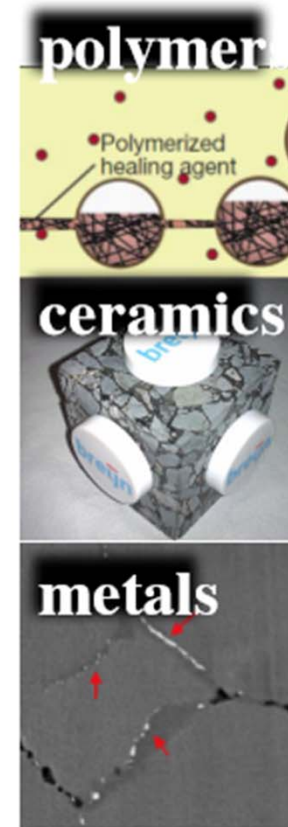
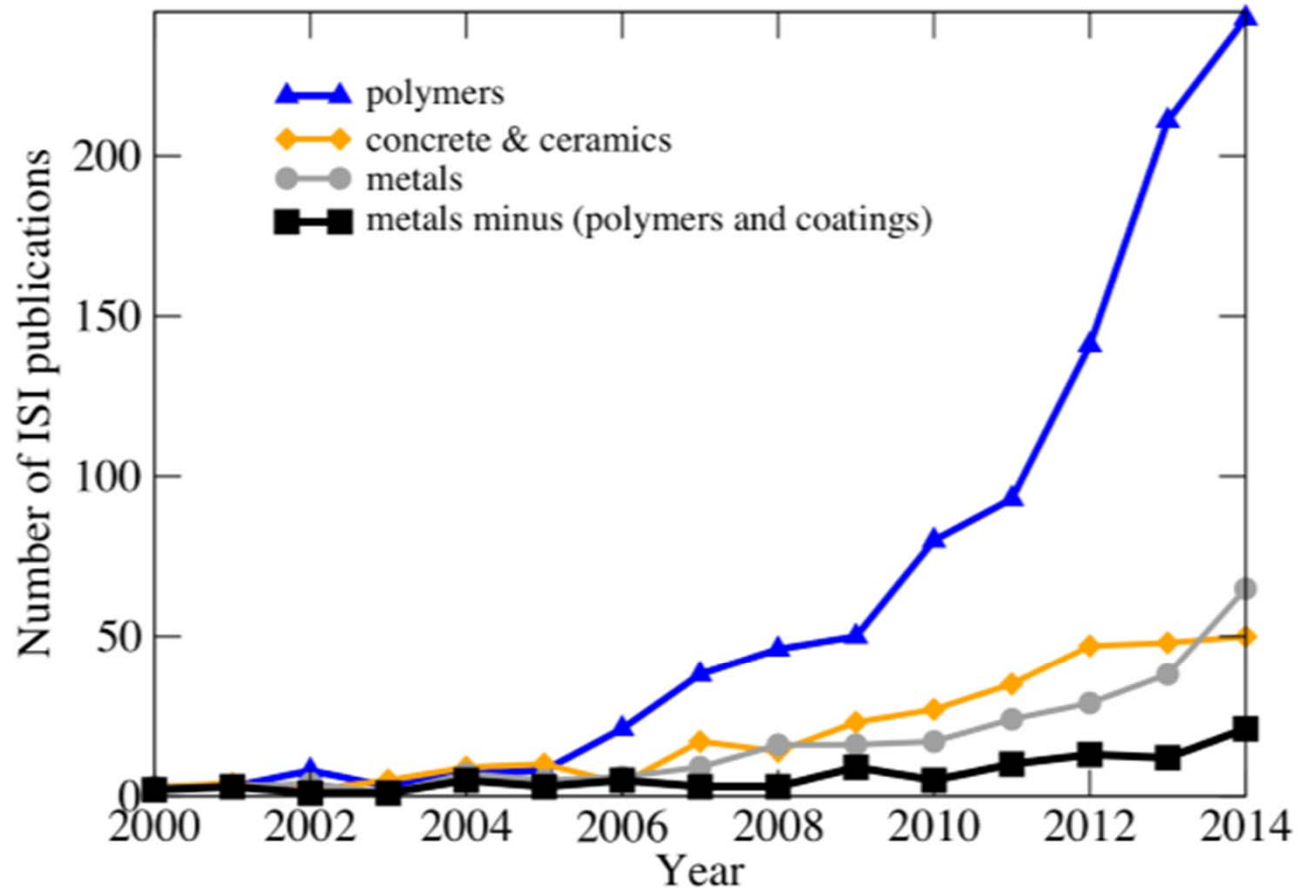


Healing agent + catalyst



• White et al, 409, Nature, 794-797, 2001

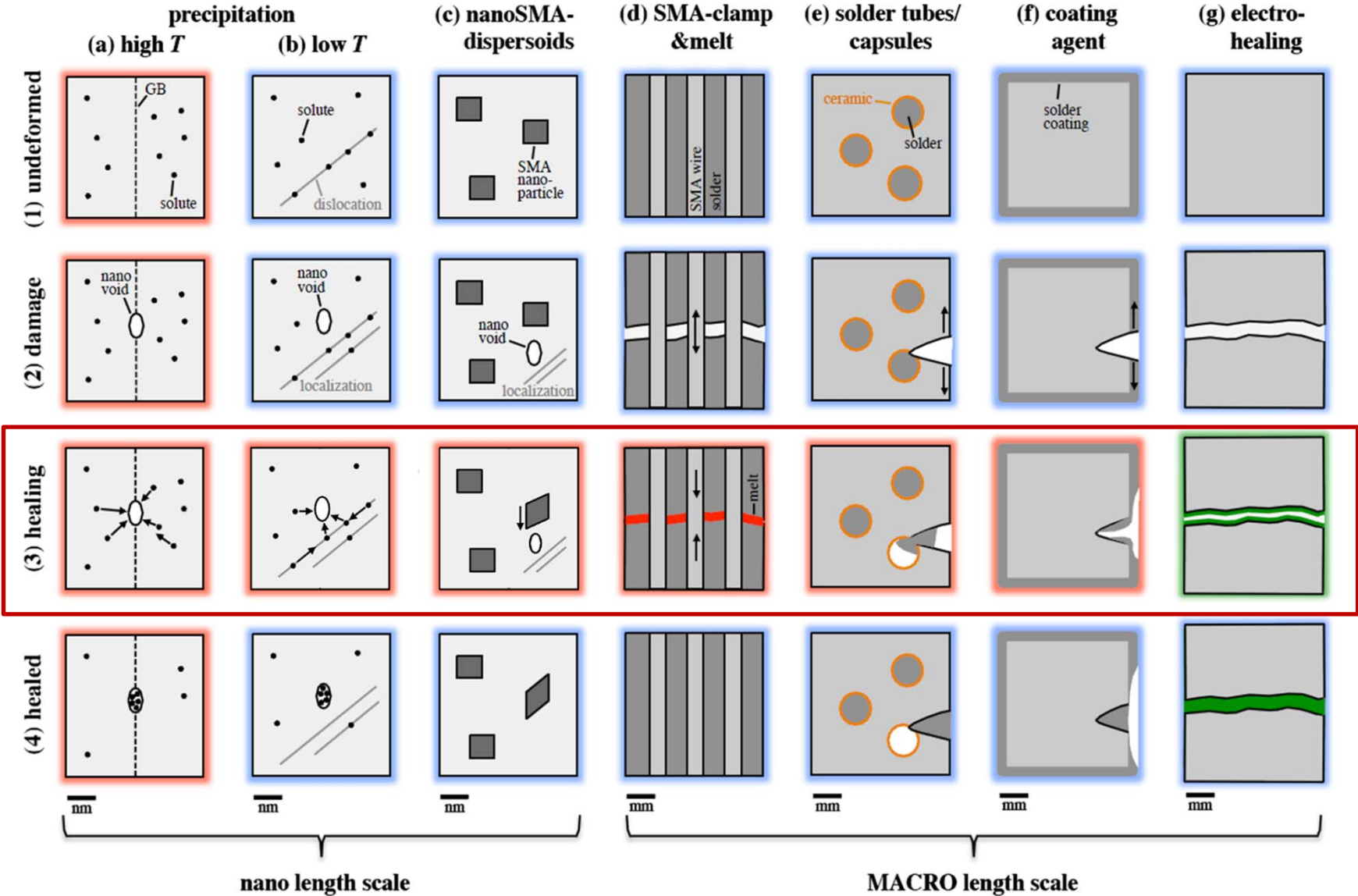
Self Healing



- Transformation kinetics in metals are slow at room temperature!

Self-healing metals

Grabowski & Tasan, *Self-healing Metals* (2016).





1) “Super-elastic Bulk Metallic Glass Composite”

**Self-healing Metallic Materials
with Recoverable 2nd phase**

Development of **New Ti-based BMGC** with High Work-hardenability

▶ Alloy system **Cu-Zr-Al system**

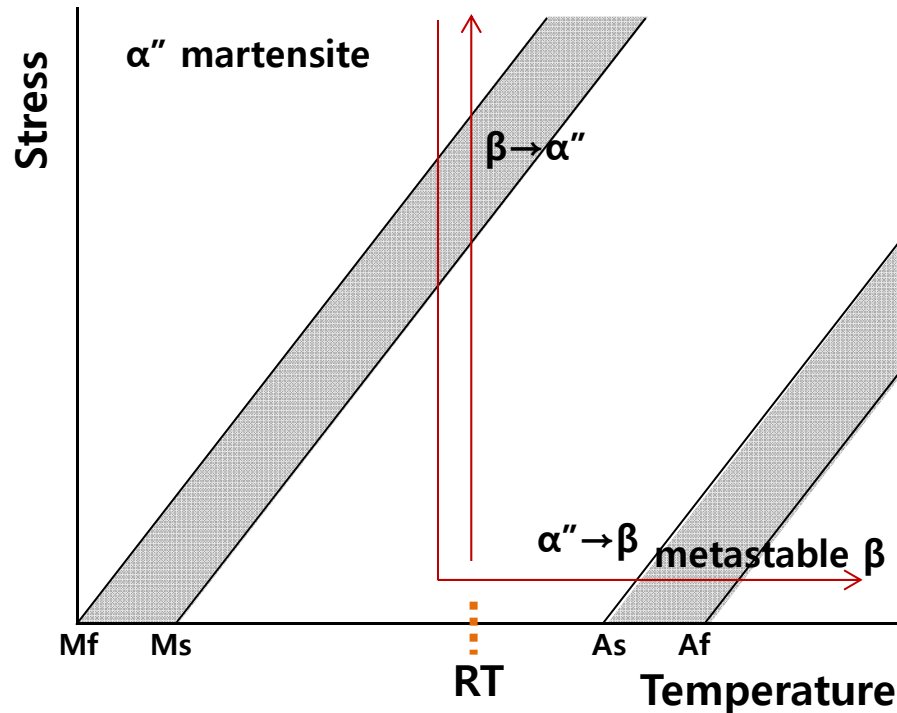
Secondary phase **CuZr**
Metastable B2 phase at RT
"Shape Memory Behavior"



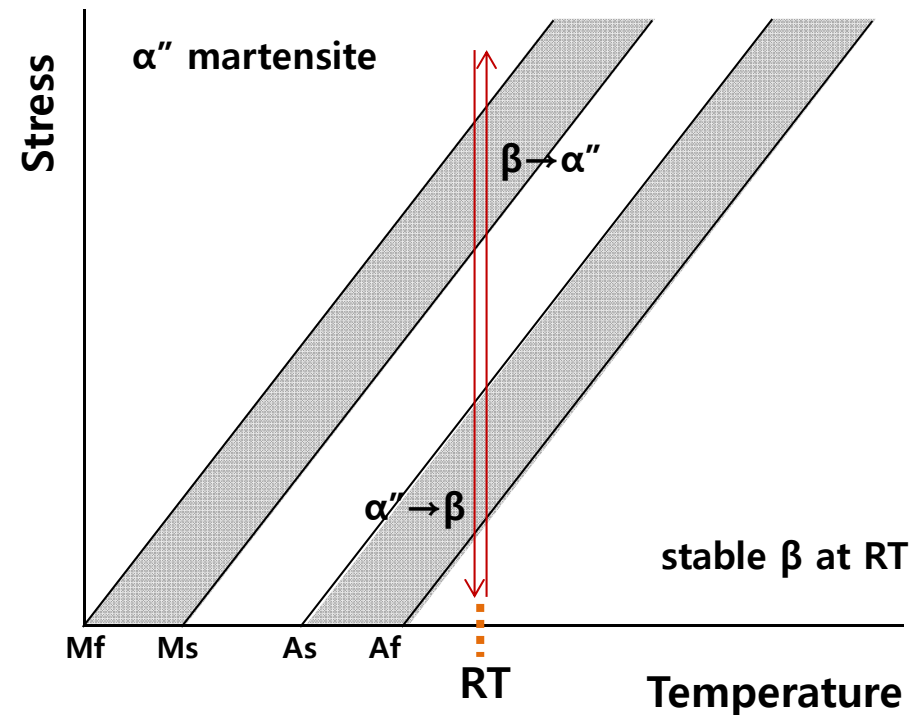
Ti-Cu-Ni system

Ti-X
Stable B2 phase at RT
"Superelastic behavior"

Shape Memory Alloy (SMA)



Super-Elastic Alloy (SE alloy)



Phase transformation in Ti-based alloys : $B_2 \rightarrow M \rightarrow B_2$

- Alloy composition:
Ti₄₉-Cu-Ni-X

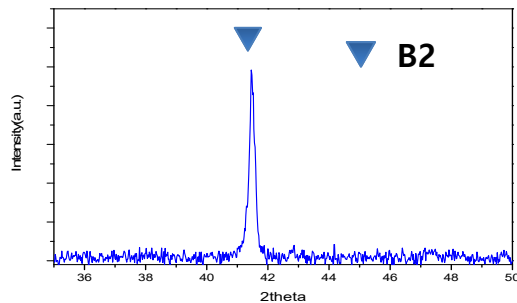
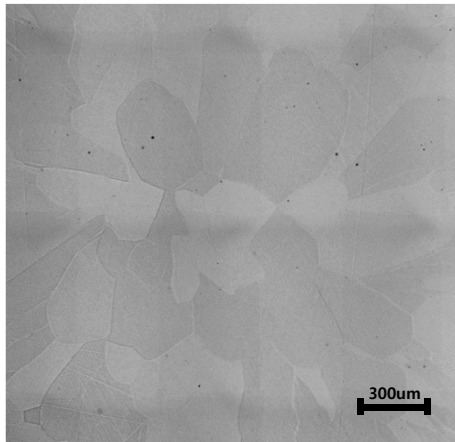
Φ3mm suction casting
-Fully crystalline B2

▶ **Stress-induced** phase transformation

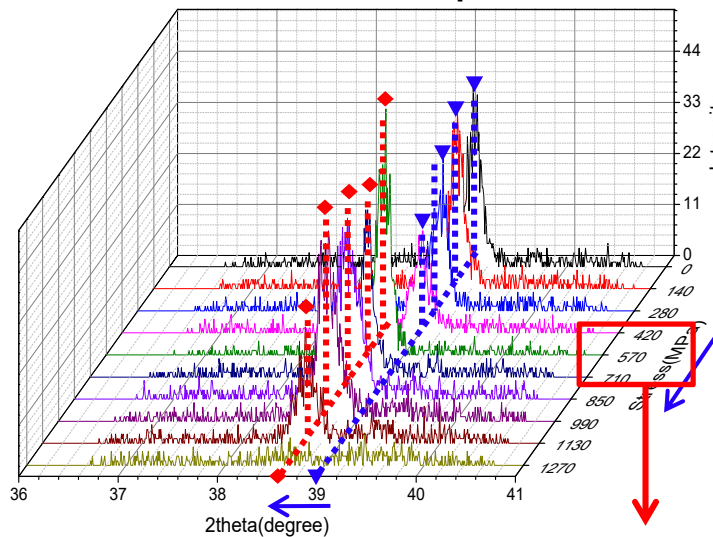
In-situ neutron diffraction measurement during compression

▶ **Temperature-induced** phase transformation

DSC measurement (during cooling)

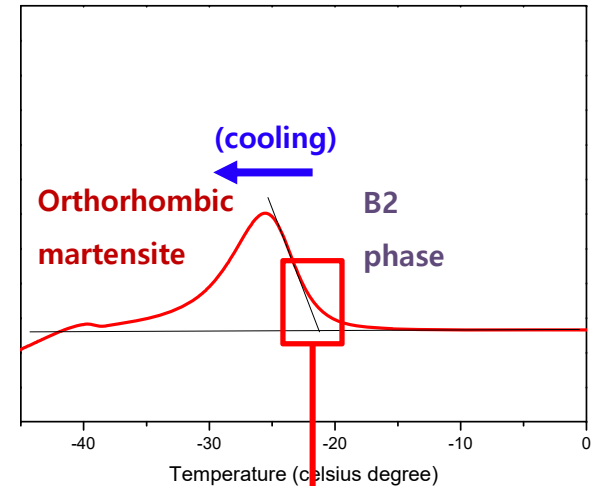


▼ B2 phase
◆ Orthorhombic martensite phase



Phase transformation stress

= 570MPa



Martensite start T (Ms)

= -22°C

➔ **Novel Ti-based Super-elastic Crystalline Alloy**

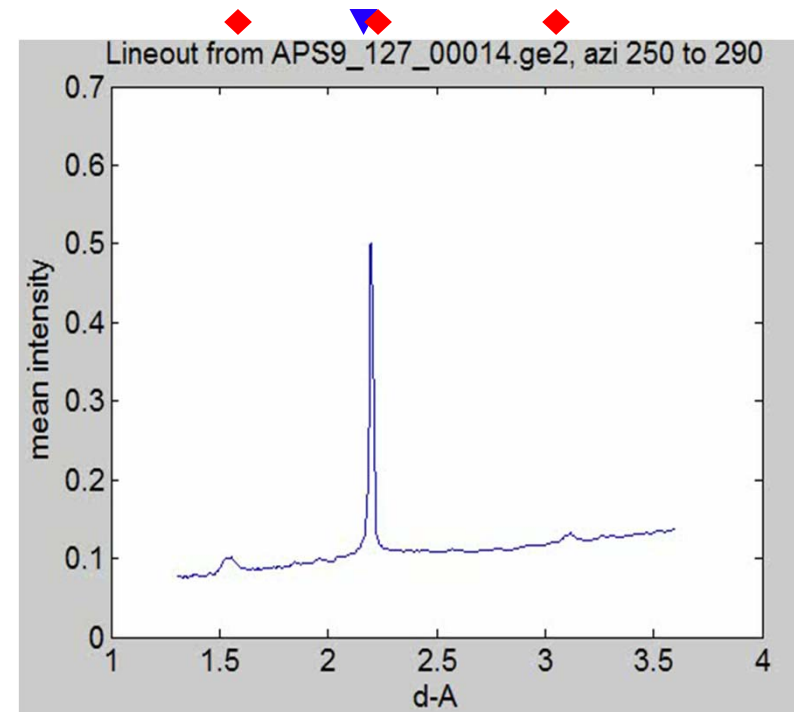
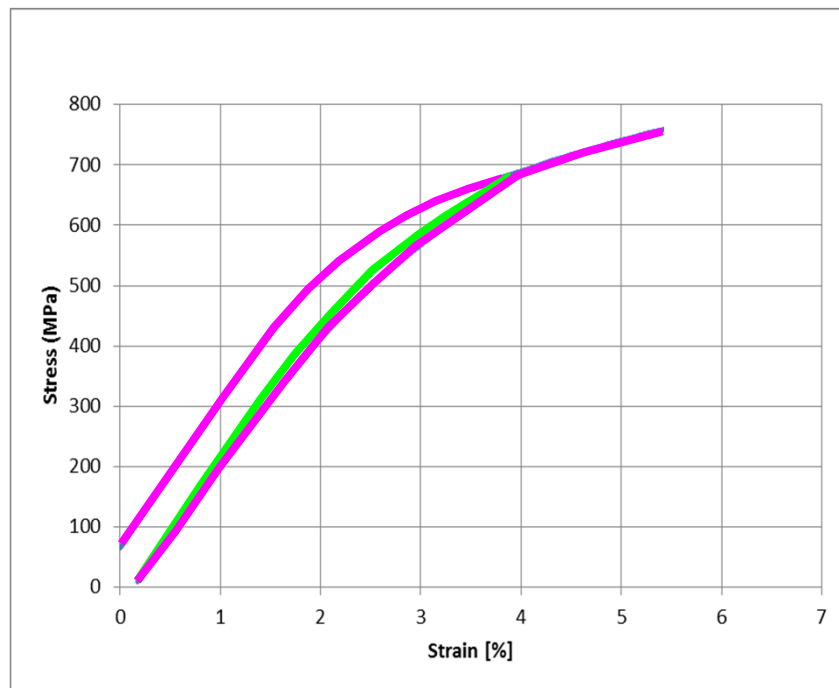
In-situ synchrotron diffraction analysis during tensile test

► Superelastic BMG composite: Reversible Phase Transformation Behavior

Ti-Cu-Ni-X Φ 3mm
Water cooled Cu mold suction casting,

Loding → Unloading → Reloading

- ▼ Initial BCC phase in as-cast sample
- ◆ Deformed martensite phase



at APS beam line, ANL





2) “TWIP/TRIP High Entropy Alloy”

- Stress-induced phase transformable HEA -

극지 개발의 글로벌 이슈



남극 장보고 과학기지 조감도



북극 항로 개척 및 활용

시베리아-베링 해협을 잇는 해상 수송 루트 개척 및 활용을 위한 첨단 선박 기술



극지 에너지 자원 개발

북극 오일샌드, 해양 플랜트, 시베리아 유전 개발에 따른 구조물 및 파이프라인 건설



극지 인프라 구축

생태, 환경 및 천체관측용 과학기지 건설에 따른 인프라(건축, 항만, 도로, 공항, 상하수도 등) 구축



극지운용 장비 및 용품 개발

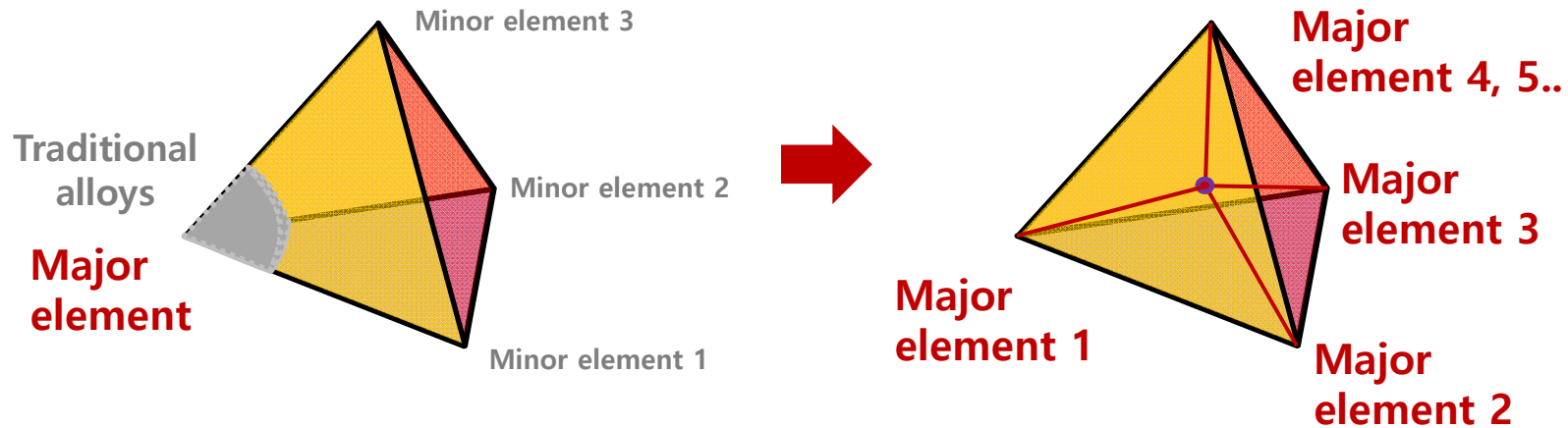
극지 건설/운영장비/관측장비, 운송/이동/탐사 수단 및 관련 용품 개발



METAL MIXOLOGY

306 | NATURE | VOL 533 | 19 MAY 2016

Basic concepts of high entropy alloy (HEA)



Conventional alloy system

Ex) 304 steel - $\text{Fe}_{74}\text{Cr}_{18}\text{Ni}_8$

High entropy alloy system

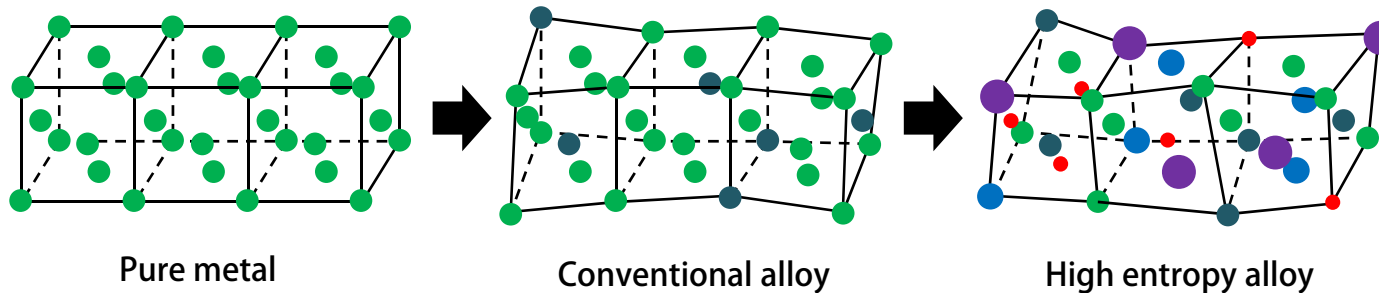
Ex) $\text{Al}_{20}\text{Co}_{20}\text{Cr}_{20}\text{Fe}_{20}\text{Ni}_{20}$

(1) Thermodynamic : high entropy effect

(2) Kinetics : sluggish diffusion effect

(3) Structure : severe lattice distortion effect

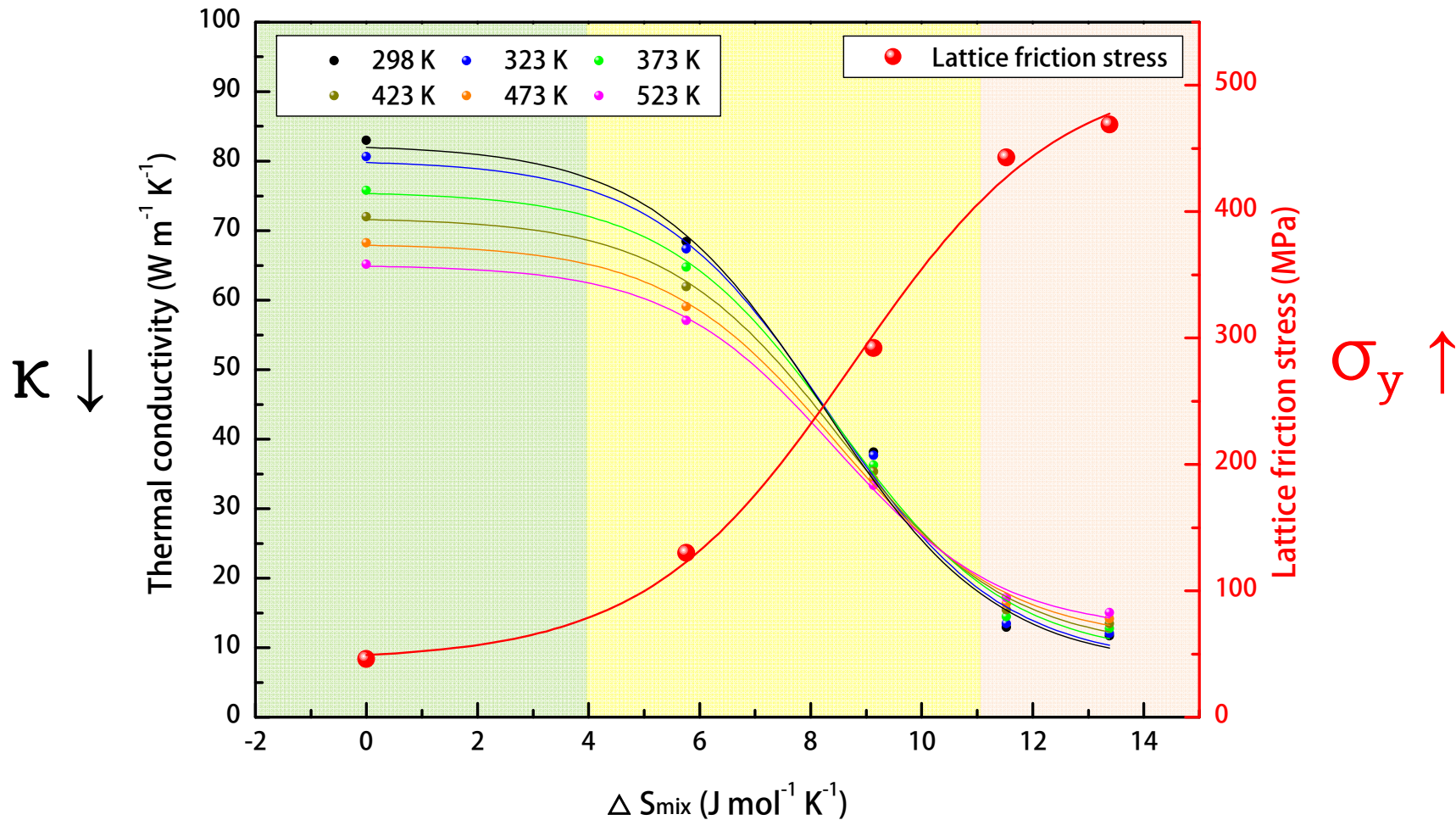
(4) Property : cocktail effect



Severe lattice distortion → Sluggish diffusion & Thermal stability

차세대 극지구조용 신소재 : “하이엔트로피 합금”

우수한 σ_y/κ ratio



하이엔트로피 합금화를 통한 저온 고인성 합금의 개발가능

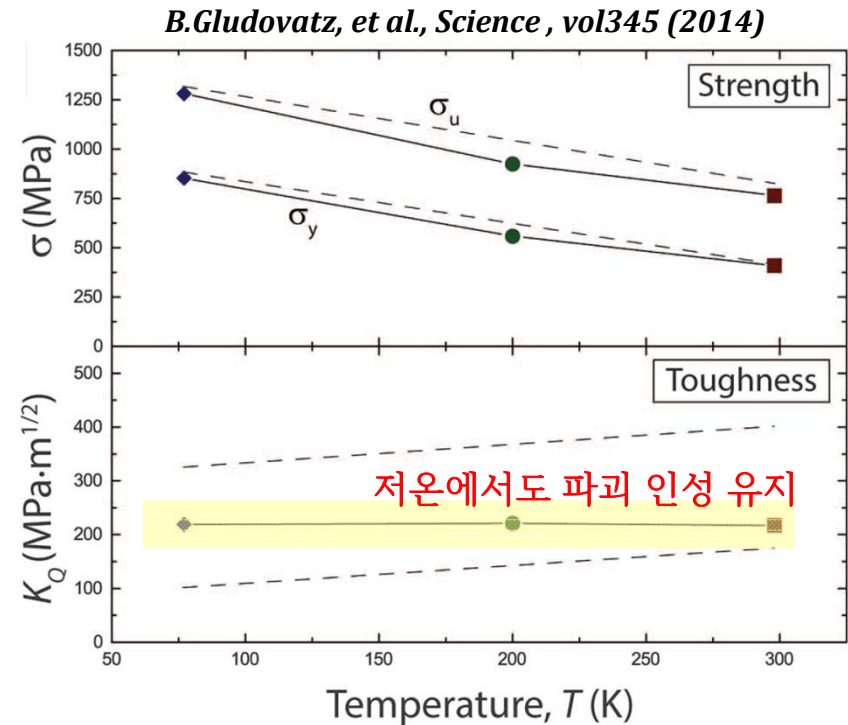
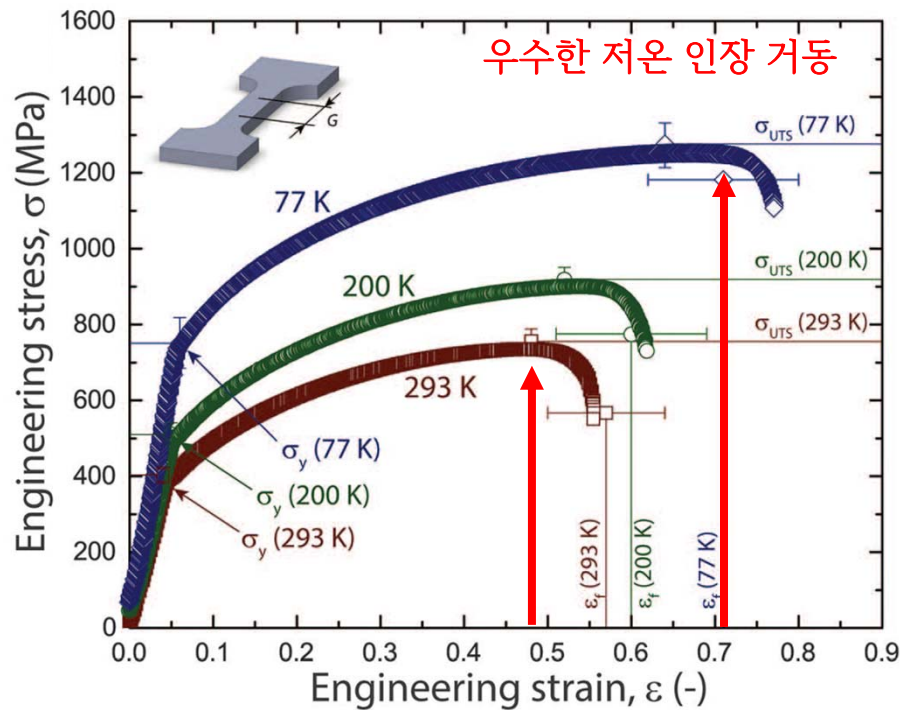


차세대 극지구조용 신소재 : “하이엔트로피 합금”

▶ FCC 하이엔트로피 합금의 극저온 특성

1) 우수한 극저온 파괴 인성 ($\sim 200 \text{ MPa}\cdot\text{m}^{1/2}$)

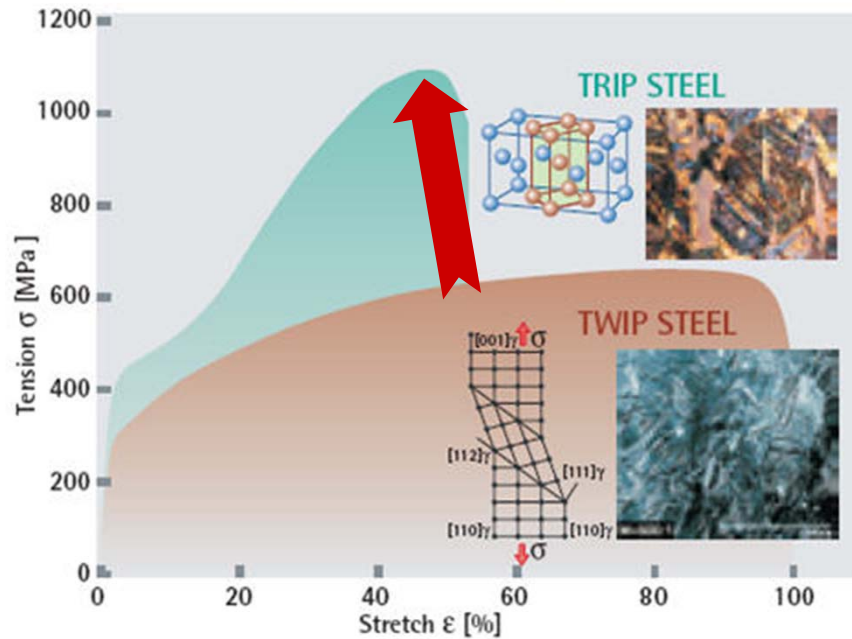
2) Nano-twin 작동으로 일반적 상용합금과는 다르게, 저온에서도 상온의 파괴 인성이 유지됨



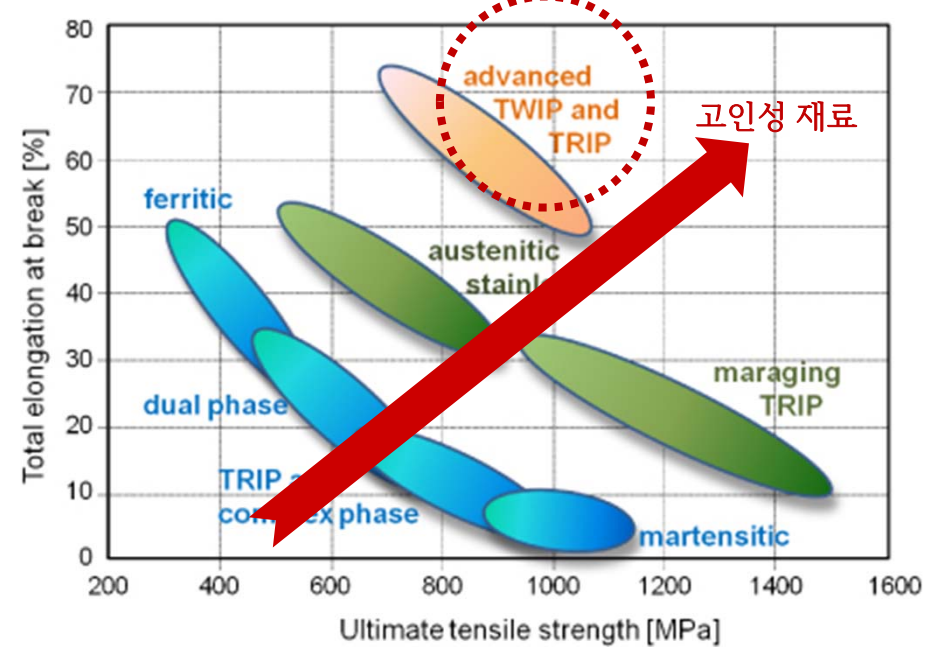
“하이엔트로피 합금화를 통한 저온 고인성 합금의 개발 가능”

TWIP/TRIP 효과 도입을 통한 기계적 물성 향상

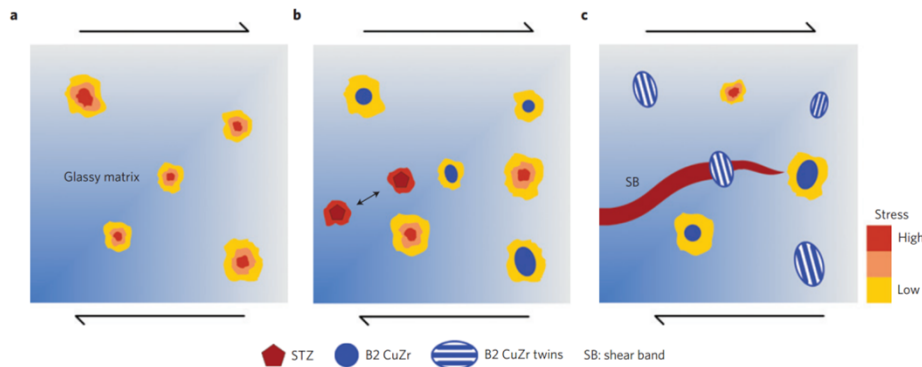
▶ TWIP/ TRIP 효과



▶ TWIP 및 TRIP Steel의 특성



▶ TRIP에 의한 균열 전파의 방지 거동

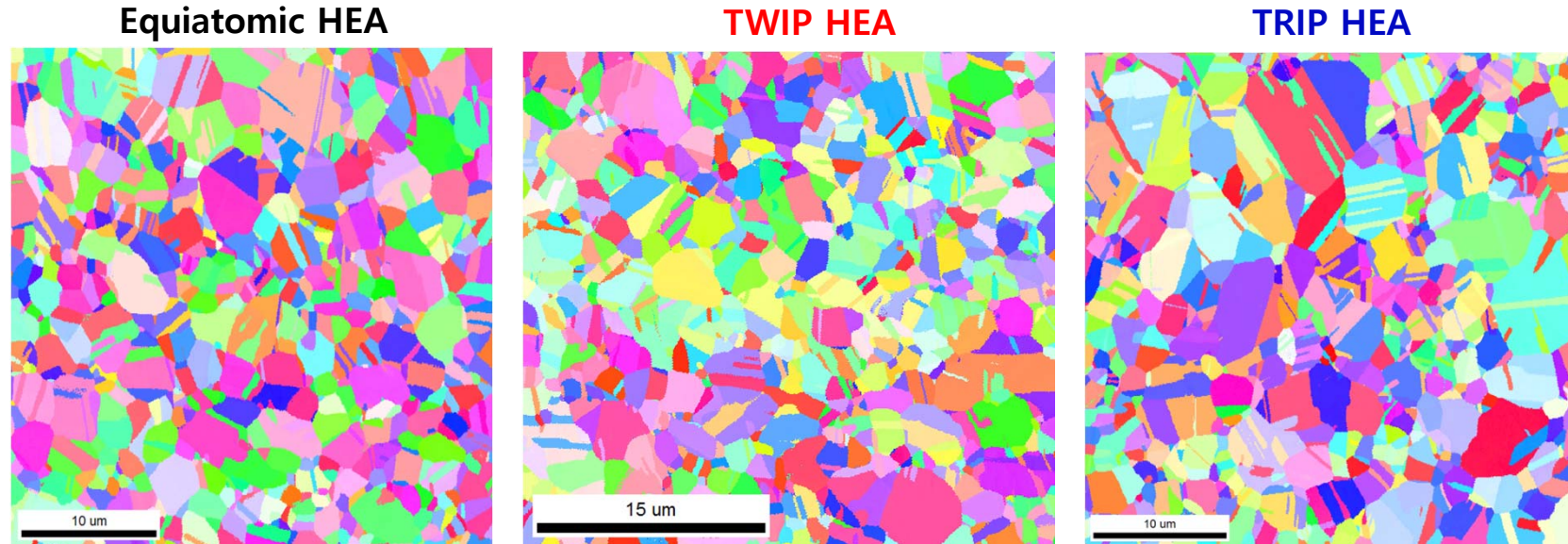


균열부 주변에서 다수의 쌍정유기소성(TWIP), 또는 상변화유기소성(TRIP)을 통한 고인성 구현

“극지 환경 피로파괴 저항성이 큰 TRIP 하이엔트로피 합금 개발”

Development of TWIP/TRIP High Entropy Alloy

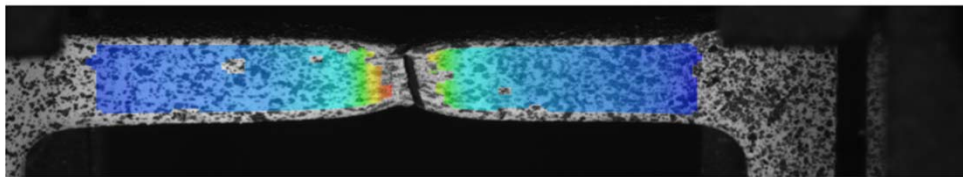
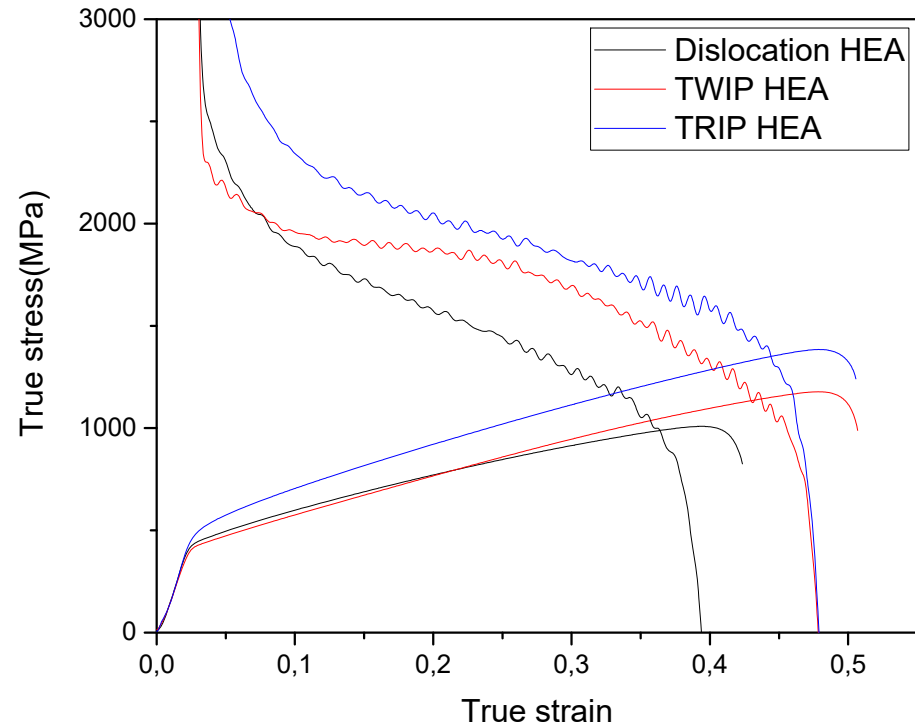
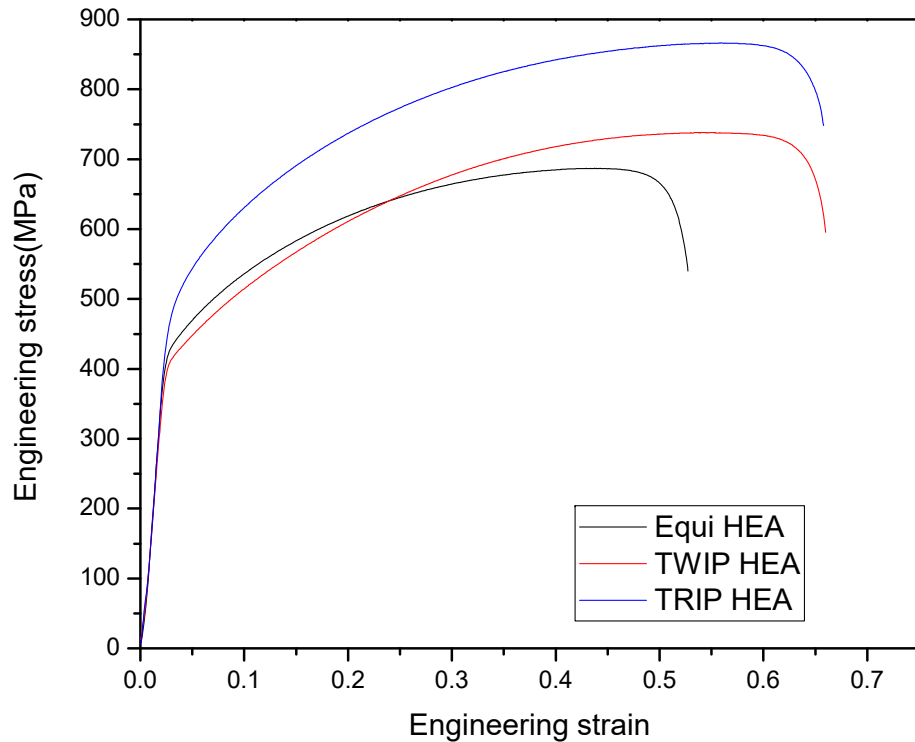
- Design of TWIP/TRIP high entropy alloy **without losing yield strength**



	Composition	Grain size (μm)
1	Equiatomic HEA	3.8
2	TWIP HEA	3.6
3	TRIP HEA	4.3

Development of TWIP/TRIP High Entropy Alloy

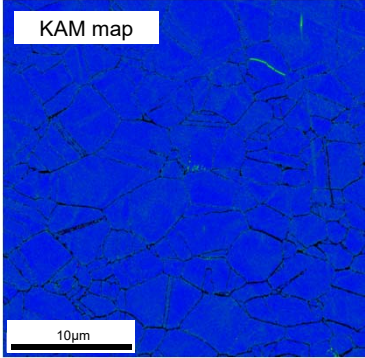
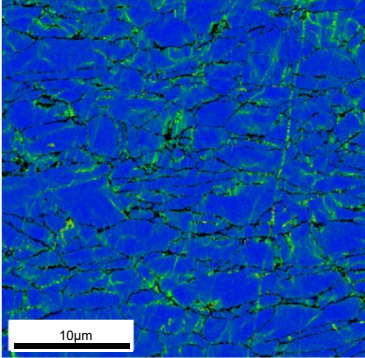
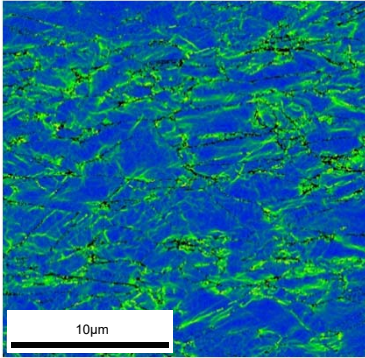
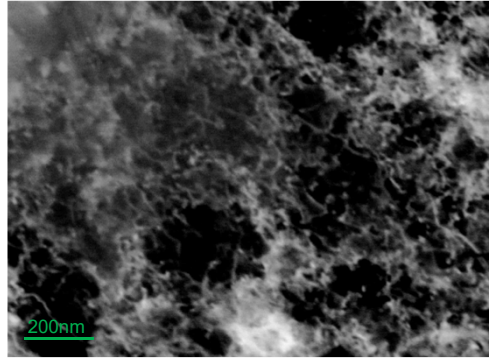
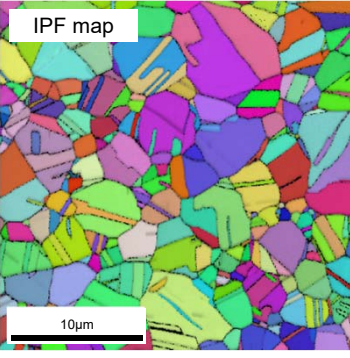
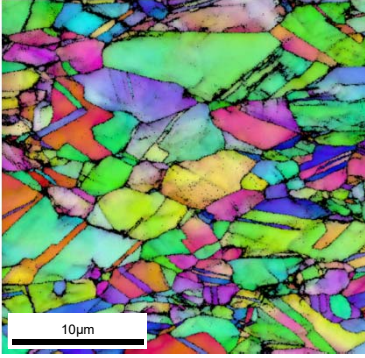
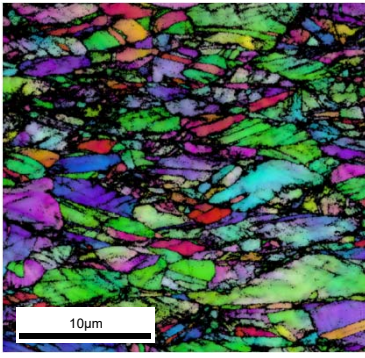
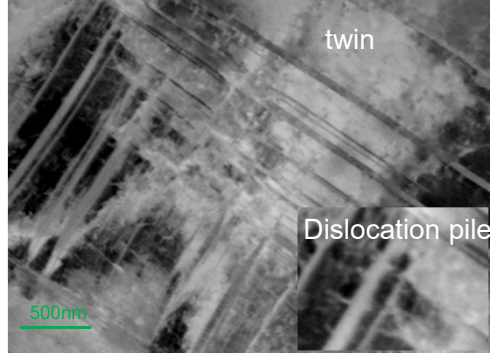
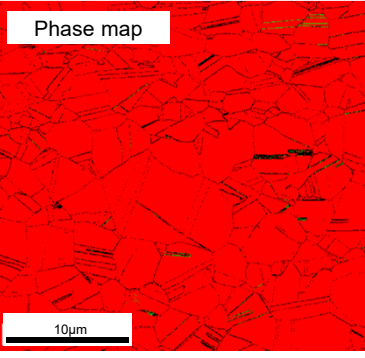
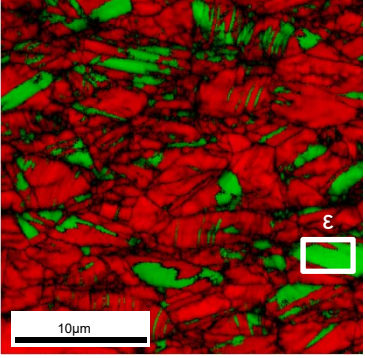
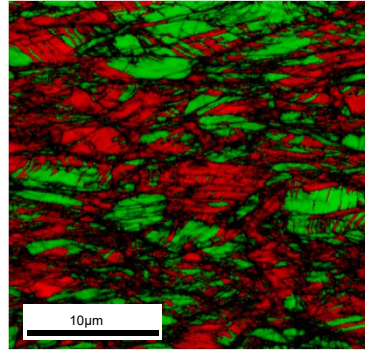
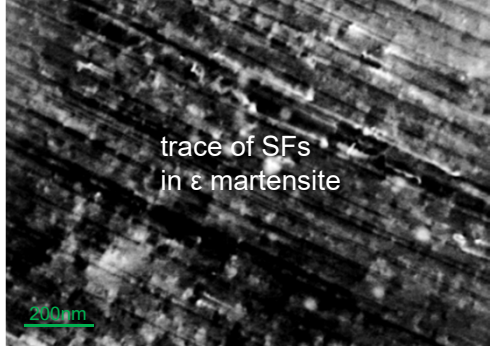
Ni-Co-Fe-Cr-Mn high entropy alloy



Considered criteria

$$\sigma = \frac{\partial \sigma}{\partial \varepsilon} : \text{Necking}$$

Development of TWIP/TRIP High Entropy Alloy

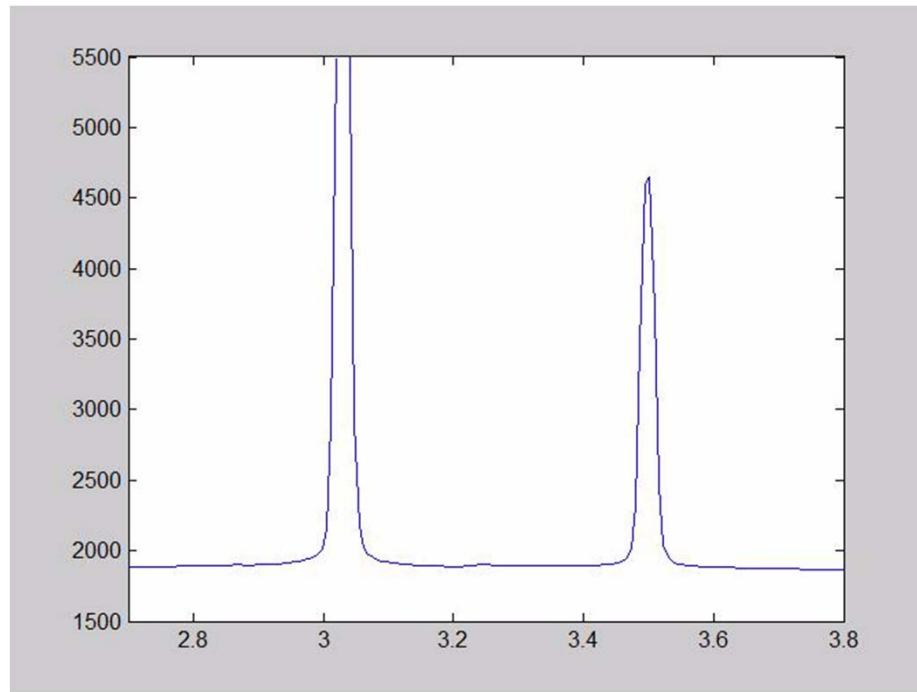
Strain	0%	30%	60%	ECCI
Equi HEA	 <p>KAM map</p> <p>10µm</p>	 <p>10µm</p>	 <p>10µm</p>	 <p>200nm</p>
TWIP HEA	 <p>IPF map</p> <p>10µm</p>	 <p>10µm</p>	 <p>10µm</p>	 <p>twin</p> <p>Dislocation pile-up</p> <p>500nm</p>
TRIP HEA	 <p>Phase map</p> <p>10µm</p>	 <p>ε</p> <p>10µm</p>	 <p>10µm</p>	 <p>trace of SFs in ε martensite</p> <p>200nm</p>



Development of TWIP/TRIP High Entropy Alloy

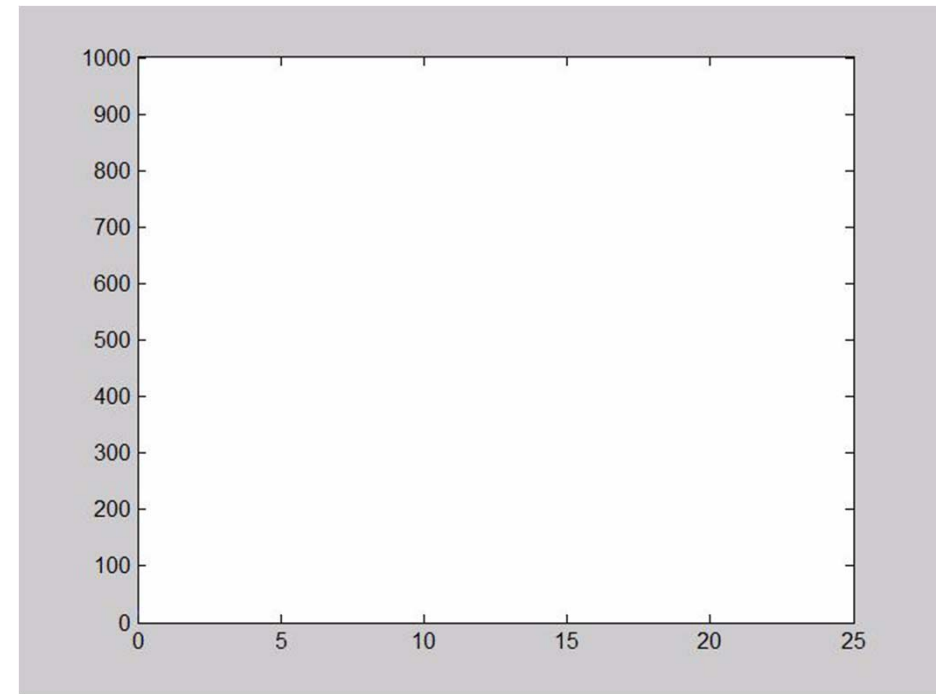
TRIP HEA

ϵ γ ϵ γ



I(Q) vs. Q

Stress-strain curve



Stress (MPa) vs. Strain (%)

at APS beam line, ANL



Contents in Phase Transformation

Background
to understand
phase
transformation

(Ch1) Thermodynamics and Phase Diagrams

(Ch2) Diffusion: Kinetics

(Ch3) Crystal Interface and Microstructure

Representative
Phase
transformation

(Ch4) Solidification: Liquid \rightarrow Solid

(Ch5) Diffusional Transformations in Solid: Solid \rightarrow Solid

(Ch6) Diffusionless Transformations: Solid \rightarrow Solid

Microstructure-Properties Relationships

Alloy design &
Processing

Performance

“Phase Transformation”

Microstructure
down to atomic scale

Properties

“Tailor-made Materials Design”

*** Homework 6 : Exercises 6**

until 19th December (before exam)

FINAL (19th December, 9 AM-1 PM)

Place: 33-328 & 330

**Scopes: Text: page 146 (chapter 3.3) ~
page 415 (chapter 6.4)/**

Teaching notes: 12~22/

QUIZ and Homeworks

Good Luck!!